Aalto University
School of Science
Department of Mathematics and Systems Analysis

**Heikki Puustinen**

# Military Aircraft Routing with Multi-Objective Network Optimization and Simulation

Thesis submitted in partial fulfillment of the requirements for the degree of Master of Science in Technology in the Degree Programme in Engineering Physics and Mathematics. The document can be stored and made available to the public on the open internet pages of Aalto University. 

Espoo, September 27, 2013

| | |
|---|---|
| Supervisor: | Professor Raimo P. Hämäläinen |
| Instructor: | Kai Virtanen, D.Sc. (Tech.) |

AALTO UNIVERSITY
SCHOOL OF SCIENCE

ABSTRACT OF THE
MASTER'S THESIS


| | | | |
|---|---|---|---|
| **Author:** | Heikki Puustinen | | |
| **Title:** | Military Aircraft Routing with Multi-Objective Network Optimization and Simulation | | |
| **Date:** | September 27, 2013 | **Pages:** | 116 |
| **Professorship:** | Systems and Operations Research | **Code:** | Mat-2 |
| **Degree Programme:** | Degree Programme in Engineering Physics and Mathematics | | |
| **Major subject:** | Systems and Operations Research | | |
| **Minor subject:** | Industrial Management | | |
| **Supervisor:** | Prof. Raimo P. Hämäläinen | | |
| **Instructor:** | Kai Virtanen, D.Sc. (Tech.) | | |



One of the most critical tasks in the planning of military air missions is the selection of the route of the aircraft, i.e., the mission route planning problem (MRPP). This thesis introduces a novel approach towards the automated solution of a dynamic optimization problem representing the multi-objective MRPP. In the approach, the optimal route for an aircraft conducting an air-to-ground (A/G) mission through enemy air defenses is solved by using multi-objective network optimization and simulation. Four objectives are considered: flight distance, consumption of fuel, and exposures to surface-to-air and air-to-air threats. Compared to the existing network formulations of the MRPP, more advanced models of the threats depending on the state of the aircraft are used. Additionally, the performance and the consumption of fuel of the aircraft are described in a more elaborate way. The optimal route is generated by aggregating the objectives with weights and by solving the resulting single objective shortest path problem with Dijkstra's algorithm. The route is then evaluated with the continuous time simulation model of the threats. Should the optimization and simulation results concur, the optimal route is accepted as the solution of the MRPP. Otherwise, the threat models are modified to reflect the simulation results and the optimization as well as the simulation are repeated.

The approach is implemented in a software named Strike Aircraft Routing Software Suite (SARSS). It is utilized in the calculation of optimal routes involving the selection of the initial and terminal bases as well as the launch point of an A/G weapon. SARSS can also be used inversely by studying optimal routes through friendly defenses in order to identify vulnerable areas. In addition, multiple targets can be considered which enables the identification of the areas that can be influenced with A/G weapons without risks posed by the threats. With the help of SARSS, the creation of mission scenarios as well as the analysis of optimization and simulation results can be easily conducted.

The new solution approach presented in this thesis can be applied to other multi-objective nonlinear dynamic optimization problems as well. Then, the original problem is approximated by a network optimization problem, and the feasibility of the optimal solution is evaluated with an appropriate simulation model. The approximation is updated according to the simulation results, and the calculations are repeated until the optimal and feasible solution is obtained.



Keywords: Computational Dynamic Optimization, Routing, Military Aircraft, Multi-Objective Network Optimization, Simulation.

AALTO-YLIOPISTO
PERUSTIETEIDEN KORKEAKOULU

DIPLOMITYÖN
TIIVISTELMÄ

| | | | |
|---|---|---|---|
| **Tekijä:** | Heikki Puustinen | | |
| **Työn nimi:** | Hävittäjälentokoneen reitin suunnittelu monitavoitteisella verkko-optimoinnilla ja simuloinnilla | | |
| **Päivämäärä:** | 27. syyskuuta 2013 | **Sivumäärä:** | 116 |
| **Professuuri:** | Systeemi- ja operaatiotutkimus | **Koodi:** | Mat-2 |
| **Tutkinto-ohjelma:** | Teknillisen fysiikan ja matematiikan tutkinto-ohjelma | | |
| **Pääaine:** | Systeemi- ja operaatiotutkimus | | |
| **Sivuaine:** | Teollisuustalous | | |
| **Valvoja:** | Prof. Raimo P. Hämäläinen | | |
| **Ohjaaja:** | TkT Kai Virtanen | | |


Lentokoneen reitin määrääminen on oleellinen osa ilmaoperaation suunnittelua. Tässä työssä esitellään uusi lähestymistapa monitavoitteista reittioptimointitehtävää kuvaavan dynaamisen optimointehtävän automatisoituun ratkaisemiseen. Lähestymistavassa määrätään optimaalinen reitti ilmapuolustuksen läpi ilmasta maahan -tehtävää toteuttavalle lentokoneelle käyttämällä verkko-optimointia ja simulointia sekä ottamalla huomioon neljä optimointikriteeriä: lentomatka, polttoaineenkulutus sekä lentomatkat ilmasta maahan ja ilmasta ilmaan -uhkien vaikutusten alla. Työssä käytetään aiempiin verkko-optimointitehtäviin verrattuna kehittyneempiä, lentokoneen tilasta riippuvia uhkamalleja sekä realistisia malleja lentokoneen suorituskyvylle ja polttoaineenkulutukselle. Reittioptimointitehtävä formuloidaan lyhimmän polun tehtäväksi, jossa optimointikriteerit yhdistetään painottamalla ja joka ratkaistaan Dijsktran algoritmilla. Optimireitin käyttökelpoisuus arvioidaan simuloimalla optimireittiä lentävään lentokoneeseen kohdistuvia uhkia. Jos optimoinnin ja simuloinnin tulokset ovat yhteneviä, saatu reitti hyväksytään reittioptimointitehtävän ratkaisuksi. Muussa tapauksessa uhkamalleja päivitetään simulointitulosten mukaisesti ja optimointi sekä simulointi toteutetaan uudelleen.

Uuteen lähestymistapaan perustuen työssä kehitetään Strike Aircraft Routing Software Suite (SARSS) -ohjelmisto. SARSS:a käytetään ilmasta maahan -tehtävän optimaalisen reitin määräämiseen valitsemalla samalla myös optimaaliset lähtö- ja saapumistukikohdat sekä ilmasta maahan -aseen optimaalinen laukaisupiste. SARSS:a voidaan hyödyntää käänteisesti tarkastelemalla optimireittiä oman ilmapuolustuksen läpi, jolloin kyetään tunnistamaan ilmapuolustusjärjestelmän mahdolliset heikkoudet. Lisäksi SARSS:lla voidaan määrittää alueita, joilla sijaitseviin maalipisteisiin kyetään vaikuttamaan ilmasta maahan -aseilla ilman, että lentokoneeseen kohdistuu uhkia. SARSS:n graafisen käyttöliittymän avulla on helppoa luoda tehtäväskenaarioita sekä tarkastella optimointi- ja simulointituloksia.

Työssä esiteltyä lähestymistapaa voidaan soveltaa myös muiden monitavoitteisten epälineaaristen dynaamisten optimointitehtävien ratkaisemiseen. Tällöin alkuperäistä optimointitehtävää approksimoidaan verkko-optimointitehtävällä ja optimointitulosten käypyys arvioidaan sopivalla simulointimallilla. Approksimoitua tehtävää tarkennetaan simulointitulosten perusteella, ja sekä optimointi että simulointi toistetaan, kunnes löydetään optimaalinen ja käypä ratkaisu.



Avainsanat: Laskennallinen dynaaminen optimointi, Reitin suunnittelu, Hävittäjälentokone, Monitavoitteinen verkko-optimointi, Simulointi.

# Acknowledgments

This work was conducted at the Systems Analysis Laboratory at Aalto University.

I thank my instructor, Kai Virtanen for his patience and guidance during the writing of this thesis. I express my gratitude to my supervisor, Raimo P. Hämäläinen for giving me the opportunity to work at the Systems Analysis Laboratory. I also thank my co-workers for creating an inspiring and warm hearted work environment. My special thanks go to my colleague, Pekka for his invaluable friendship and willingness to discuss my ideas during these years.

I am also grateful to my parents, Harri and Helka-Maija for their support and care during my academic pursuits. Finally, I thank my wife, Laura for standing beside me through my seemingly endless studies.

Espoo, September 27, 2013

Heikki Puustinen

# Contents

# Chapter 1

# Introduction

The planning of an air mission (e.g., [1]) is a complex process that involves several tasks. The optimization of the route of the aircraft conducting the mission is called the mission route planning problem (MRPP) (e.g., [2, 3, 4]) and it is one of the critical tasks of the planning process. It is especially important in an air-to-ground (A/G) mission where an aircraft tries to deliver an A/G weapon to a target. The target is usually defended by air-to-air (A/A) and surface-to-air (S/A) weapon systems. The optimal route from the initial base to the launch point of the A/G weapon and back to the terminal base should avoid the threats posed by these systems. In addition, other objectives such as minimizing flight time and the consumption of fuel are considered. In this thesis, the novel approach to the automated solution of a dynamic optimization problem representing the multi-objective MRPP based on network optimization (e.g., [5]) and simulation (e.g., [6]) is introduced.

Several approaches towards solving the MRPP have been proposed in the existing literature. The methodologies of optimal control (e.g., [7, 8, 9, 10, 11]), mixed integer linear programming (e.g., [12, 13, 14, 15, 16]), network optimization (e.g., [2, 3, 17, 18]), game theory (e.g., [19, 20, 21, 22, 23]), and simulation (e.g., [24, 25, 26]) have been applied in the context of MRPPs. Solving the multi-objective optimization problem discussed in this thesis with an optimal control approach is computationally demanding. To achieve optimal routes in feasible time, realistic models of aircraft and threats must be discarded to simplify the optimal control

problem. Mixed integer linear programming formulations of the MRPP may be easier to solve but only simple models for the aircraft and the threats can be used. In game theory formulations, assumptions of the behavior of the counterpart, e.g., enemy aircraft, must be made. This leads to challenges in the interpretation of the optimal routes. In simulation-optimization approaches, large number of possible routes must be evaluated with the simulation model. This too would need excessively large computational resources. In the context of the thesis, the solution of the MRPP should be optimal, realistic, comprehensible, and acquired in a reasonable time. In this thesis, network optimization and simulation are used to achieve these goals. Using network optimization, optimal routes through enemy defenses are found fast as the solution time is not affected by the complexity or the number of threats. However, the network optimization formulation is less accurate than, e.g., optimal control formulations, and the costs caused by the threats as well as the movement of the aircraft might not be realistic. This issue is overcome by using an elaborate simulation model to evaluate the optimization results.

The MRPP considered in this thesis contains multiple objectives including minimizing the threats caused by enemy aircraft and surface-to-air missiles as well as minimizing flight distance and fuel consumption. The solution procedure of such a MRPP consists of three main phases. In the first phase, the mission under consideration is defined including the information on the area of operations, locations of bases as well as positions of enemy A/A and S/A threats. In addition, the structure of the optimization network is defined. In the second phase, the weights of the objective costs are elicited from the decision maker (DM) with trade-off statements [27]. The optimal route is generated by aggregating the objectives with the weights and by solving the resulting single objective shortest path problem [5] with a modified version of Dijkstra's algorithm [28, 29]. The resulting route is evaluated both visually and by examining the objective costs. If the route is unacceptable, the weights are updated and the second phase is repeated. In the third phase, a continuous time simulation model of the threats [30] is applied for analyzing the optimal route. In the simulation, the threats on the optimal route are taken into account more accurately than in the second phase. The optimal route is evaluated by comparing the optimization and simulation results. For example, flying edges that have objective cost related to surface-to-air

missiles should also result to successful launches of surface-to-air missiles in the simulation. Should the optimization and simulation results conflict, the threat models are modified to reflect the simulation results, and optimization as well as simulation are repeated. Otherwise, the optimal route is accepted as the solution of the MRPP.

The approach is implemented in a software named Strike Aircraft Routing Software Suite (SARSS) that consists of a graphical user interface (see, Figure 1.1) as well as mission planning, optimization, and simulation modules. The user interface provides an intuitive and transparent way for defining A/G missions as well as analyzing optimization and simulation results. The optimization and simulation modules are designed to operate automatically so that the DM does not need prior knowledge of network optimization or simulation. She provides only the definition of the mission under consideration and the preference information in the form of the weights of the objective costs. The results of optimization and simulation are presented with visualizations and numerical data of the optimal route and the objective costs. The updating of the weights is implemented in the interface, and the comparison of alternative routes acquired with different weight sets is enabled. Additionally, the evaluation of the optimal routes with simulation and the comparison of the simulation results to the results of optimization can be conducted with little effort. Furthermore, the updating of threat models and repeating optimization and simulation in the case that the results differ can be conducted.

While SARSS produces the solution of the MRPP for an A/G mission, the simulation of the threats can be used to determine which enemy bases and launch platforms of surface-to-air missiles pose the greatest threat on the optimal route. This information can be used to plan suppression of enemy air defenses (SEAD) missions (e.g., [31]) where one or more of the threats are neutralized in order to find a new optimal route with less threat. SARSS can also be utilized inversely by studying optimal routes through friendly air defenses. By evaluating the threats posed by the friendly defenses to the enemy aircraft, probable targets, critical defense assets as well as vulnerable areas in the defenses can be identified.

In addition to the calculation of optimal routes, SARSS can be used for determining areas having targets that can be influenced with A/G weapons without

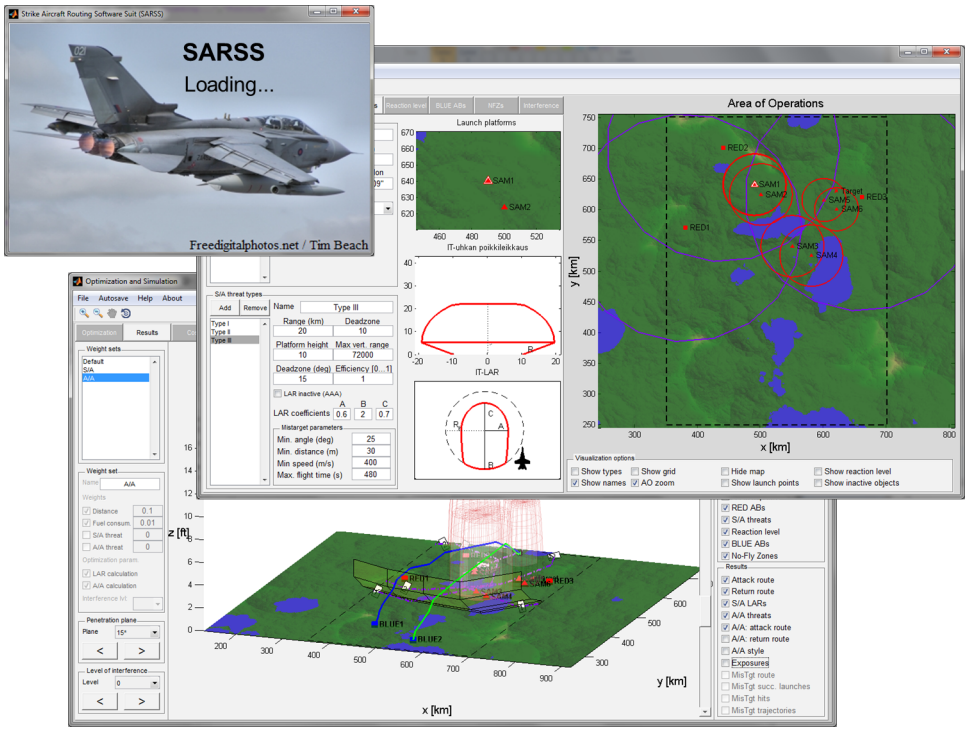


Figure 1.1: Graphical user interface of SARSS.

exposing the aircraft to the threats. Here, the calculation and the evaluation of the optimal routes are conducted for multiple targets whose locations form a target area. This feature of SARSS is called the area of influence calculation. Using this feature, the targets of an A/G mission that involve high and low risks are easy to determine. The high risk targets cannot be influenced without exposure to surface-to-air missiles while the low risk targets can be influenced safely. In addition, the feature can be used in the planning of SEAD missions by extending the target area to consider the locations of the threats. Then, the low risk targets form the potential targets of SEAD missions. In order to evaluate the effect of the SEAD mission, a threat is removed from the mission description and the optimization is repeated. As a result, the original A/G mission is likely to become less risky to execute as a shorter and safer route is often found. The area of influence calculation can also be used inversely to assist the allocation of friendly S/A and A/A resources. This means revealing the areas that are vulnerable to A/G weapons so that the defenses can be reallocated accordingly.

Compared to the existing network optimization formulations dealing with the MRPP, the approach to the automated solution of the MRPP innovated in this

thesis provides several improvements. First, multiple objectives are taken into consideration including two threats, flight distance, and fuel consumption. Earlier, only one or two objectives with varying number of constraints (e.g., [17, 32]) are used. In addition to the threat posed by S/A weapon systems, a new threat representing A/A threat, which is not considered in the previous studies, is taken into account. Second, the threat posed by surface-to-air missiles is treated so that it depends on the state of the aircraft and thus reflects the kinematic capability of the missile opposite to static circular or spherical models that are used previously (e.g., [17, 18]). Third, the performance and flight capabilities of the aircraft are represented more accurately than in the existing network optimization formulations (e.g., [17, 18, 32]) by allowing the aircraft to descend and ascend in various angles. Fourth, the fuel consumption of the aircraft is based on actual data and depends on flight altitude as well as ascent or descent angle. Fifth, multiple initial and terminal bases for the mission along with multiple targets coupled with alternative weapon systems and their launch points are considered, and the optimal combination of these is determined when solving the optimal route. According to the author's knowledge, such a combination has not been treated before even though it increases the computational effort negligibly while providing new information for supporting the planning of A/G missions. Finally, the novel feature of the approach is also the evaluation of the optimal route with an accurate simulation model in order to guarantee the feasibility and practicality of the route. Based on the evaluation, the threat models are updated if necessary and the calculations are repeated. Such an evaluation aspect has not been addressed in the context of the MRPP.

The rest of the thesis is structured as follows. Chapter 2 gives an introduction to the planning of military air missions and reviews the existing approaches to the solution of MRPPs. Chapter 3 discusses single and multi-objective shortest path problems and their solution methods. In Chapter 4, the approach to the automated solution of the MRPP is introduced. The formulation of the MRPP as a multi-objective shortest path problem is presented, and the phases of the approach are discussed. The details of the optimization and simulation models are also presented. In Chapter 5, the implementation of the approach, SARSS, is presented. The structure, modules, and functionalities of SARSS are discussed. Additionally, the computational performance and the utilization of SARSS are

addressed. Chapter 6 demonstrates the approach and the utilization of SARSS using an example MRPP. First, an optimal route in the case of an A/G mission is considered. Second, the area of influence calculation allowed by SARSS is applied for supporting in the planning of a SEAD mission. Further research avenues and conclusions are given in Chapters 7 and 8, respectively.

# Chapter 2

# Planning of military air missions and aircraft routes

The planning of military air missions has become increasingly important in air warfare (see, e.g., [1]). In the recent military conflicts, effort has been allocated towards the precision and accuracy of air missions to increase efficiency and to avoid collateral damage [33, 34]. Air mission planning can be summarized as a preparation to provide an aircraft crew with the necessary information and material to carry out a mission such as delivering a weapon to a target [35]. The planning starts by gathering information related to the mission. The next task is to select the goal or goals of the mission, e.g., destruction of a key building, neutralization of an enemy unit or search and rescue of a crashed air crew. The following task is to decide what material such as aircraft, weapon systems, and crew are available and needed to successfully carry out the mission. The final task is to form the step-by-step plan of the mission where the use of the resources to achieve the goals is described. For a detailed description of the air mission planning process, see, e.g., [1, 35, 36].

In air mission planning, the goal of the mission is often selected from a large set of possible goals. The decision process dealing with the selection of the goal is called targeting [33] and it aims to evaluate the vulnerabilities of the enemy military, economic, and political systems as well as the effects of damaging or destroying them. Choosing the correct type and amount of ammunition to achieve

the desired effect is known as weaponeering [33]. The planning of the mission considers the costs of successfully completing the mission including weapons and fuel costs as well as possible material and crew losses. The losses are evaluated through assessing the risks involved in the mission. For example, the positions and types of enemy air defenses must be taken into account in such a risk analysis. The actual flight route of the mission is decided based on all available information. This thesis addresses this essential part of air mission planning by introducing a novel approach to the determination of optimal routes. In the following sections, existing approaches to the planning of aircraft routes employed in air missions, i.e., existing methods for solving the MRPP are discussed.

## 2.1 Existing approaches to planning of military aircraft routes

Mission route planning is the process of deciding how an aircraft gets from a starting point to a single or multiple targets and back [37]. Its purpose is to ensure the completion of missions with as little risks and other costs as possible. Traditionally, air force personnel have planned routes manually based on doctrine and experience. Nowadays, different computational methods on aiding the planning of routes by solving the MRPP are utilized (see, e.g., [38]). These approaches are used for solving the optimal route based on given objectives such as the risk of being spotted by enemy radars or material losses (see, e.g., [9, 18]).

The nature of the resulting route plan varies depending on the method used for calculating the route. It can be in the form of providing aircraft controls as a function of time or a set of way points. The methods providing optimal routes can be categorized into three branches depending on how the route planning problem is formulated. If the problem involves only deterministic parameters, optimization based methods are often used (see, e.g., [9], [18]). If the parameters of the problem hold stochastic properties, simulation based methods can be used (see, e.g., [26, 39]). Game theory based methods suit formulations where the modeling of decision making of actors with conflicting goals must be taken into account (see, e.g., [19, 21]). The summary of the methods used for solving the

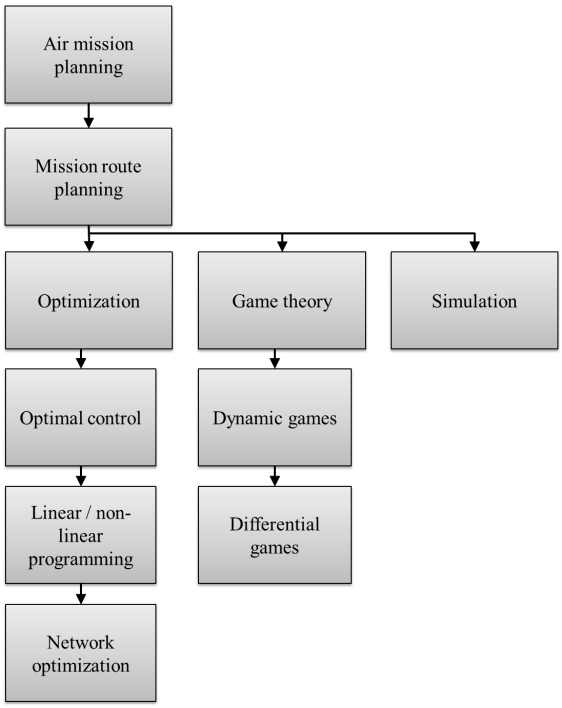


Figure 2.1: Methods for solving the route planning problem.

MRPP is presented in Figure 2.1.

### 2.1.1 Optimal control based approaches

Optimal control theory [40] is used when the MRPP is formulated as a continuous time optimization problem. Using an optimal control formulation, one can determine the route in terms of a control law for the aircraft that transforms the state of the aircraft, i.e., a dynamic system, from its initial state to its final state while minimizing the objective function and satisfying the control and state constraints (see, e.g., [8]). One objective, such as flight time [7] or radar exposure [10], is minimized. The resulting control law gives the optimal control as a function of time leading to the optimal route. In optimal control formulations, aircraft are usually represented as a point mass object with up to three degrees of freedom [41]. The optimal routes are therefore close to flyable in real life. In addition, accurate threat models, such as the effect of the radar cross section of the aircraft to the ability to track the aircraft by a radar, can be applied (see, e.g., [9, 10]). The objective and constraint functions are required to be continuous and smooth, i.e.,

their derivates are continuous functions of the control and state variables. This means that the objective and constraint functions must be approximated with smooth ones if necessary. Discrete time and linear approximations [42] are often used since closed form solutions are rarely found for continuous time and non-linear problems. Therefore, the computational resources needed to solve these problems can be extensive. The problem settings are also limited as realistic objectives and constraints, such as avoiding multiple radars, are hard to formulate and incorporate into the optimization problem. The use of the optimal control theory in route planning is called trajectory optimization [42]. A review of the studies related to trajectory optimization can be found in [43]. In the context of this thesis, trajectory optimization is not suitable as the large number of threats and the long planning horizon result in excessive computational requirements.

### 2.1.2 Mixed integer linear programming based approaches

Mixed integer linear programming (MILP) is a case of linear programming where some of the decision variables can have discrete values instead of continuous ones [5]. Efficient software to solve MILPs, such as CPLEX [44], are widely available. MILP is used in MRPPs where obstacle avoiding is emphasized [12, 45]. On the other hand, the MILP approach with reasonable size enables route planning for more complex missions than optimal control since the required computational effort for solving the problem is smaller. For example, a greater number of actors or threats can be involved. The solution of the MILP formulation is a discrete set of points that reflect the optimal route. However, using discrete decision variables means that the optimization problem is not as accurate as optimal control formulations. Because solving a large MILP problem can take considerable time, the MRPP under consideration is usually solved in smaller parts. An optimal subroute is sought within some planning horizon that is usually far less than the total length of the final route. This means that the globally optimal route is not necessarily found (see, e.g., [46]). While MILP is useful for large scale route planning with multiple actors and goals, the complex dynamics of aircraft and elaborate threat models require large amount of variables and restrictions. For this reason, approaches using MILP formulations do not suit the problem addressed in this thesis.

### 2.1.3 Network optimization based approaches

One of the common methods to solve the MRPP is to use network optimization [5] and formulate the problem as a shortest path problem [47] or a travelling salesman problem [48]. Compared to MILP, network optimization formulations are purely combinatorial problems [49]. When applying network optimization for the MRPP, a grid of nodes representing the possible way points is formed. The solution is a sequence of edges between the nodes that minimize the cost attached to them. Multiple objectives as well as constraints can also be taken into account. The performance of the aircraft dictates the structure of the network, i.e., the edges between the nodes that reflect the possible flying segments. Additionally, turning constraints can be introduced to avoid unrealistic routes [18]. Edge costs, such as fuel consumption, radar detection probabilities or obstacles are easy to implement but their modeling accuracy is dependent on the structure of the network.

In general, network optimization suits complex missions better than optimal control or MILP approaches as adding more costs, e.g., threats, do not add to the complexity of the formulation. Using efficient shortest path and other network algorithms [50], MRPPs can be solved faster than the other formulations and the solution time is not affected by the complexity or the number of objective costs of the problem. Network optimization suits well to the MRPP considered in this thesis as the number of threats can be significant and long flight distances are considered. A grid of nodes adequately represents the possible waypoints of the aircraft, and unnecessarily detailed flying mechanics can be omitted which enables the calculation of optimal routes promptly. The symmetry of the grid also lowers the computational effort when calculating the objective costs. Examples of network optimization formulations for the MRPP can be found in [3, 17, 2, 10, 18].

### 2.1.4 Game theory based approaches

Optimization approaches discussed above consider the MRPP as a one-sided optimization problem. In the cases where the behavior of an opposing actor is dependent on the actions of the friendly aircraft, game theory [51] can be applied. Game theory formulations are utilized in route planning when two adversaries

with conflicting interests are studied (see, e.g., [19, 20]). In a game, the outcome of an action, e.g., the move of an aircraft in some direction, depends also on the counterpart's action. Two different types of games are considered in route planning depending on the problem setting. Differential games, where usually two actors try to control the states of a dynamic system such that the outcomes of the actors are maximized, are used in pursuit-evasion situations [52, 53]. Such situations are, e.g., aircraft evading a missile [54] or an enemy aircraft [41]. The solution of these games is in the form of the time depended optimal control for each actor. Aircraft and threats can be represented as in the optimal control approach. Dynamic game [55] formulations are used in more complex route planning where multiple actors are involved. For example, whole air operations with multiple attackers and defenders can be treated (see, e.g., [21, 22]). In dynamic games, the solution is a sequence of actions similar to the MILP approach. While game theory allows the analysis of decision making for multiple actors, the evaluation of the outcomes of the possible series of actions, can be demanding. The solution times for game formulations are usually much longer than in the optimization formulations. In the case of the dynamic games, the solution time can be shortened by limiting the number of actions to be considered by setting a planning horizon that is shorter than the entire planning horizon of the route planning problem. Similar to MILP approaches with the same modification, the global optimum might not be reached. The usability of the results achieved with game formulations can be challenging due to the assumptions associated with them. The optimal actions are based on the assumptions of the opponent's behavior which might be difficult to predict. Therefore, the game formulations do not give as transparent solutions to the MRPP as the optimization approaches. Because the interaction of the decision making of the actors is not taken into account in the MRPP considered in this thesis, game theory based approaches are unnecessarily complex to be used for determining optimal routes.

### 2.1.5 Simulation based approaches

Simulation e.g. [6]) is applied to MRPPs when the problem setting is too complex to handle with other methods. This is the case when the number of decision variables associated with the actions of multiple actors is large or the setting has

stochastic elements. Simulation allows accurate models for aircraft and threats including realistic representations of flight mechanics and avionics systems. In addition, decision making for a large number of actors can be treated (see, e.g., [25, 56]). Because a simulation model transforms its input parameters to its outputs according to the simulation logic, optimization in the traditional sense is not possible. Therefore, simulation suits studies where the number of the possible input parameters is limited and their effects on the output are analyzed. For example, the optimal values of the inputs maximizing the values of the outputs could be identified. Using simulation in this context is called simulation-optimization (e.g., [57]). The computational effort of simulation-optimization greatly depends on the complexity of the simulation model. The issue is that the simulation has to be run several times if the number of the values of the inputs is large. In addition, in the presence of uncertainty, achieving desirable accuracy in the estimation of the outputs increases the number of simulations. In the MRPP discussed in this thesis, the number of the inputs dealing with the movements of the aircraft is large. Thus, the time to execute simulations would exceed reasonable limits and the MRPP at hand is not feasible to solve using simulation-optimization.

### 2.1.6 Software

Various software have been developed to aid the planning of air missions (e.g., [58]). Some software evaluate the costs such as the threats and fuel consumption, of routes planned manually [59, 60]. Other software tools provide routes automatically, e.g., using network optimization, based on inputs such as threats and aircraft models [61, 62, 63, 64]. There are also software that calculate optimal trajectories for rockets and aircraft as well as aircraft and missiles in pursue and evasion settings using the optimal control theory [7, 65, 66, 67, 68, 69]. However, all these software focus on certain specific aspects of the MRPP. In addition, most of the existing software require that the DM is well trained and dedicated to use them. In this vein, the goal of this thesis is to develop a tool that solves optimal routes for MRPP promptly and with little orientation of the DM as well as takes into consideration the various costs and threats related to flying the route. As a result, this thesis introduces a software suite named SARSS that solves MRPPs fast and with little effort.

# Chapter 3

# Multi-objective network optimization

Network optimization has wide ranging applications in, e.g., operations research [70], biology [71], telecommunications [72], economics [73], and sociology [74]. Network optimization is a part of graph theory [75] that was conceived in the 18th century by Euler with his famous Seven Bridges of Konigsberg problem [76]. It is used to study graphs that represent relations between discrete objects. Network optimization provides means to solve, for example, shortest path, max-flow, assignment, transportation, and travelling salesman problems. In military applications, network optimization has been used in, e.g., aircraft route planning [18], resource allocation [77], and career planning of personnel [78].

A weighted graph, i.e., the relations between the objects representing, e.g., lengths, costs, or capacity is called a network. A network, denoted with $G(V, E)$, consists of nodes $V_i \in V$ and their connections to each other that are called edges $(i, j) \in E$. A network is directed if the cost $c_{ij}$ of moving between nodes $V_i$ and $V_j$ depends on the direction of the movement. MRPPs discussed in this thesis mainly deal with directed networks as the costs, e.g., the fuel consumption of an aircraft, differ whether the aircraft is ascending or descending.

Simple networks can be visualized as two-dimensional drawings such as the one in Figure 3.1. The nodes can represent, e.g., points in space and the edges possible movements with corresponding distances between the nodes. A network can also

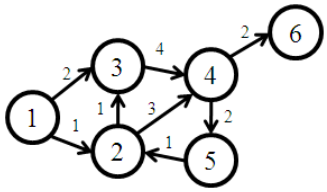


Figure 3.1: Example network.

be represented as an adjacency list which is a list of nodes that are connected to each other with edges. Software implementations usually use adjacency matrices, i.e., matrix representations of adjacency lists, because they are easy to manipulate and store in memory. In the adjacency matrix, the element $A_{ij}$ represents the cost of travelling from node $V_i$ to node $V_j$. The adjacency matrix of the example network presented in Figure 3.1 is

$$A = \begin{pmatrix} 0 & 1 & 2 & 0 & 0 & 0 \\ 0 & 0 & 1 & 3 & 0 & 0 \\ 0 & 0 & 0 & 4 & 0 & 0 \\ 0 & 0 & 0 & 0 & 2 & 2 \\ 0 & 1 & 0 & 0 & 0 & 0 \\ 0 & 0 & 0 & 0 & 0 & 0 \end{pmatrix}. \tag{3.1}$$

In the following sections, single and multi-objective shortest path problems with their solution methods are discussed. In addition, the weighting of the objective related costs of the multi-objective shortest path problem is discussed.

## 3.1 Single-objective shortest path problem

The single-objective shortest path problem (SPP) is a classical optimization problem where the object is to find a sequence of edges, i.e., a path between two given nodes in a network, that minimizes the sum of the costs associated with the edges of the path [79]. This problem is also called the single-pair shortest path problem. There are numerous versions of the shortest path problem depending on what kind of shortest path is sought. For example, in the travelling salesman

problem [80, 81], the goal is to minimize the travelled distance while visiting all the nodes of the network exactly once. Applications of the shortest path problem also include finding optimal routes in traffic networks [82] and least congested paths in communication networks [83] where the edges of the network represent driving distances or delay times. The shortest path formulations have also been used to identify associations in criminal networks [84].

The shortest path problem is formulated as follows: For a network $G(V, E)$ with nodes $V_i \in V$ and edges $(i, j) \in E$ associated with costs $c_{ij}$ , the length of a path $P$ is

$$\sum_{(i,j)\in E} c_{ij}x_{ij}, \tag{3.2}$$

where

$$x_{ij} = \begin{cases} 1 & \text{if } (i,j) \in P, \\ 0 & \text{otherwise.} \end{cases} \tag{3.3}$$

The shortest path problem is to find the set of edges $(i, j) \in E$ such that

$$\begin{aligned} \min \sum_{(i,j)\in E} c_{ij}x_{ij} & \\ \text{s.t.} \sum_{\{j|(i,j)\in E\}} x_{ij} - \sum_{\{j|(i,j)\in E\}} x_{ji} &= \begin{cases} 1 & \text{if } i = s, \\ -1 & \text{if } i = t, \\ 0 & \text{otherwise.} \end{cases} \\ x_{ij} \in \{0,1\} \; \forall \; (i,j) \in E, & \end{aligned} \tag{3.4}$$

where $s$ is the source node and $t$ the destination node of the path. In other words, the path from node $s$ to node $t$ minimizing the cost of the edges is determined.

The generalizations of the problem are the single-pair shortest path problem described above, the single-source shortest path problem, the single-destination

shortest path problem, and the all-pair shortest path problem [5]. In these cases, the goal is to find the shortest paths from a source node to a destination node, the shortest path from a source node to all the other nodes, the shortest path from all the other nodes to a single destination node, and all shortest paths between all the nodes in the network, respectively.

### 3.1.1 Solution methods

A great amount of research has been carried out to develop efficient algorithms to solve alternative versions of the shortest path problem. Dijkstra's algorithm [28] based on dynamic programming [85], is probably the best known. It is used for solving the single-source shortest path problem and can be used to solve the single-pair shortest path problem by terminating the algorithm once the destination node is reached. Using the big O notation (see, e.g., [86]), the original Dijkstra's algorithm runs in $O(|E|^2)$, i.e., the solution time is related to the number of the edges squared. Another widely used algorithm for solving the shortest path is the A* search algorithm [87]. A* search is based on Dijkstra's algorithm and uses heuristics to shorten the solution time. Performance of the proposed shortest path algorithms, that enumerate all the possible paths, have been compared in [88, 89]. Evolutionary algorithms have also been proposed to solve the single-pair shortest path problems (see, e.g., [90, 91]). Evolutionary algorithms suit cases where enumeration of the paths is not feasible due to computational constraints. On the other hand, optimality of the achieved path is not guaranteed.

Dijkstra's algorithm and its modifications are readily available in many software libraries. The algorithm solves the single-source problem discussed in Section 3.1 for a network with nonnegative edge costs. A modification of Dijkstra's algorithm [29] is the fastest known single-source shortest path algorithm that runs in $O(|V|) + |V|log|V|)$. Steps of the algorithm are summarized in Table 3.1.

For the example network, shown in Figure 3.2, the steps of the algorithm are presented in Table 3.2. The shortest path from node 1 to node 5 is 17 units in length and goes through nodes 1, 3, 6, and 5. The illustration of the algorithm for solving the example network is depicted in Figure 3.3.

Table 3.1: Steps of Dijkstra's algorithm.

| |
|---|
| **Step 1**<br>Set the distance, i.e., the label, for all nodes: zero for the initial node and infinity for all the other ones. Set the initial node as the current node. |
| **Step 2**<br>Set all nodes as unvisited. |
| **Step 3**<br>Calculate distances to all unvisited nodes connected to the current node as the label of the current node plus the length of the edge from the current node to the node in question. If the distance is less than the label of the node, overwrite it with the smaller distance. |
| **Step 4**<br>When distances to all neighboring unvisited nodes have been updated, mark the current node as visited. |
| **Step 5**<br>Select the next current node as the unvisited node with the smallest distance from the current node. |
| **Step 6**<br>If all nodes are visited, finish. Otherwise go to Step 3. If the shortest path to a specific destination node is to be determined, finish when the destination node becomes the current node. The resulting labels of the nodes depict the distances of the shortest paths from the source node. |

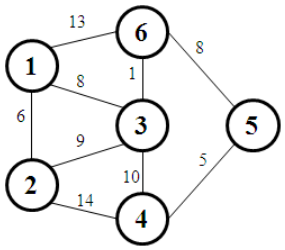


Figure 3.2: Example network solved with Dijkstra's algorithm.

Table 3.2: Example illustrating Dijkstra's algorithm.

| Iteration # | Candidate list $V$ | Node labels | Node out of $V$ |
|---|---|---|---|
| 1 | {1} | ( 0, ∞, ∞, ∞, ∞, ∞) | 1 |
| 2 | {2,3,6} | ( 0, 6, 8, ∞, ∞, 13) | 2 |
| 3 | {3,4} | ( 0, 6, 8, 20, ∞, 13) | 3 |
| 4 | {4,6} | ( 0, 6, 8, 18, ∞, 9) | 6 |
| 4 | {5} | ( 0, 6, 8, 18, 17, 9) | - |

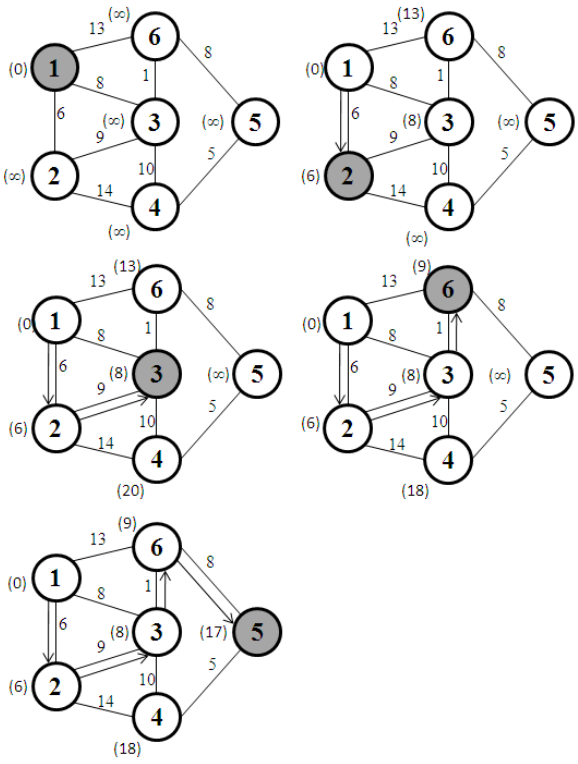


Figure 3.3: Progress of Dijkstra's algorithm when solving the example network.

## 3.2 Multi-objective shortest path problem

In a multi-objective shortest path problem (MSPP), several types of costs related to the objectives are associated with each edge of the network [92]. The optimal path is determined with respect to all the objectives. The MSPP is formulated as

$$\begin{aligned} &\min \left[\sum_{(i,j)\in E} c_{ij}^1 x_{ij}, ..., \sum_{(i,j)\in E} c_{ij}^k x_{ij}, ..., \sum_{(i,j)\in E} c_{ij}^M x_{ij}\right] \\ &\text{s.t.} \sum_{\{j|(i,j)\in E\}} x_{ij} - \sum_{\{j|(i,j)\in E\}} x_{ji} = \begin{cases} 1 & \text{if } i = s, \\ -1 & \text{if } i = t, \\ 0 & \text{otherwise.} \end{cases} \\ &x_{ij} \in \{0,1\} \; \forall \; (i,j) \in E, \end{aligned} \tag{3.5}$$

where $c_{ij}^k, k = 1, ..., M$ represent the costs associated with different objectives, $M$ is the number of the objectives, and $s$ and $t$ denote the source and destination nodes.

The goal is to find efficient, i.e., non-dominated, paths as the solutions to the problem 3.5 because such a path that is optimal in terms of all objectives does not usually exist. This is especially true when the objectives are conflicting. In general, a solution for a multi-objective optimization problem is non-dominated if no other solutions exist that are a better one with respect to all the objectives, i.e.,

$$\nexists \; x' \in X \; s.t. \; f_k(x') \geq f_k(x) \; \forall \; k = 1, ..., M, \tag{3.6}$$

where at least one of the inequalities is strict and $X$ refers to the set of feasible paths. In the case of MSPP (3.5), $x$ is a feasible path, i.e., it fulfills the constraints (3.5), and the cost function $f_k$ is the sum of the edge costs corresponding to the objective $k$, i.e., $f_k = \sum_{(i,j)\in E} c_{ij}^k x_{ij}$. An illustration of the set of efficient paths in the case of two objectives is depicted in Figure 3.4.

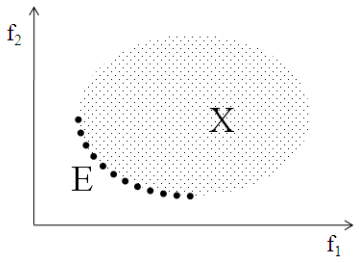


Figure 3.4: $E$ (black dots) denote the set of efficient paths, $X$ (grey dots) the set of feasible paths, and $f_1$ and $f_2$ the value of the path in terms of the objectives, respectively

### 3.2.1 Solution methods

Approaches for solving the multi-objective optimization problem are classified into three methods based on the way the preference information of the DM is utilized [93]. This classification also applies for the MSPP. Here, the preference information refers to the DM's view on how important the objective related costs are with respect to each other. The information is used to form the weights $w^k$ of the objective costs in Equation (3.7). The first method, called *a priori* method, aims to solve a single efficient path using an aggregate objective function that is determined as, e.g., a weighted sum of cost functions $f_k$ associated with the objectives [94]. The second method, called *a posteriori* method, solves all the efficient paths of the problem, or a sufficient approximation of these paths if the set of efficient paths is too large to enumerate, and then lets the DM choose the preferred path. The third approach, called the interactive method, generates one efficient path at a time according to the weights, i.e., the DM revises the weights as more solutions are generated. The solution method can be selected on the basis of how large the set of feasible paths is. If there are only few feasible paths, it is convenient to calculate all the efficient paths. On the other hand, if the number of possible solutions is large such that all the paths cannot be calculated in reasonable time, *a priori* and interactive methods might be more appealing. Classification and characteristics of some solution methods of the MSPP are reviewed in [95].

#### 3.2.1.1 *a priori* method

In the *a priori* method, the preference information related to the costs is elicited from the DM before the generation of efficient paths. Relative importances between the costs are used to assign a non-negative weight $w^k$ ($w^k \in \mathbb{R}_{\geq 0}$) to each objective $k$. Then, the MSPP is reduced to a single-objective SPP by forming an aggregate objective function as a weighted sum of the objective functions that is minimized.

Using the weights $w^k$, the MSPP (3.5) is converted into the following single-objective SPP:

$$\begin{aligned} &\min \textstyle\sum_{k=1}^{N} \sum_{(i,j)\in E} w^k c_{ij}^k x_{ij} \\ &\text{s.t.} \textstyle\sum_{j|(i,j)\in E} x_{ij} - \sum_{j|(i,j)\in E} x_{ji} = \begin{cases} 1 & \text{if } i = s, \\ -1 & \text{if } i = t, \\ 0 & \text{otherwise.} \end{cases} \\ &x_{ij} \in \{0,1\} \; \forall \; (i,j) \in E. \end{aligned} \tag{3.7}$$

The use of the *a priori* method requires that the preference information is available before the optimization so that the weights $w^k$ can be determined. Often, this is not the case as the elicitation of the preference information, that defines the weights, can be complicated. Comparing objective costs that are not intuitively comparable can be difficult. Furthermore, the magnitudes of the objective costs are not known beforehand.

#### 3.2.1.2 *a posteriori* method

In the *a posteriori* method, preference information on the objective costs is not needed prior to the optimization because the whole set of efficient paths is calculated. This is done by enumerating all the feasible paths and selecting the set of efficient paths as the paths that are not dominated. Then, the DM is given the choice of choosing the preferred path. In the case that the number of feasi-

ble paths is too large to enumerate, sufficient number of paths is generated and paths that are not dominated are selected to form an approximation for the set of efficient paths.

After the set of efficient paths has been generated, the DM still has to choose the preferred path. The preference information of the DM is needed, much like in the *a priori* method. However, as all the possible levels of the costs are now known, the preference information is easier to acquire, e.g., using multi-criteria decision analysis (e.g., [96, 97]) techniques.

#### 3.2.1.3 Interactive method

When preference information about objectives is not available or the set of efficient paths or an adequate approximation of it cannot be calculated, an alternative approach is needed to acquire a solution in feasible time. This can be achieved by eliciting the preference information of the DM interactively. Interactive methods commonly present an initial solution or a set of solutions from the efficient set to the DM to choose from. The DM then decides if the solution is acceptable. If not, the preference information is updated until a satisfying solution is found. When updating the preference information at each iteration, the DM learns what kinds of paths are attainable. The steps of a general interactive method [98] are presented in Table 3.3.

The interactive methods can be classified into three branches depending on the type of preference information used [98]. These are methods based on trade-off information, reference points, and classification of objective functions. In methods based on trade-off information, the DM is asked two types of trade-off questions. In the first case, the DM is presented with several trade-offs between the objective costs and he has to decide whether the trade-offs are desirable, undesirable or indifferent (see, e.g., [99]). In the second case, the DM is asked for straight comparisons on how much of loss in one objective he is willing to give up to gain some amount of gain in another objective (see, e.g., [100]). Based on the information gathered from these questions, a new efficient path is generated. In the reference point based methods, the DM is asked to specify a reference point consisting of desired values for each objective related cost at every iteration (see,

Table 3.3: Steps of a general interactive method.

| |
|---|
| **Step 1** |
| Initialize, e.g., calculate the highest and lowest values of each objective cost and present them to the DM. |
| **Step 2** |
| Generate an efficient path as a starting point with, e.g., even weights of the objective costs or use a path given by the DM. |
| **Step 3** |
| Ask for preference information from the DM, e.g., which objective cost or costs should be lower. |
| **Step 4** |
| Generate one or more new efficient paths according to the preference information given in step 3. |
| **Step 5** |
| If several paths are generated, ask the DM to choose the most preferred one. |
| **Step 6** |
| Stop if the DM is satisfied with the preferred path. Otherwise, go to step 3. |

e.g., [101]). Corresponding efficient paths are then calculated and presented to the DM. In the classification based methods, the DM is asked which objective related costs could improve and which worsen from their current values (see, e.g., [102]). Additionally, desirable amounts of improvements and tolerable amounts of impairments may be asked. Again, based on the given information, a new efficient path is generated.

### 3.2.2 Interpretation of weights of objectives

When applying the weighted sum method discussed in Section 3.2.1 to solve the MSPP (3.7), the question is how to determine the weights of the objective costs in order to generate efficient paths that reflect the preferences of the DM. The weights are generally seen as the relative measures of importance between the objectives costs. However, this is only true when the magnitudes of the objective costs are the same [103]. In this special case, the *a priori* methods provide efficient paths where the weights represent the relative importance between the objective costs. If the magnitudes of the objective costs differ and a common unit to measure the costs cannot be selected, the meaning of the weights becomes unclear. This is usually the case in MSPPs.

One possibility to choose the weights is to use the weighted sum simply as a mathematical tool to produce efficient paths. Every combination of the weights corresponds to an efficient path when $w^k \geq 0, \forall k$ [94]. Evaluating the sum with different weights, the whole set of efficient solutions or an approximation of it can be calculated. Then, the DM chooses the solution that satisfies his preferences as in the *a posteriori* method. However, using the weighted sum in this way does not give the weights any interpretation. Generating efficient paths by systematically varying the weights of the objective costs has several deficiencies. First, even if the weights are varied consistently, the resulting set of efficient paths is not guaranteed to be evenly spaced over the actual set of efficient paths [104]. Viable efficient paths might be left undiscovered. For example, if the absolute value ranges of the objective costs differ greatly, the objective that systematically has larger costs tends to dominate the other objectives no matter how small weight it is assigned. Secondly, even if all the possible combinations of the weights are evaluated, the resulting paths do not include the possible non-convex parts of the

set of efficient paths [105]. Finally, the set of efficient solutions can be too large and it cannot be generated in feasible time. These shortcomings are discussed in detail in [106].

If the weights are interpreted as representing trade-offs between the objective costs (e.g., [27]), the different magnitudes of the costs do not have an effect on the interpretation. When trade-offs between the objective costs are used to form the weights, two equally preferred paths are constructed at a time. This statement implies the trade-off the DM is willing to make between the objective costs. The statements are usually generated by asking the DM how large an increase ($x_i^\circ \rightarrow x_i^*$) of the objective cost $x_i$ the DM is willing to trade to a predetermined decrease ($x_j^* \rightarrow x_j^\circ$) of the objective cost $x_j$ when other objective costs stay the same. An example of such a trade-off statement is

$$(x_1, x_2, ..., x_i^\circ, x_j^*, ..., x_n) \sim (x_1, x_2, ..., x_i^*, x_j^\circ, ..., x_n), \tag{3.8}$$

where $\sim$ refers to equal preference. The ratio between the two weights of the objective costs is determined as the ratio between the value ranges of the increase and the decrease of the objective costs in the statement, i.e.,

$$w^i(x_i^* - x_i^\circ) = w^j(x_j^* - x_j^\circ) \Rightarrow \frac{w^i}{w^j} = \frac{x_j^* - x_j^\circ}{x_i^* - x_i^\circ}. \tag{3.9}$$

If there are $n$ objective costs, $n-1$ comparisons between the costs form a system of equalities and the weight ratios between all the objective costs can be solved [107]. It should be noted that only the relative values of the weights is needed which gives the DM the freedom to choose the absolute values of the weights as any nonnegative numbers.

There are also methods for generating the set of efficient paths that overcome the issues of the weighted sum method. These methods include physical programming [108], normal boundary intersection [109], normal constraint [110], and compromise programming [111]. These methods can, e.g., produce the paths that lie in the non-convex parts of the set of efficient paths. In addition, there are methods providing an approximation for the set of efficient paths. Simulated annealing

[112], evolutionary algorithms [4, 113, 114], ant colony optimization [115], and particle swarm optimization [116] have been successfully applied to the solution of multi-objective shortest path problems.

# Chapter 4

# The approach to the automated solution of the mission route planning problem (MRPP)

This chapter presents the approach to the automated solution of MRPP. The approach consists of optimization (Section 4.2) and simulation (Section 4.3) models that are used to solve and evaluate the optimal route. In the optimization model, the MRPP is formulated as a MSPP discussed in Chapter 3. The simulation model is used to evaluate the optimal route with continuous time deterministic simulation. The procedure of determining the solution to the MRPP with the above models is described in Section 4.4. The procedure consists of parameterization, optimization and simulation phases, and it results in the optimal route as the solution of the MRPP.

## 4.1 Description of MRPP

In a MRPP, two opposing forces, Blue and Red, are taken into account. The goal of the Blue force is to find an optimal route within the area of operations from a friendly base to the launch point of an air-to-ground (A/G) weapon and back to a base. The optimal route minimizes the exposure to the threats posed

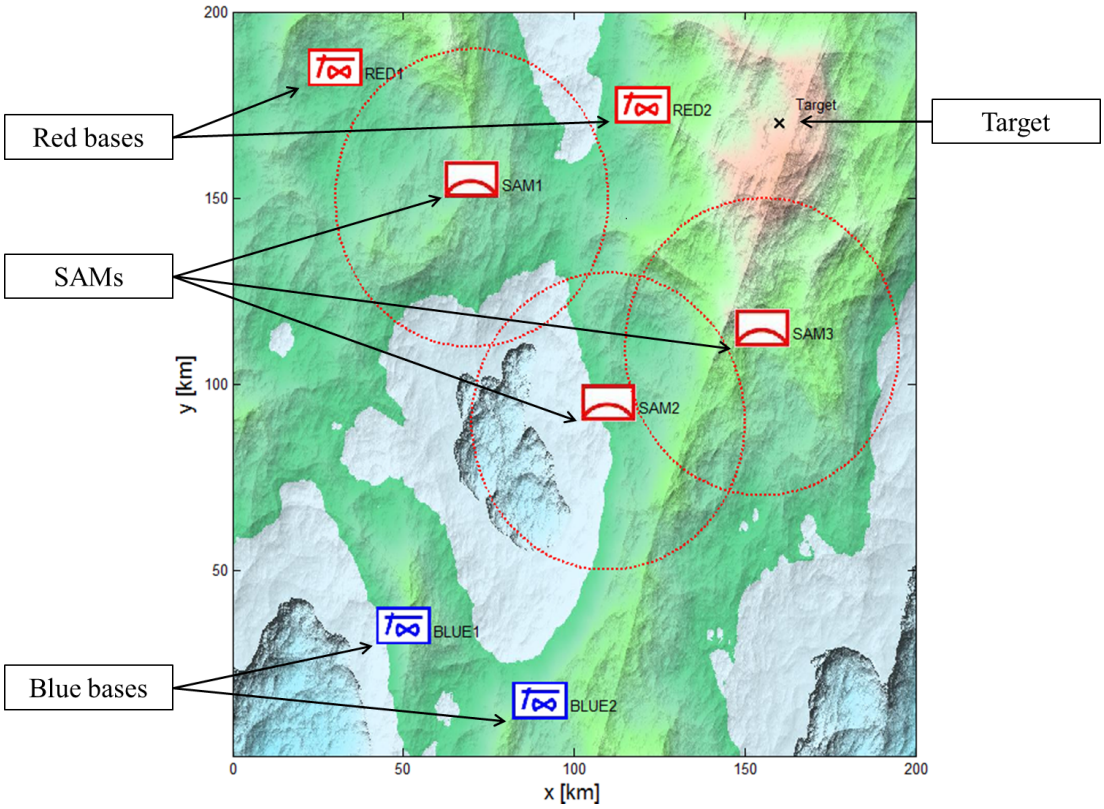


Figure 4.1: Example A/G mission.

by the Red force as well as the flight distance and the consumption of fuel. The threats consist of the possibility of the Blue aircraft being shot down by Red surface-to-air (S/A) and air-to-air (A/A) weapons. The S/A weapons include Red surface-to-air missiles (SAM) and anti-aircraft artillery (AAA) while the A/A weapons are deployed by the Red defensive counterair aircraft that try to intercept the Blue aircraft. The MRPP includes the determination of the optimal route, the selection of the optimal bases where the mission starts from and ends as well as the selection of the optimal A/G weapon and its launch point.

An example MRPP is depicted in Figure 4.1. The Blue bases are shown in the bottom left of the figure and the Red bases in the top of the figure. The Red SAMs are denoted with SAM1-3. The dotted circles represent the maximum ranges of the weapon systems. The target is located in the upper right corner of the area of operations and it is denoted with an $X$.

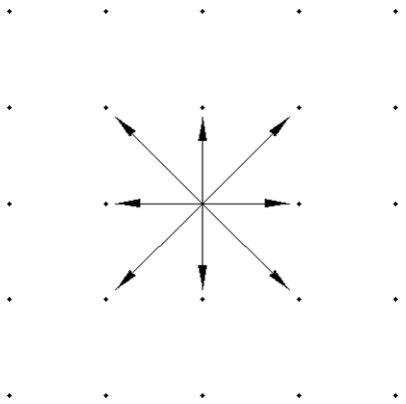

Figure 4.2: Horizontal movements.

## 4.2 Optimization model for MRPP

### 4.2.1 Structure of optimization network

The area of operations is depicted as the three-dimensional lattice of nodes that represent the possible points between which the aircraft can move. Together with the edges that represent the possible flying segments between the nodes, they form the network of the optimization model. The dimensions of the area of operations are set to reflect the combat radius as well as the minimum flight altitude and the service ceiling of the aircraft. On the horizontal plane, the nodes are evenly spaced and the distance between the nodes is selected to best suit the performance of the aircraft or the accuracy of the route. The movements on the horizontal plane are depicted in Figure 4.2.

The vertical spacing of the nodes depends on the ascending and descending capabilities of the aircraft. The altitude between consecutive planar lattices determines the smallest ascent and descent angles defined for the aircraft when moving to a neighboring node. The aircraft is allowed to move through more than one planar lattice at once. Therefore, the maximum descent and ascent angles of the aircraft have to be known in order to connect the right amount of planar lattices together. The nodes are connected to their nearest neighbors in the same plane and in as many planes below and above so that the maximum angles are taken into account. Movements in the nodes directly under and above the current node are prohibited due to physical constraints. Vertical movements are shown in Fig-

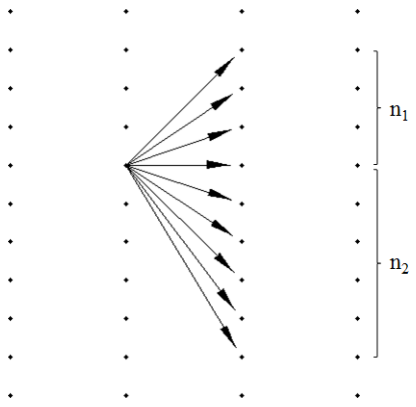


Figure 4.3: Vertical movements. $n_1$ and $n_2$ are the number of planes the aircraft can ascend or descend in one move.

ure 4.3. As the aircraft can descend in a greater angle than ascend, there are usually more downward than upward edges.

Allowing the aircraft move through multiple horizontal planes between neighboring nodes requires that the maximum descent and ascent angles of an aircraft at different altitudes are known (see, Figure 4.4). Typically, the higher the aircraft is flying, the less its maximum sustainable ascent angle is. The edges exceeding these angles are removed from the network to avoid unrealistic routes. Multiple upward and downward edges lead to more realistic flight routes as the optimal ascent and descent angles can be selected. It also enables more complex routes that take better into account the dead zone of the ascending radar horizon of a S/A weapon system. The aircraft can make steep dives and climbs which enables maneuvering below the reach of an S/A threat or achieving altitude required to launch a A/G weapon. These kinds of maneuvers are typical for a general high-low-low-high profile of an A/G mission [117] presented in Figure 4.5 where ingress and egress are conducted at higher altitudes to save fuel and the attack and withdrawal phases at lower altitudes to avoid radar detection and S/A threats.

The aircraft uses a fuel efficient airspeed of Mach 0.84 in the optimization network. In the case of the constant Mach number as airspeed, the corresponding ground speed is different in various altitudes. Mach 1 at ground level is approximately 662 knots as in 50,000 feet it is 574 knots. The ground speed of the aircraft is needed in the calculation of the flight time of the optimal route as well as in the simulation of the threats.

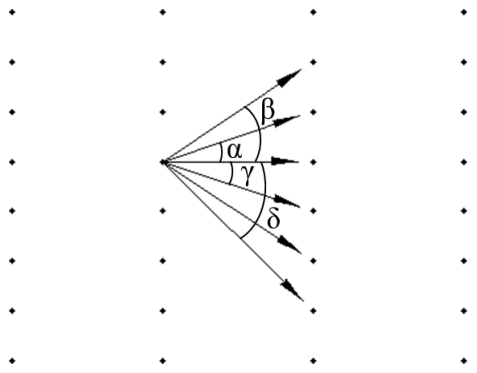


Figure 4.4: Minimum and maximum ascent and descent angles $\alpha$, $\beta$, $\gamma$ and $\delta$.

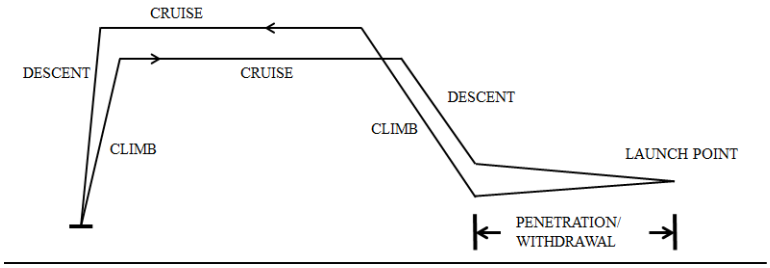


Figure 4.5: High-low-low-high mission profile.

The optimal initial and terminal bases for the mission as well as the optimal launch point are determined by inserting two dummy nodes into the network. The first dummy node is connected to all the Blue bases and the second one to all the possible launch points. The edges that originate from an end to the dummy nodes are assigned equal costs. For the attack route, the first dummy node is used as a source node for the shortest path problem and the second dummy node is used as a destination node. When the optimal route is determined, it automatically includes the optimal initial base as well as the optimal launch point. For the return route, the optimal launch point is used as a source node and the first dummy node is used as a destination node. Again, the optimal route automatically includes the optimal terminal base. The dummy nodes and their connections are depicted in Figure 4.6.

To summarize, the parameters of the network are

- Width, depth, and height of the network
- Minimum and maximum flight altitude
- Spacing of nodes in horizontal direction

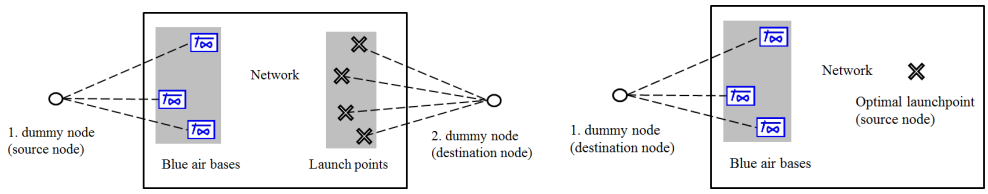


(a) Attack route. (b) Return route.

Figure 4.6: Dummy nodes in attack and return routes.

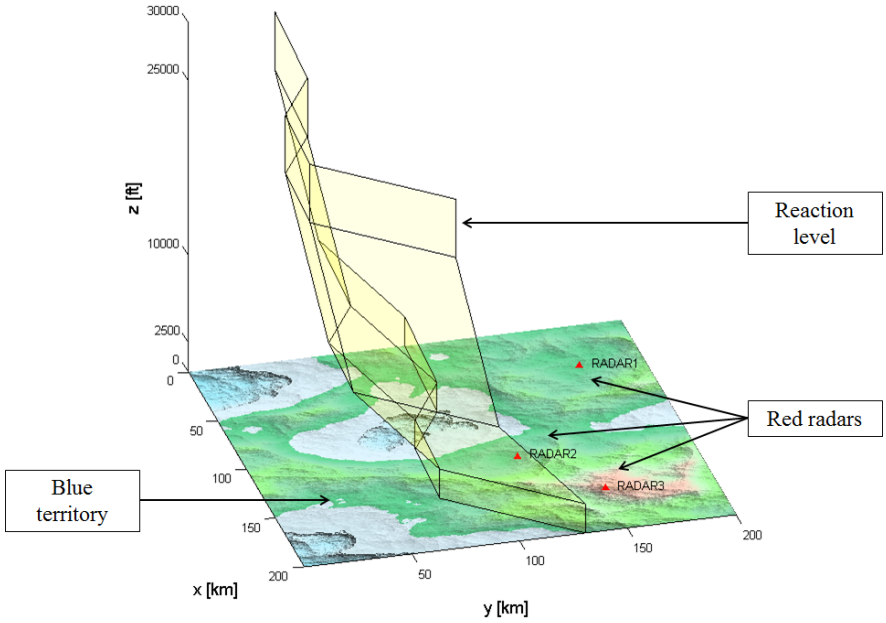


Figure 4.7: Reaction level.

- Minimum and maximum angles of ascent and descent

### 4.2.2 Network constraints

The network of the MRPP is constrained in two ways. First, a reaction level that determines when the Red aircraft, equipped with A/A missiles, are scrambled to intercept the Blue aircraft, is introduced. Second, no-fly zones (NFZ) are defined as parts of the network where flying is restricted.

The basic concept of the reaction level is that the A/A threat, i.e., the Red aircraft, starts to expand uniformly from the Red bases as the Blue aircraft penetrates the reaction level. This level, depicted in Figures 4.7 and 4.8, is derived

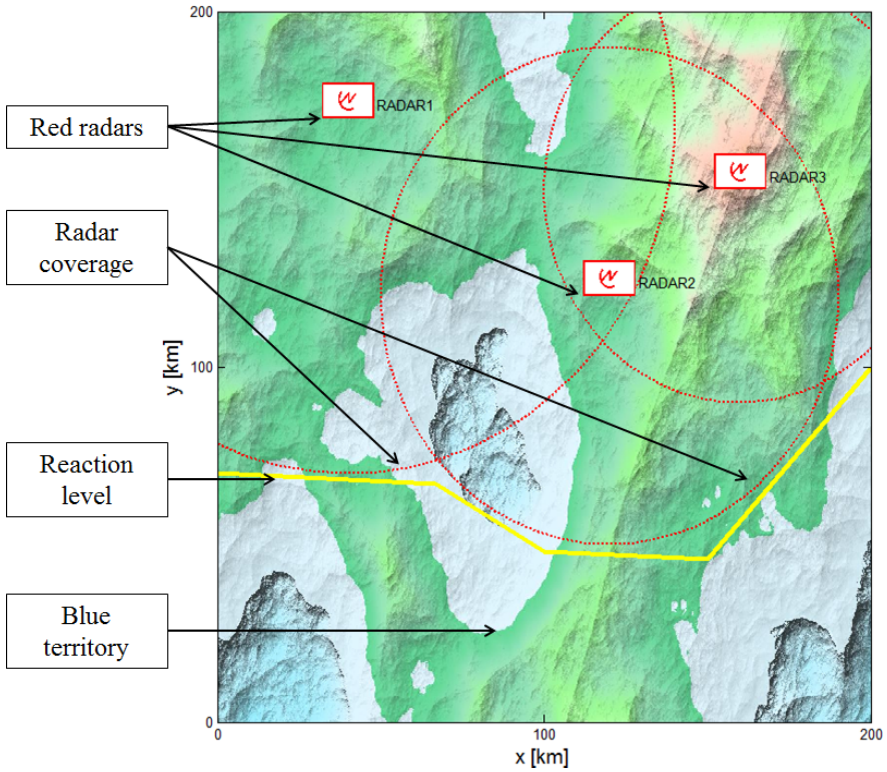


Figure 4.8: Coverage of the radar network.

using the detection capability of the Red radar network at different heights. A cost is incurred in every edge leading from a node the A/A can expand to before the Blue aircraft. Therefore, the A/A threat depends on the point where the reaction level is penetrated as it determines the nodes the Blue aircraft cannot reach before the Red aircraft (see, Figure 4.9). Due to computational restrictions, the reaction level must span opposite sides of the area of operations.

Because the network used for solving the MRPP is static in the way that the costs of the edges cannot be changed during the run of the optimization algorithm, the A/A threat has to be fixed before the optimization. The dynamic nature of the A/A threat is taken into account such that the MRPP is divided into two MSPPs considering the attack and return routes separately. The attack route is defined as the route from a Blue base to a launch point and the return route as the route from the launch point back to a Blue base. The A/A threat is calculated separately for each route.

In order to calculate every possible case of the A/A threat related to the attack

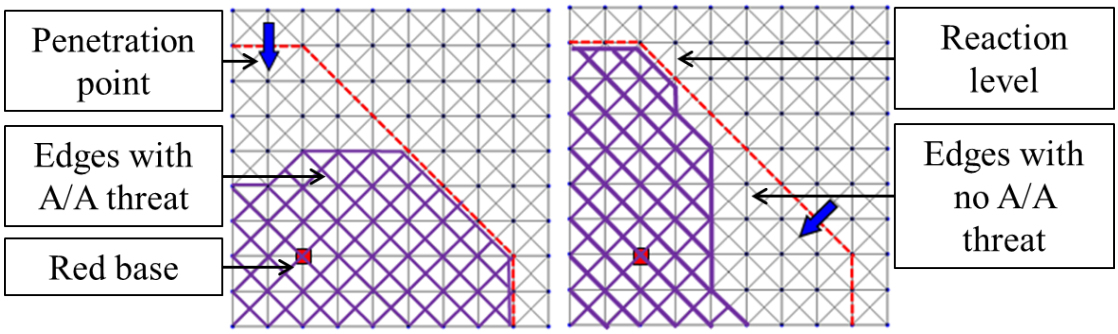


Figure 4.9: A/A threat in the case of different penetration points.

route would mean that the optimization would have to be conducted for every possible penetration point of the reaction level. However, the number of edges that penetrate the reaction level can be large and conducting the optimization through all of them is not feasible. As a compromise, the reaction level is divided into 16 planes in a four-by-four grid. Within each plane, the penetration point is assumed to be at the center of the plane. The flying time to the nodes of the network is then calculated from that point, i.e., the A/A threat is the same for every penetration point within a plane. The optimal attack route is determined by calculating the optimal route through each plane of the reaction level and choosing the one with the least total cost. In this way, 16 cases of the A/A threat for the attack route are considered.

NFZs are areas in which flying is not permitted. The reason could be, e.g., that there are other critical operations carried out in the area. Additionally, the vicinity of a friendly SAM or an AAA is often set as a NFZ to avoid friendly fire. The NFZs are determined by polygons that have minimum and maximum altitudes. Then, edges from the nodes within the polygons are deleted from the network. The NFZs can be set as active during the attack route, the return route or both.

To summarize, the parameters of the network constraints are

- Coordinates of the reaction level
- Coordinates of the NFZs
- Active NFZs for attack and return routes

### 4.2.3 Objectives

The total cost of travelling an edge depends on four kinds of costs: the travelled distance, the consumption of fuel as well as the travelled distance under the influence of the S/A and A/A threats. An adjacency matrix depicting the cost of travelling between the nodes of the optimization network is formed for each objective. The individual costs are explained in detail in following.

#### 4.2.3.1 Travelled distance

The length of an edge is determined as the Euclidean distance between its origin and destination nodes. The length of an edge is also used to calculate the rest of the costs to make them more comparable.

#### 4.2.3.2 Fuel consumption

To be able to fly, an aircraft needs thrust to generate lift to counteract gravity. The aircraft moving through air also induces drag which is an opposite force to the thrust, and the main contributor to the fuel consumption of the aircraft. As the efficiency of a jet engine depends on the density of the air, flight altitude has a significant role in fuel consumption as well.

Accurate modeling of fuel consumption in the MRPP is essential as the mission starts and ends at the ground level. The takeoff and landing trajectories have a significant effect on the overall fuel consumption. In addition, the mission profile often has altitude variations that increase fuel consumption. Fuel consumption is now calculated using the consumption data for a fighter aircraft with full fuel tanks and typical weapons for an A/G mission. While the fuel consumption data is also available in the case that the aircraft is lighter and has less drag, i.e., it has delivered its weapons, it is not now taken into consideration. The rationale is that the calculated return routes would be possible to fly in the situations where, for some reason, the weapons are not released. This guarantees that the aircraft is able to return to a base in either case.

In order to assign realistic fuel consumption to each edge, data where the con-

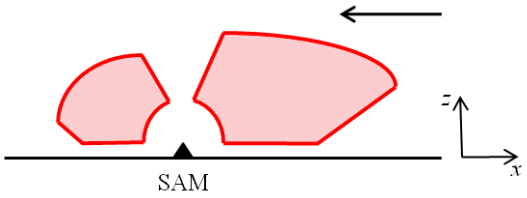


Figure 4.10: Typical LAR of a SAM.

sumption is presented as a function of airspeed, altitude and ascent or descent angle is needed. However, the fuel consumption of an aircraft flying with a typical weapon setting is given as a function of altitude and Mach number. In addition, the consumption of a jet engine at maximum thrust at different altitudes is available. If the maximum ascent angle with the maximum thrust of the aircraft at different altitudes is known, the data can be combined by interpolating between the altitudes and the angles. In the case of fighter jets, maximum ascent angles and fuel consumption with after burner is also required as using it is a viable option in some cases. In this way, realistic fuel consumption can be assigned to each edge in the network. Additionally, taking different maximum ascent angles at different altitudes into account, edges that have too steep angles can be identified and removed from the network.

#### 4.2.3.3 Surface-to-Air threat

The S/A threat is caused by the Red SAMs and AAAs. In the case of an AAA that fires unguided ammunitions, a shape based on the maximum range of the threat adequately represents the area where the Blue aircraft incur a cost. If the threat represents a SAM, the kinematics of the missile and the aircraft should be considered. For example, the SAM reaches the aircraft that is moving towards the launch platform more easily than when the aircraft is moving away. The area, in which the aircraft must be at the time of the launch for the SAM to achieve a successful launch, is called launch acceptability region (LAR) [118]. A typical LAR of a SAM is depicted in Figure 4.10. The area shaded red represents the LAR and the arrow represents the direction in which the target is moving.

In this thesis, the kinematic capability of a missile to reach an aircraft instead of just the capability of a radar to detect it is taken into account. First, the

curvature of the Earth and the curvature of a radar beam that travels through air are taken into consideration when modeling the maximum range of a S/A threat. This results in dead zones that can be exploited by the Blue aircraft. Second, the kinematic capability of the SAM is represented as the LAR of the weapon system.

When the dead zones are taken into account, the part of an edge inside a threat can vary significantly. Therefore, it is important to calculate how much of the edge is inside the threat to accurately describe the cost associated with flying the edge. The part of the edge that is inside the threat is calculated by determining the intersections of the edge and the threat. When the cost is determined like this, the routes containing edges that intersect the threat only a little become viable. The total cost of the SAM and AAA threat is depicted as the distance travelled inside their LARs ($nm_{S/A}$).

A SAM requires that in the early stage of its flight the target is tracked by a tracking radar that communicates the state of the target to the missile [119]. In the case of missiles with a passive homing system, the target is illuminated by the radar so that the sensors of the missile can observe the target. The theoretical maximum range of SAMs is therefore the distance at which the tracking radar can detect and track the target.

For a radar with the antenna height of $h_a$, the minimum altitude of the target that can be detected at distance $r$ is [120]

$$h = \sqrt{r^2 + k_e^2 R^2 + 2rk_e R \sin\theta} - k_e R + h_a. \tag{4.1}$$

Here, $k_e$ is the standard refraction coefficient, $R$ the radius of the Earth, and $\theta$ the angle between the line $t$ parallel to the tangent of the Earth and the minimum angle the antenna can be aligned to. Targets above $h$ can be detected within the maximum range $r$. The minimum detection altitude is illustrated in Figure 4.11.

When the radar beam is presented in Cartesian coordinates, the form of the beam resembles an inverted cone as shown in Figure 4.12. To describe the greater maximum vertical range at small distances, a half sphere is added on the top of the cone.

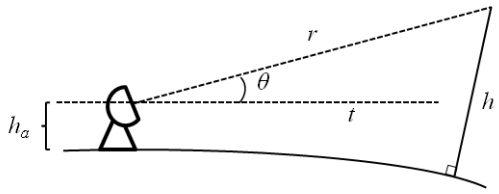


Figure 4.11: Height $h$ of the radar beam at distance $r$.

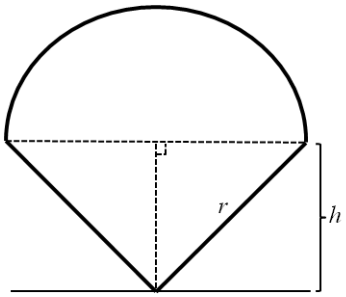


Figure 4.12: Maximum range $r$ of a surface-to-air threat in Cartesian coordinates.

In order to better represent the form of the actual threat presented in Figure 4.10, a distance $r_0$, until which the dead zone of the threat is neglected, is determined. Additionally, a limit $h_{max}$ is set to the vertical range. These modifications are depicted in Figure 4.13.

In the case of a SAM, the threat model based just on radar detection is not adequate as the symmetrical threat in Figure 4.13 does not resemble the real threat of the SAM presented in Figure 4.10. In order to incorporate the kinematic capability of the SAM, the threat should begin sooner when the aircraft is moving towards the threat and also end sooner when the aircraft is moving away from the threat.

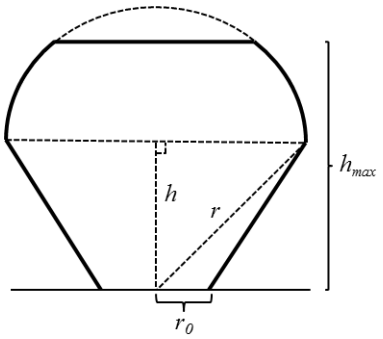


Figure 4.13: Adjustment of the dead zone and the vertical range.

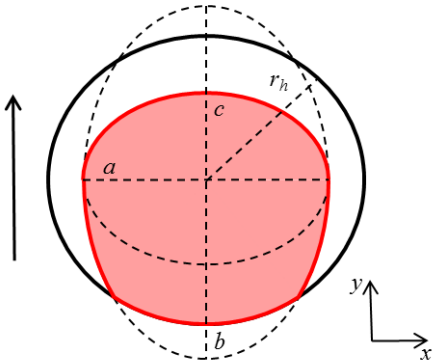


Figure 4.14: Launch acceptability region.

The symmetrical threat is modified to resemble the real threat by setting two partially overlapping ellipses over the cross section of the threat (see, Figure 4.14). The larger of the ellipses forms the threat when the aircraft is moving towards the threat and the smaller one when the aircraft is moving away. Together these half ellipses form the LAR of the SAM represented by the red area in Figure 4.14. The lengths of the axes of the ellipses $a$, $b$, and $c$ are defined relative to the maximum horizontal range $r_h$ of the SAM at the height of the cross section. The arrow represents the direction the aircraft is flying. The close range dead zone is rarely exploited so it is omitted to simplify the calculations. In addition, the LAR calculation is not considered in the case of an AAA as the kinematics of the projectiles can be represented with a maximum range based on the curvature of the Earth.

To summarize, the parameters of the S/A threats are

- Maximum horizontal and vertical range of the missile
- Minimum operating angle of the tracking radar
- Dead zone adjustment parameter
- Height of the tracking radar antenna
- LAR coefficients $a$, $b$, and $c$

#### 4.2.3.4 Air-to-Air threat

The A/A threat represents the threat posed by the Red aircraft equipped with A/A missiles. After the reaction level has been penetrated, the threats start

to expand uniformly from the Red bases, i.e., the Red aircraft are scrambled to intercept the Blue aircraft. The uniform expansion is based on a worst case assumption that the Red aircraft can fly to the optimal interception point without having to chase the Blue aircraft. A reaction time that determines how long after the penetration the threats start to expand can be taken into account. The number of the A/A threats is limited by the number of Red bases, i.e., there is one type of threat in each base. The threats are divided into types that have different expansion speeds and maximum ranges. This reflects the possibility to have different types of aircraft in the bases. The number of aircraft in a base can be set to reflect the magnitude of the threat. The cost of travelling within the extent of the threat is multiplied by this number. The cost of the A/A threat is incurred in every edge that starts from a node the Red aircraft can reach before the Blue aircraft. The amount of the threat is calculated as the distance travelled under its influence, which is denoted with $nm_{A/A}$.

The A/A threat cost for the attack route is calculated as explained in Section 4.2.2. For the return route, the optimal launch point is set as the starting point of the Blue aircraft. Again, the nodes that the Red aircraft can reach before the Blue aircraft are determined as the extent of the threat. However, the time that the Blue aircraft uses to fly from the reaction level to the launch point is reduced from the flying time of the Red aircraft. This reflects the worst case scenario where the Red aircraft could predict that the optimal intersection point is on the return route rather than on the attack route. An example of the extent of the A/A threat on the attack and return routes are shown in Figures 4.15 and 4.16. The area shaded purple denotes the extent of the threat.

To summarize, the parameters of the A/A threats are

- Speed of the Red aircraft
- Reaction time
- Number of aircraft in the base

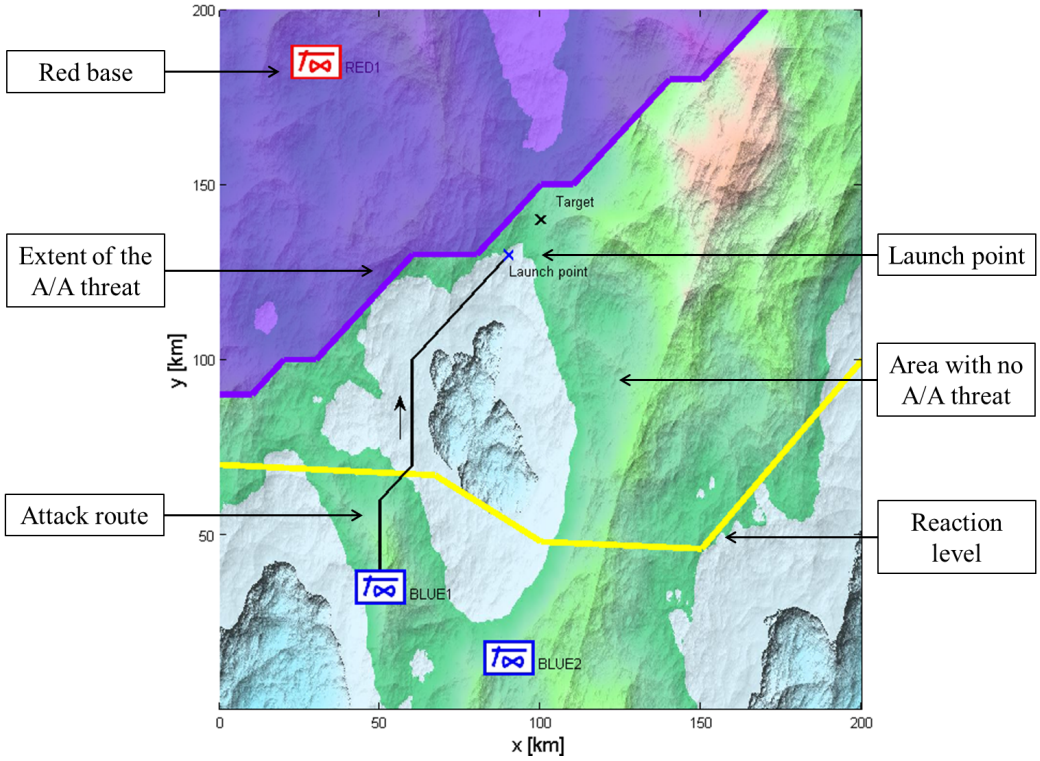


Figure 4.15: A/A threat on the attack route.

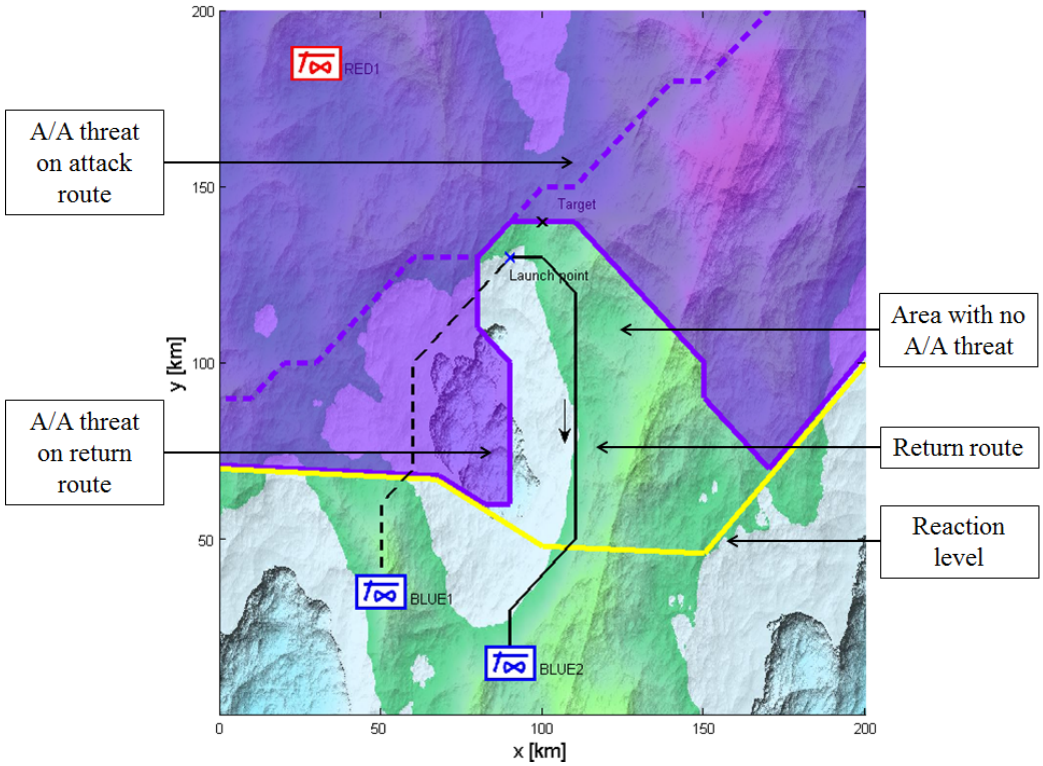


Figure 4.16: A/A threat on the return route.

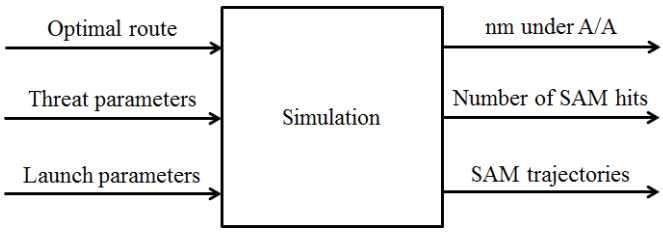


Figure 4.17: Inputs and outputs of the simulation model.

## 4.3 Simulation model for MRPP

The dynamic nature of a MRPP cannot be fully captured using a static network optimization formulation. First, the extent of an A/A threat has to be set prior to the optimization. The Blue aircraft might not use a straight route to the launch point which is assumed when calculating the A/A threat. In reality, the Red aircraft can reach the Blue aircraft even though the optimization model does not indicate so. In addition, the expansion of the threat is restricted along the edges of the network which leads to longer flight times to the nodes as flying a straight line is not always possible. Second, in the calculation of a LAR of a SAM it is assumed that the Blue aircraft does not change its direction after the SAM is launched. Depending on the route of the aircraft after the launch, the capability of a SAM to reach it can vary significantly. In most cases, this capability is reduced as the SAM needs to correct its course according to the change of the direction of the aircraft. Therefore, the modeling of the LAR generally leads to the assignment of unnecessary costs caused by SAMs.

In order to handle the issues pointed out above, the optimal routes are evaluated with a deterministic continuous time simulation model describing the threats caused by the SAMs and the Red aircraft. In the simulation, the Blue aircraft is set to fly the optimal route and the costs are calculated based on more realistic models than in the optimization model. The simulation model takes the optimal route as well as threat and launch parameters of SAMs as input. Here, launch parameters consist of the launch interval between SAMs as well as the criteria for a successful launch. The outputs are the nautical miles travelled under the influence of the A/A threat as well as the number of successful SAM launches and their trajectories. The simulation model with its inputs and outputs are depicted in Figure 4.17.

### 4.3.1 Surface-to-air threat

Before the simulation, the optimal route is divided into parts that correspond to a flight time of one second to help calculations. A moving average is then applied to smoothen the route in order to remove sharp turns because the simulation of SAM launches requires that the route's derivative is continuous.

The simulation of SAM launches is conducted with MisTarget simulation model [30] that is developed to simulate both air-to-air and surface-to-air missiles against a moving target. The Simulation is conducted whenever the Blue aircraft is within the maximum range of a SAM. In MisTarget, different kinds of SAMs such as infrared or radar guided missiles can be simulated. The SAMs are represented with pseudo 5 degree-of-freedom equations of motion. These are used when numerically integrating the trajectory of the missile. The missiles are guided by proportional navigation [121]. The effects of countermeasures, e.g., flares, as well as of evasive maneuvering can be taken into account.

In evasive maneuvering, an S-veawe or a barrel roll maneuver presented in Figure 4.18 is applied to the parts of the route that are inside the maximum range of a SAM. The moves are defined so that the maximum g-forces do not exceed the operational limits of the aircraft. The evasive maneuvering forces the missile to repeatedly calculate a new interception point. In proportional navigation [121], the missile changes its direction by an amount that is proportional to the change in the line-of-sight between the missile and the target. The larger the change in the line-of sight, the larger correction in the course of the missile is needed. These changes in the course slow down the missile and consume propellant [122]. Countermeasures are modeled by reducing the updating frequency of the SAM's navigation system. This reflects the situation where the aircraft, e.g., dispenses flares or chaff in order to produce false tracks.

Because the target acquisition and the fire control of a SAM weapon system are not treated in MisTarget, the exact times of the SAM launches must be set prior to the simulation. The SAM launches are set to occur at short time intervals whenever the Blue aircraft is within the theoretical maximum range of the SAM. This ensures that the optimal launch times of the SAMs are taken into account even though it results in the simulation of additional launches that would not

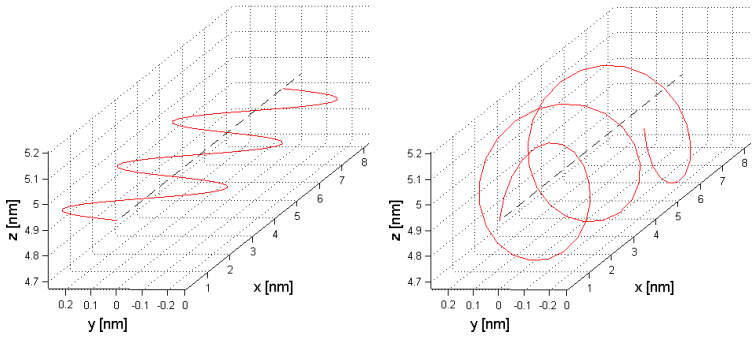


(a) S-weave. (b) Barrel roll.

Figure 4.18: Evasive maneuvers.

occur in reality. Using the theoretical maximum range of the SAM as a launch criterion rather than the LAR also increases the number of simulations. It is used to ensure that launches are not omitted in the case that the LAR in the optimization model is not accurate.

The simulation of SAM launches gives the missile trajectories as a function of time as the output of the simulation. Additionally, the terminal ground speed and distance to the target are provided. The launch can be considered as successful if the missile reaches the Blue aircraft with a speed that is greater than a missile specific minimum speed called miss speed. On the other hand, the type of the missile determines the minimum distance, called miss distance, between the missile and the target in order to the launch to be successful.

The simulation parameters related to S/A threat are

- Size of the subset of moving average used in the smoothing of the optimal route
- Launch interval of SAMs
- Minimum launch angles of SAMs
- Maximum flight times of SAMs
- Criteria, i.e., miss speed and miss distance, of successful launches of SAMs
- MisTarget missile model files determining the performance of SAMs
- Optional: Type of evasive maneuver, time period of the maneuver, and maximum sustainable g-force
- Optional: Effect of countermeasures on the updating frequency of the proportional navigation

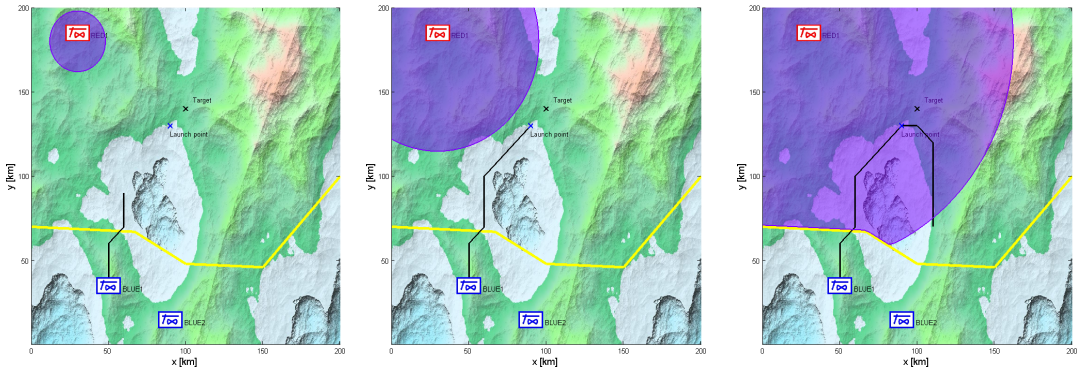


(a) t = 10 min 49 s (b) t = 21 min 18 s (c) t = 36 min 8 s

Figure 4.19: Simulation of the A/A threat. The purple area denotes the extent of the threat and the black line the optimal route, respectively

### 4.3.2 Air-to-air threat

The extents of A/A threats are simulated as cylinder shaped areas expanding continuously from the Red bases with constant speeds (see, Figure 4.19). At every step of the simulation, the extent of the A/A threat is checked in order to determine if it covers the current position of the Blue aircraft. Because the route of the Blue aircraft is divided into parts equaling a flight time of one second, the time that the Blue aircraft spends in the extent of the A/A threat can be calculated within the same accuracy. Based on this time, the corresponding distance in nautical miles is derived. The distances flown within the extents of the A/A threats originated from different bases are calculated independently and added to each other.

The simulation parameters related to A/A threat are

- Speed of the Red aircraft
- Reaction time

## 4.4 Solution of MRPP

The solution procedure of the MRPP introduced in this is presented in Figure 4.20. The procedure starts with the parameterization phase in which the A/G

mission is defined and the parameters of the optimization network as well as the threats are set. In the optimization phase, weights of the objective costs are determined and the optimal route is calculated as the solution to the MSPP formulation of the MRPP. Finally, the optimal route is evaluated in the simulation phase. The phases of the solution procedure are explained in more detail in the following sections.

### 4.4.1 Parameterization phase

The parameterization phase consists of steps where the parameters of the MRPP are determined. In step 1 of the solution procedure presented in Figure 4.20, the A/G mission is defined. The parameters of the optimization network, e.g., spacing of nodes discussed in Section 4.2.1 are set. In step 2, the parameters of the S/A and A/A threats, discussed in Sections 4.2.3.3 and 4.2.3.4, are determined.

### 4.4.2 Optimization phase

In the optimization phase, the MSPP formulation of the MRPP is solved. According to Equation 3.7, the MRPP is presented as the following MSPP:

$$\begin{aligned} &\min \textstyle\sum_{(i,j)\in E} w^D c_{ij}^D x_{ij} + \sum_{(i,j)\in E} w^F c_{ij}^F x_{ij} + \\ &\textstyle\sum_{(i,j)\in E} w^{S/A} c_{ij}^{S/A} x_{ij} + \sum_{(i,j)\in E} w^{A/A} c_{ij}^{A/A} x_{ij} \\ &\text{s.t.} \textstyle\sum_{j|(i,j)\in E} x_{ij} - \sum_{j|(i,j)\in E} x_{ji} = \begin{cases} 1 & \text{if } i = s, \\ -1 & \text{if } i = t, \\ 0 & \text{otherwise.} \end{cases} \\ &x_{ij} \in \{0,1\} \; \forall \; (i,j) \in E, \end{aligned} \tag{4.2}$$

where $E$ denote the set of edges connecting the nodes $V$. $c_{ij}^D$ denote the distance (see, Section 4.2.3.1), $c_{ij}^F$ the consumption of fuel (see, Section 4.2.3.2), $c_{ij}^{S/A}$ the distance inside the LAR of S/A threats (see, Section 4.2.3.3), and $c_{ij}^{A/A}$ the distance under the influence of A/A threats (see, Section 4.2.3.4) related to the edge

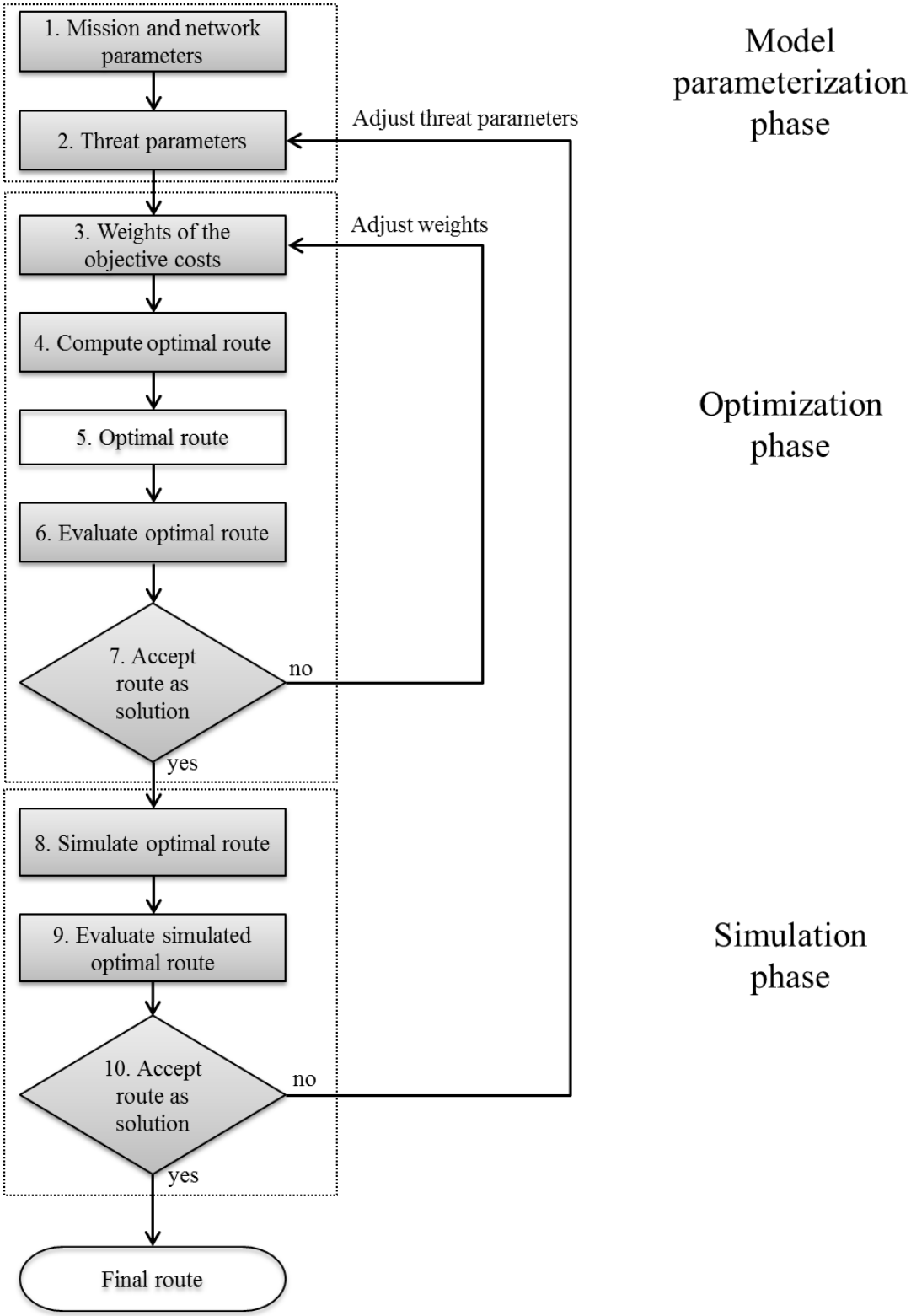


Figure 4.20: Flowchart of the solution procedure.

$(i, j)$. In addition, $w^D$, $w^F$, $w^{S/A}$ , and $w^{A/A}$ denote the weights of the objective costs associated with the travelled distance, the consumption of fuel, the travelled distance within the extent of the A/A threats, and the travelled distance within the LAR of the SAMs, respectively.

Since the number of efficient routes for the MRPP in question is large even for small networks, the *a posteriori* methods are ill-suited for the problem. It would take too much time to calculate even a modest approximation for the set of efficient solutions. On the other hand, the use of the *a priori* method is unfeasible because the minimum and maximum levels of each objective cost are not known beforehand. The efficient solution acquired with *a priori* weights can result in, e.g., too much exposure from any of the threat types. The interactive method for solving the MSPP overcomes these problems. When the preference information related to the objective costs can be revised on the basis of the unacceptable solution, it is more likely that the new solution is acceptable or at least less undesirable. When the preference eliciting process is performed thoroughly, the potential number of routes that need to be calculated is significantly lower than in *a posteriori* methods.

In step 3 of the solution procedure, the weights $w^k$ in the problem (4.2) are elicited with the trade-off method described in Section 3.2.1. The DM expresses the preference information in terms of ratios between the objective costs. The ratios represent the trade-offs of the objective costs the DM is willing to make between equally preferred routes. For example, the DM may be indifferent about spending additional 1000 lbs of fuel to avoid flying 10 nm inside the LAR of a SAM when other costs stay the same. In this case, the ratio $w^F/w^{S/A}$ would be 0.01. Linking the other costs with similar comparisons, the rest of the weights can be determined.

After the weights are determined, the shortest path problem is solved using a modified version of Dijkstra's algorithm in step 4. In step 5 of the solution procedure, the visualization of the optimal route is presented to the DM. Additional metrics such as the total flight time and the cumulative threat costs are also provided. In step 6 of the solution process, the evaluation of the optimal route is conducted by examining the objective costs and the feasibility of the route. If the DM is not satisfied with the optimal route, e.g., the flight time is too long, it

is rejected in step 7, the weights are revised and the optimization is repeated. If the DM is content with the optimal route, the solution procedure continues with the evaluation of the route in the simulation phase.

### 4.4.3 Simulation phase

After the optimal route has been generated, it is evaluated with the simulation model described in Section 4.3. If the results of the simulation phase are similar to the results of the optimization phase, the optimal route is accepted as the solution to the MRPP. Otherwise, the threat parameters used in the optimization model are corrected according to the simulation results, and the optimization phase is repeated. In the simulation phase, the results of the simulation are compared to the costs of the S/A and A/A threats on the optimal route acquired in the optimization phase.

The parameters of the S/A threats are evaluated by examining the trajectories as well as the miss distances and miss velocities of the SAMs in the simulation of SAM launches. In general, successful launches in the simulation should only occur when the Blue aircraft is within the LAR of a SAM used in the optimization model. In the case that the SAM achieves a successful launch even though the Blue aircraft is not inside the LAR at the time of the launch, the LAR parameters must be updated. The LAR is increased so that the successful launches would occur only when the Blue aircraft is within the LAR. Similarly, if there are unsuccessful launches that take place when the aircraft is inside the LAR, the LAR should be reduced. On the other hand, if the SAM reaches the Blue aircraft outside the theoretical maximum range, the maximum range of the SAM should be increased. Once the successful launches take place only when the aircraft is within the LARs of the SAMs and the aircraft is reached only within the maximum ranges of the SAMs, the optimal route is considered as feasible in terms of the S/A threat.

The evaluation of the parameters of the A/A threats is conducted by examining the points on the optimal route where the threats reach the Blue aircraft. Same points should be identified with both, the optimization and the simulation results. In the optimization model, the Red aircraft are restricted to fly along the edges

of the optimization network contrary to the simulation model where the threat expands without restrictions. This can lead to a situation where the extent of the A/A threat in the simulation model covers the parts of the optimal route that are free of the threat in the optimization model. If such a situation occurs, the speed of A/A threat is increased so that the extent of the threat in the optimization corresponds to those of the simulation. When the optimization and simulation models provide similar results, the route can be determined as feasible in terms of the A/A threat. It should be noted that the extent of the A/A threat in the simulation model is always equal or greater than in the optimization model. This is due to the aircraft being restricted to fly along the edges in the optimization model.

Although the optimal route is feasible in terms of the threats, it can involve more exposure to the threats than the DM prefers. If successful launches occur in the simulation of SAM launches, the weight of the S/A threat is increased in order to provide routes with less exposure. In the case of the A/A threat, the weight can similarly be increased in order to achieve routes involved with less A/A threat. After updating the weights, the optimization and simulation phases are repeated.

When the results of the optimization and simulation phases concur for both of the threat types, the solution procedure is terminated. The resulting optimal route is the final solution of the MRPP with the given weights of the objective costs. For missions that involve unavoidable successful launches of SAMs, the simulation model has an option to examine the effects of evasive maneuvering and countermeasures, employed during the optimal route, on the ability of the SAMs to reach the Blue aircraft.

## 4.5 Calculation of area of influence

The approach towards the automated solution of the MRPP presented in this thesis can also be applied to determine areas having targets that the Blue aircraft can influence with A/G weapons without exposing itself to the S/A threat. This feature is now called the area of influence calculation. Its idea is to optimize and simulate the route for multiple targets and then identify the targets that involve

a safe route.

First, a polygon shaped target area within the AO is defined. The target area is then divided into an evenly spaced grid of targets. Similarly to the calculation of a single route, each target is assigned launch points of A/G weapons. If the parameters of the threats are not yet evaluated with the help of the simulation model, a single route related to one of the targets is calculated and evaluated using the solution procedure in Section 4.4.2. Optimal route is then determined and evaluated for each target in the target area. As a result, the risks, i.e., the number of successful launches of SAMs, related to flying the optimal route in case of each target is identified. Therefore, areas having targets that involve low risk can be identified and the information can be used when deciding possible targets of A/G and SEAD missions as well as identifying vulnerabilities of friendly air defenses. Multiple simulations for a given target area can be conducted to study the effects of different simulation parameters, e.g., dealing with evasive maneuvers. Additionally, the criteria for the successful launch, i.e., the miss distance and the miss velocity, can be varied. This enables the analysis on how well the SAMs reach the Blue aircraft and how the changes in the launch criteria affect the area of influence. If the criteria are fulfilled only barely, applying evasive maneuvering or countermeasures on the parts of the optimal route that are within the maximum range of the SAMs can result in recognizing more targets that can be influenced without risks.

# Chapter 5

# Strike Aircraft Routing Software Suite (SARSS)

The solution procedure as well as the optimization and simulation models of the MRPP described in Chapter 4 are implemented in a software suite called Strike Aircraft Routing Software Suite (SARSS). SARSS is controlled through a graphical user interface (GUI). The GUI is used to create the mission to be analyzed, to set the parameters of the threats, as well as to display optimization and simulation results. In addition, the area of influence calculation can be conducted. The optimization and simulation phases of the solution procedure are implemented in the optimization and simulation modules of SARSS which are embedded in the GUI. MATLAB [123] is chosen as a programming environment because of its efficiency in matrix calculation and ability to produce GUIs with modest effort. In addition to the GUI and the modules, the suite uses MisTarget simulation model [30] in the simulation of SAM launches. The structure of the software suite and the relations between its components are presented in Figure 5.1.

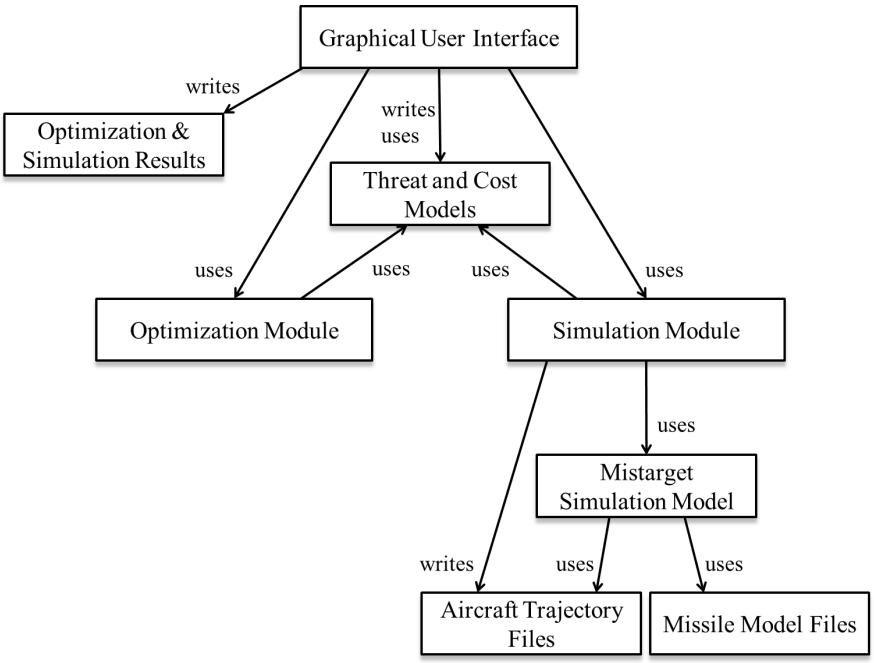


Figure 5.1: Structure of SARSS.

## 5.1 Graphical user interface (GUI)

The GUI of SARSS, depicted in Figure 5.2, is built using MATLAB [123]. It is programmed to function without the need of optional toolboxes of MATLAB in order to maximize compatibility among different MATLAB releases and configurations. The GUI is divided into components by functionality to make updating simple and to provide logical user experience. The GUI includes mission planning, optimization, and simulation windows. In addition, the area of influence calculation is implemented in a separate window that is accessed from the mission planning window.

Each main window of the GUI contains panels that group similar components together. The panels are controlled via tab buttons on the upper edge of the window. The window hierarchy of the GUI is depicted in Figure 5.3. A more detailed description of each window and its panels is given in the following sections.

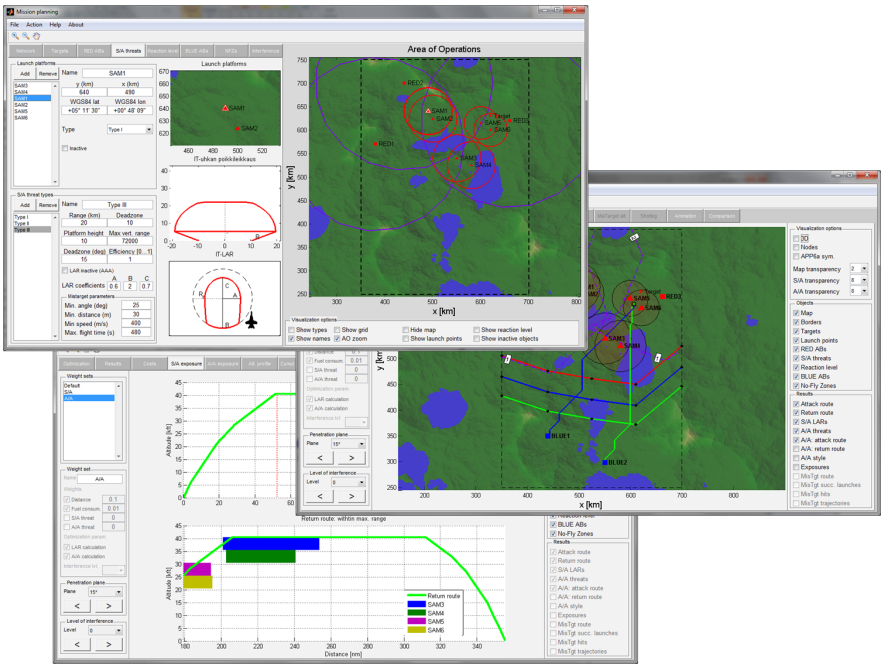


Figure 5.2: GUI of SARSS.

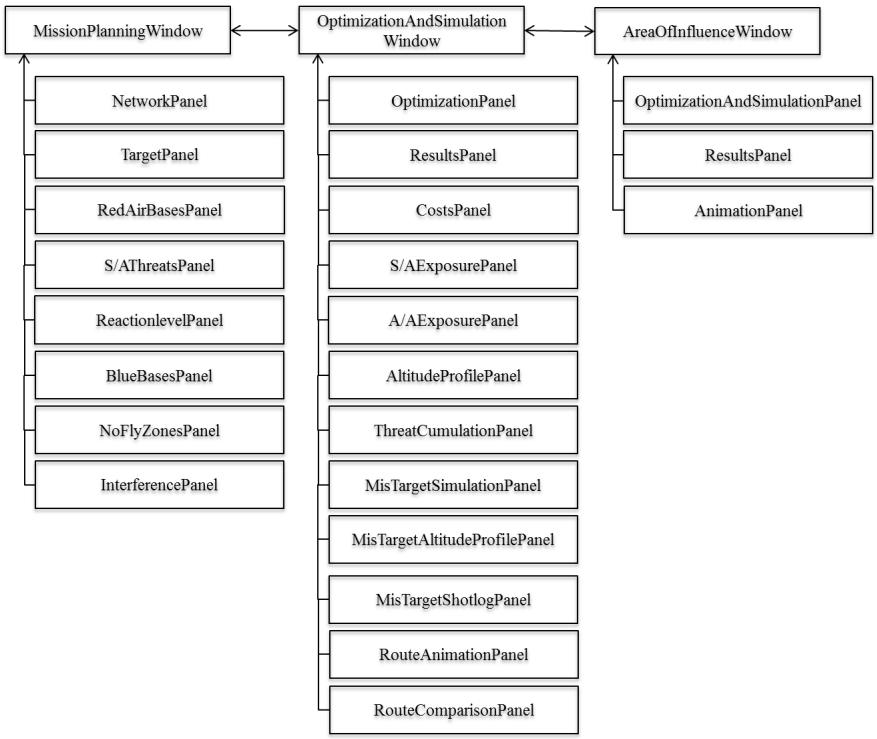


Figure 5.3: Structure of the GUI.

### 5.1.1 Mission planning window

In the mission planning window (Figures 5.4-5.11), the structure of the optimization network is determined and the definition of the mission under consideration is given. The window is shown first after the software suit is started. It consists of eight tab panels and a map figure. The map is generated with the Fractal Terrains 3 software [124]. The map is updated in real time as the parameters of the tab panels are changed. All the edit fields have error checking algorithms and they are colored red if the input is not feasible. Missions can be saved and loaded from the menu bar of the window. An option to load coordinates of bases and launch platforms of SAMs from a Microsoft Excel file is also provided. When moving between the mission planning and other windows, an error checking routine is employed to guarantee that unfeasible inputs are not used.

The network panel (Figure 5.4) of the mission planning window is used to define the structure of the optimization network as well as the dimensions of the area of operations. The area of operations is defined by using Cartesian coordinates or latitudes and longitudes associated with the WGS84 system as well as minimum and maximum flight altitudes. The definition of the optimization network includes minimum ascent and descend angles, the number of planes that can be ascended or descended in one move, and the distance between the nodes of the network in horizontal lattice. The vertical spacing of the nodes is determined by the horizontal spacing and the minimum ascend and descend angles. The direction of the reaction level, that dictates the opposite sides of the area of operations between which the reaction level spans, is set. The network panel also displays the table of all the ascent and descent angles in the network as well as the memory needed to store the optimization network.

In the target panel (Figure 5.5), the coordinates related to the targets and launch points are defined. The targets are set either in Cartesian coordinates or the WGS84 coordinate system. Multiple targets can be defined in a mission. A single target has one or more groups of launch points. These groups are determined by first setting a launch sector that dictates the launch direction in relation to the target. Next, the launch distance from the target as well as the launch height are set. The launch points are then evenly spread on the launch sector. Parameters of the weapon system can be set to automatically calculate the launch distance

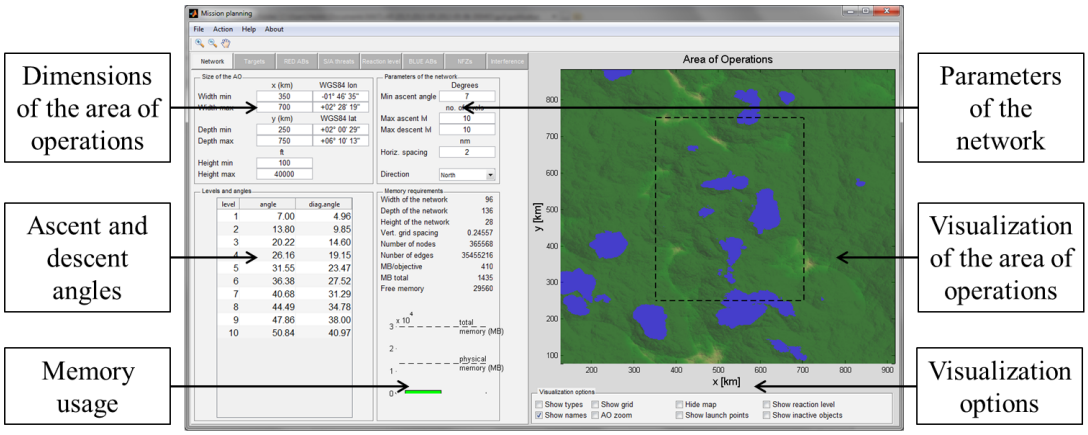


Figure 5.4: Network panel.

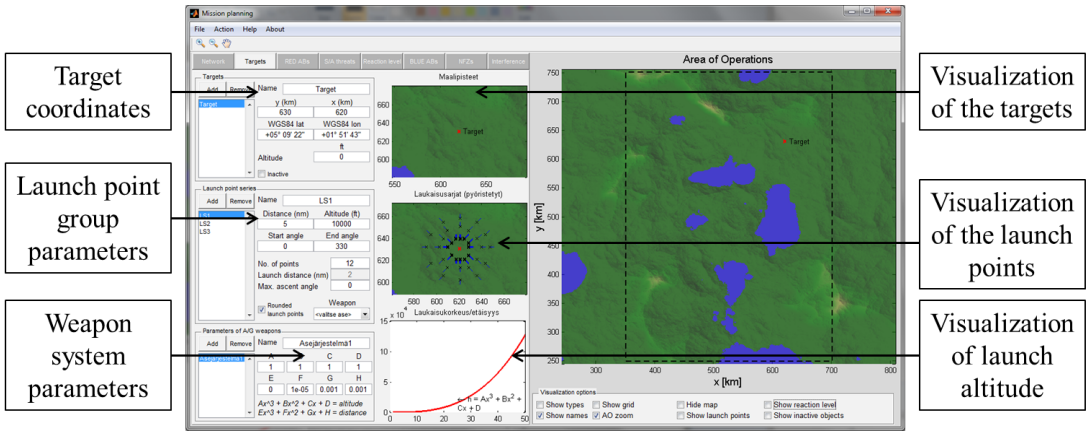


Figure 5.5: Target panel.

or launch altitude if the other is known. These parameters are defined as the coefficients of a third-degree function between the launch distance and altitude. Depending on the weapon system, a maximum ascent angle can be set so that the launch can occur while travelling an upward edge. The targets and the launch point groups along with the functions of launch distance in terms of launch altitude are presented in figures within the panel.

The locations of Red bases and A/A threats are set in the Red bases panel (Figure 5.6). The bases are given by their coordinates as well as the type of the A/A threat. The A/A threat types are defined with parameters that reflect a type of aircraft located in the base including maximum combat radius, reaction time, and speed. A smaller figure, where the selected base is shown on a more accurate map, is embedded in the panel. On the larger map in the mission planning window,

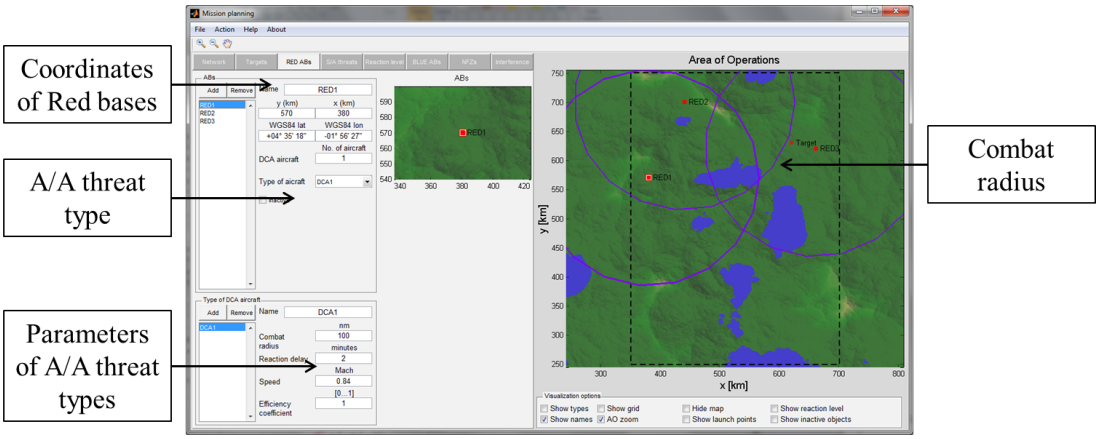


Figure 5.6: A/A threat panel.

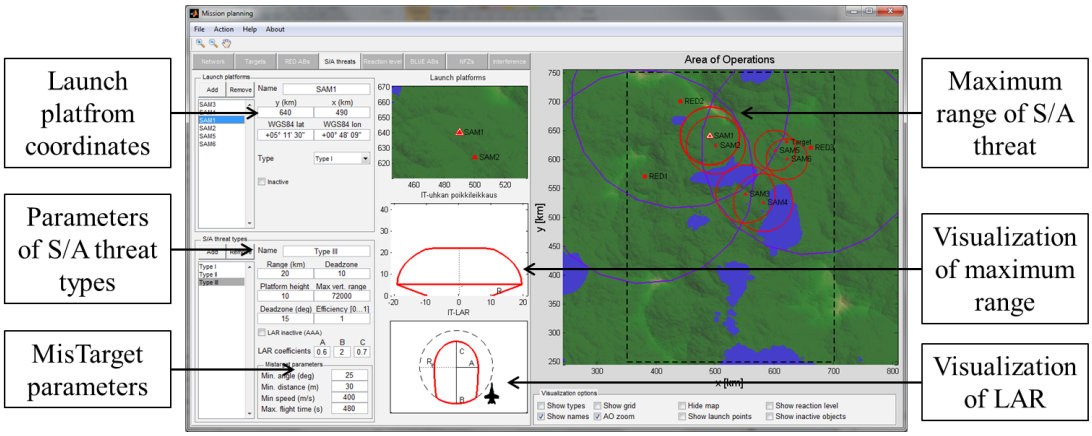


Figure 5.7: S/A threat panel.

the bases are shown with circles representing the maximum combat radiuses of the aircraft located in the bases.

In the S/A threat panel (Figure 5.7), parameters for enemy air defenses are defined. The parameters include the locations of the S/A threats as well as the types of the threats. An option to omit the LAR calculation is available if an AAA is considered. The S/A panel includes three smaller figures where the S/A installations are shown on a more detailed map and the side profile of the range and the LAR of a SAM are depicted. The maximum ranges of all the S/A installations are plotted on the larger map.

The parameters of the reaction level are determined in the reaction level panel (Figure 5.8). The reaction level is defined as five consecutive line segments in

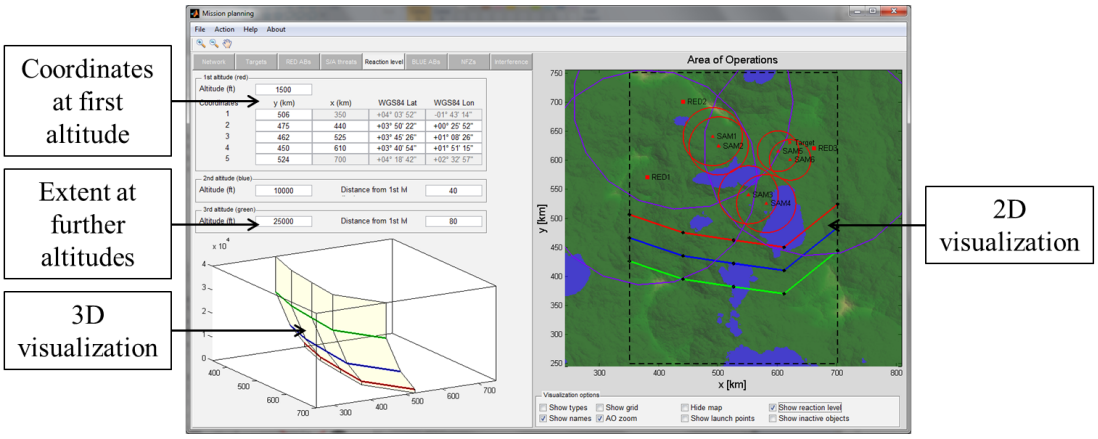


Figure 5.8: Reaction level panel.

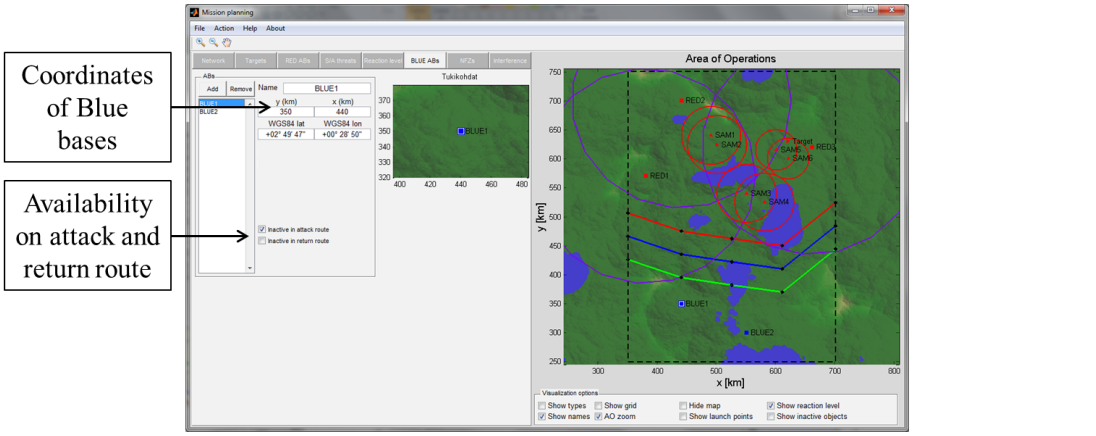


Figure 5.9: Blue bases panel.

three altitudes. The level is automatically extrapolated to the minimum and maximum flight altitudes if necessary. The coordinates of the level are set only at one altitude. The consecutive segments are defined by setting their altitude and distance from the first segment. If the direction that determines the opposite sides of the area of operations over which the reaction level is spanned is changed, the reaction level is automatically aligned accordingly. The panel also has an embedded figure with the three-dimensional representation of the reaction level.

In the Blue base panel (Figure 5.9), the number and coordinates of the Blue bases are determined. These bases act as the initial and terminal points of the A/G mission. A base can be set as inactive on the attack or the return route.

NFZs are defined by polygons with three to five coordinates and minimum and

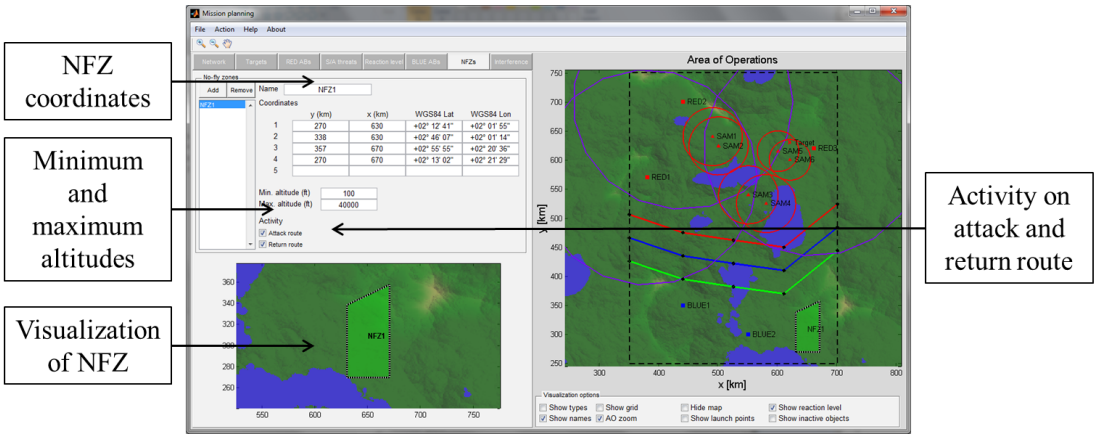


Figure 5.10: No-fly zone panel.

maximum height (Figure 5.10). The NFZ can be set as inactive for the attack or the return routes. The panel also has a detailed map in order to aid the determination of the coordinates.

In the interference panel (Figure 5.11), the qualitative and quantitative effect of interference to the threats in the optimization model is determined. This option enables to conduct what-if analysis in the case that the threats can be influenced by interfering them with, e.g., electronic countermeasures or that there is uncertainty about the parameters of the threats. The idea is to analyze how the optimal route changes if the threats are reduced from their original size. Additionally, the interference can affect the threats by reducing their costs by some factor. In the panel, the S/A and A/A threat types are listed and three levels of the effect can be assigned to each threat type. In the case of the S/A threat, the percentage of reductions of the maximum range and cost are determined. For the A/A threat, the reduction of range is determined in nautical miles. This depicts the distance of how much closer, compared to the situation without interference, the Red aircraft must be in order to achieve radar lock on the Blue aircraft.

### 5.1.2 Optimization and simulation window

The optimization of routes, the simulation of the routes, and the evaluation of results are conducted in the optimization and simulation window (Figures 5.12-5.23). The window consists of twelve tab panels and visualization options. Op-

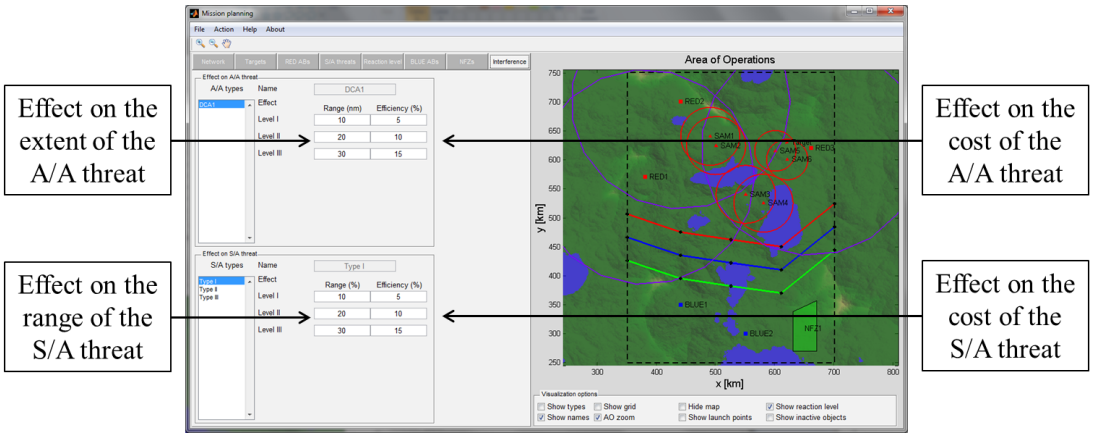


Figure 5.11: Interference panel.

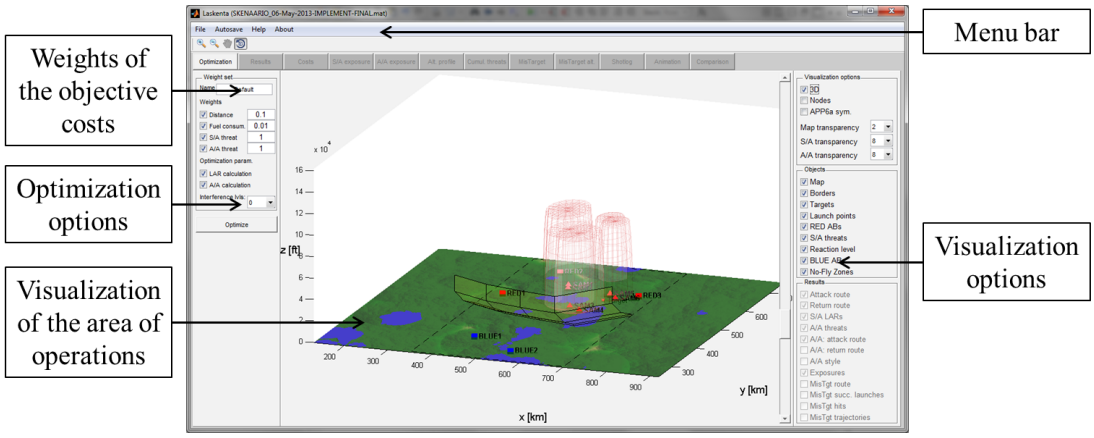


Figure 5.12: Optimization panel.

timization and simulation results can be saved and old results can be loaded through the menu bar of the window.

The optimization panel (Figure 5.12) displays 2D and 3D visualizations of the area of operations. In addition, the weights of objective costs along with a name for the weight set can be edited by using the edit fields of the panel. The panel also includes the settings for the calculation of effects of interference on the threats.

After completing the optimization routine, the results panel (Figure 5.13) is displayed. In the panel, the optimal route is visualized and the exposures to the threats are highlighted. The extent of the A/A threat is depicted with dashed contour lines that indicate how much threat is present in different parts of the area of operations. A list of weight sets is shown and the optimal route corre-

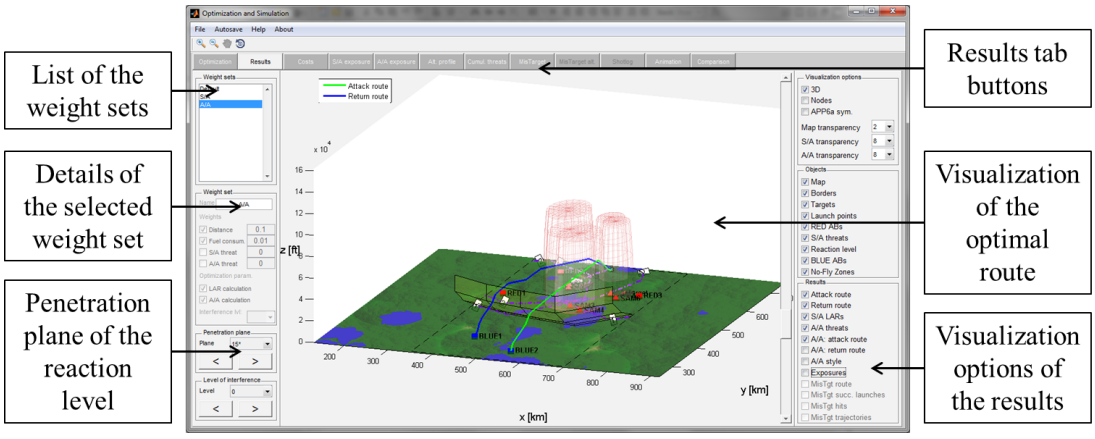


Figure 5.13: Results panel.

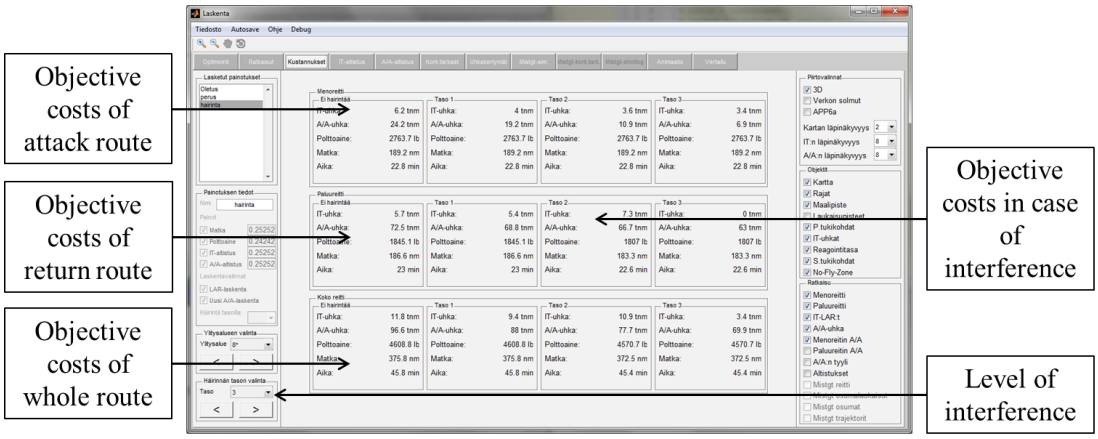


Figure 5.14: Costs panel.

sponding to a given weight set can be displayed. The panel also has options to study the non-optimal routes through different penetration planes of the reaction level. The effects of different levels of interference can be examined if the interference calculation has been conducted. The original sizes of the threats are shown with dashed lines to aid the examination of the effects of the reduced threats on the optimal route.

The costs panel (Figure 5.14) provides objective costs for a given weight set, penetration plane and interference level related to the optimal route. The costs are presented for both attack and return routes as well as for the route in whole. In the case of the travelled distance as well as S/A and A/A threats, the cost is given as nautical miles and for the fuel consumption, the cost is given as pounds of fuel.

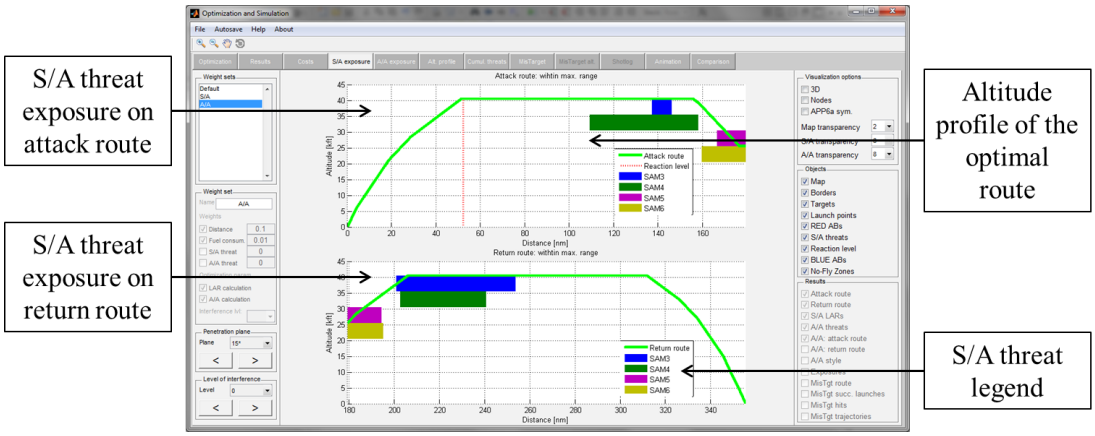


Figure 5.15: S/A threat exposure panel.

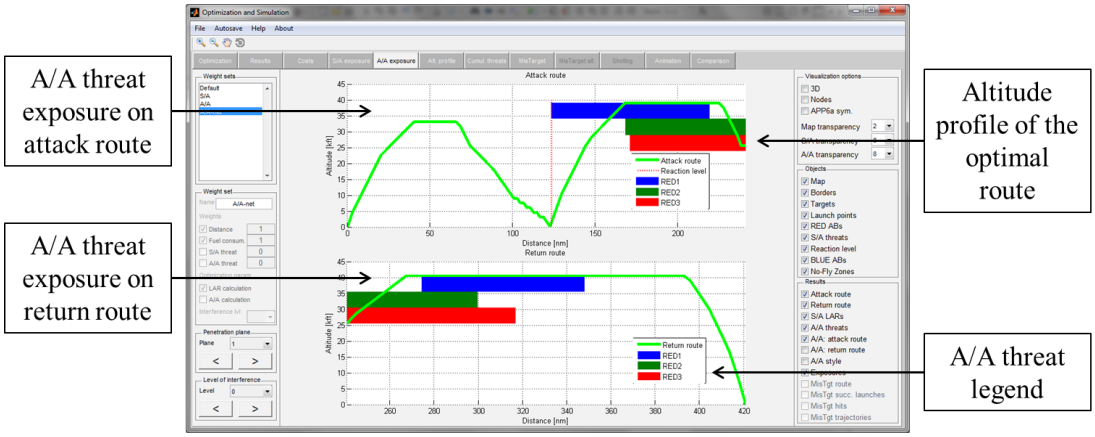


Figure 5.16: A/A threat exposure panel.

The S/A threat exposure panel (Figure 5.15) depicts the altitude profile of the attack and return parts of the optimal route along with the information about the S/A threat exposure. A colored bar is drawn on the background of the altitude profile when the Blue aircraft is within the maximum range of a threat. Different threats are separated with stacked bars and a legend linking the colors to the individual S/A launch platforms is presented.

The A/A threat exposure panel (Figure 5.16) displays similar information as the S/A threat panel but for the threat posed by the Red aircraft. The bars represent the parts of the route where the Red aircraft from different bases have reached the Blue aircraft. The point where the reaction level is penetrated is indicated with a dashed line.

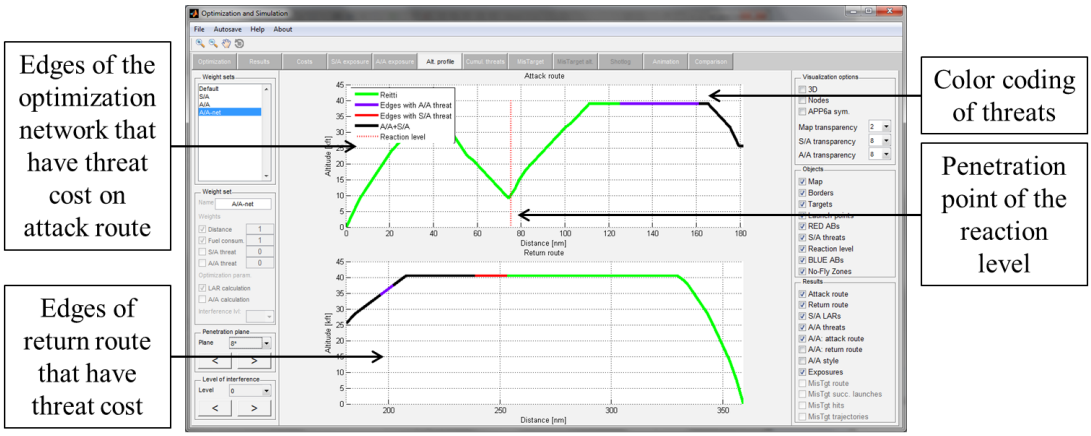


Figure 5.17: Altitude profile panel.

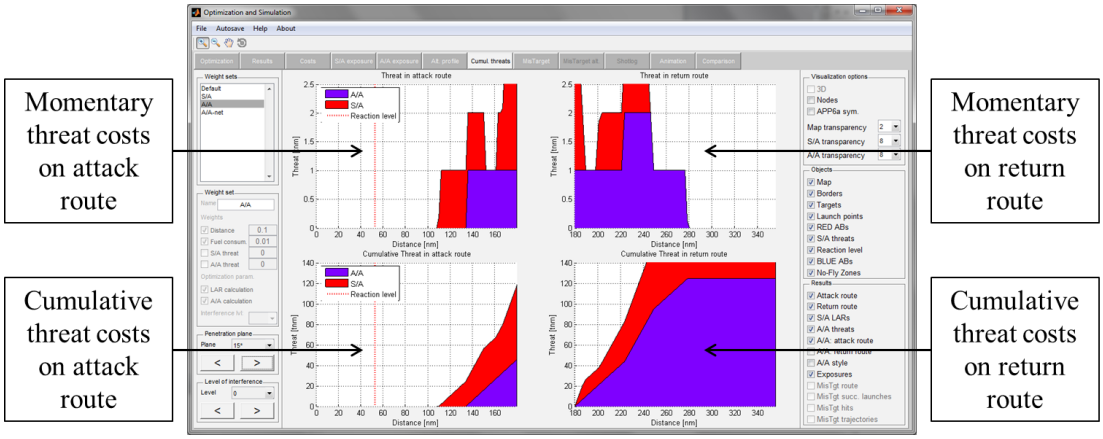


Figure 5.18: Cumulative threat exposure panel.

In the altitude profile panel (Figure 5.17), the edges of the route in the optimization network that have S/A and A/A threat are highlighted. The edges that have S/A threat are colored red and the edges with A/A threat are colored purple. If an edge has both types of threat, it is colored black. In the case of the S/A threat, the costs in the network can be significantly different from the representation in the S/A threat exposure panel since the costs are based on the LARs of the SAMs rather than the maximum ranges.

The momentary and cumulative threat exposures on the optimal route are displayed in the cumulative threat exposure panel (Figure 5.18). The threats are shown as a stacked graph as a function of the distance travelled using the same color scheme as in the altitude profile panel.

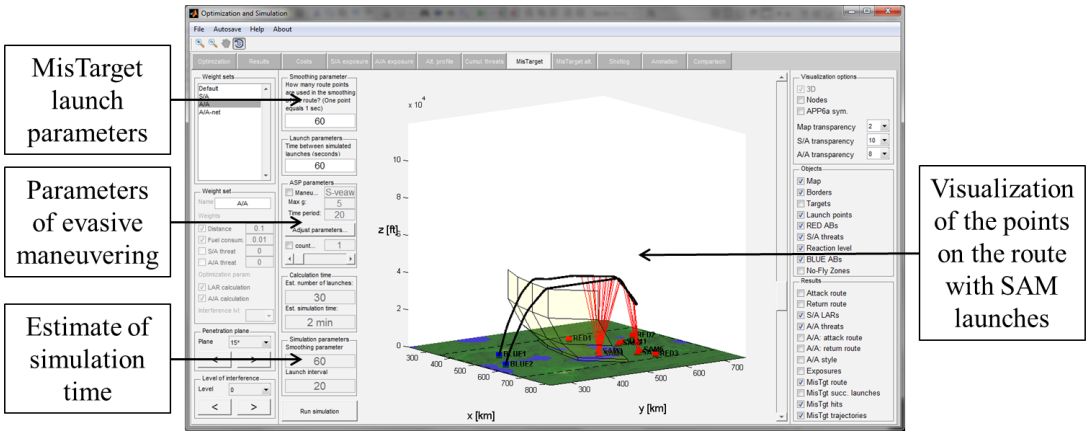


Figure 5.19: MisTarget simulation panel.

The parameters of the simulation of SAM launches are set in the MisTarget simulation panel (Figure 5.19). The smoothened optimal route used in the simulation is displayed on a map. The points of the smoothened route that correspond to the launch times with the current launch interval parameter of the SAMs are highlighted. Additionally, the optional evasive maneuvers are shown in the visualization.

Once the MisTarget simulation is completed, the MisTarget altitude profile (Figure 5.20) and shotlog panels (Figure 5.21) are enabled. The altitude profile panel shows in which points the aircraft is when a successful launch is carried out and where it is when the SAM reaches it. The points of the optimal route where the simulated launches occur are connected with a line to represent the part of the optimal route that is associated with successful launches. One can also study the S/A threat exposure of the optimal route in the network so that the difference between the results obtained with the network optimization and the MisTarget simulation model can be examined.

The shotlog panel lists all the simulations carried out with a given weight set. Additionally, the simulation can be conducted for the non-optimal routes related to different penetration planes as well as in the case of interference. In the list, the simulation, evasive maneuvering and countermeasures parameters are presented in order to enable the comparison of the simulation results with different parameters. A table of all the simulated launches with given simulation parameters is also presented. This table lists the launch information such as the name of the

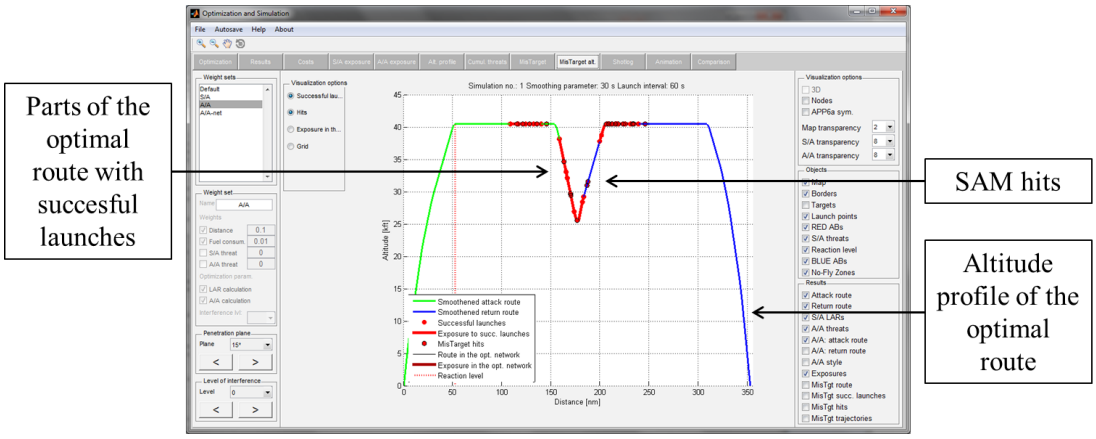


Figure 5.20: MisTarget altitude profile panel.

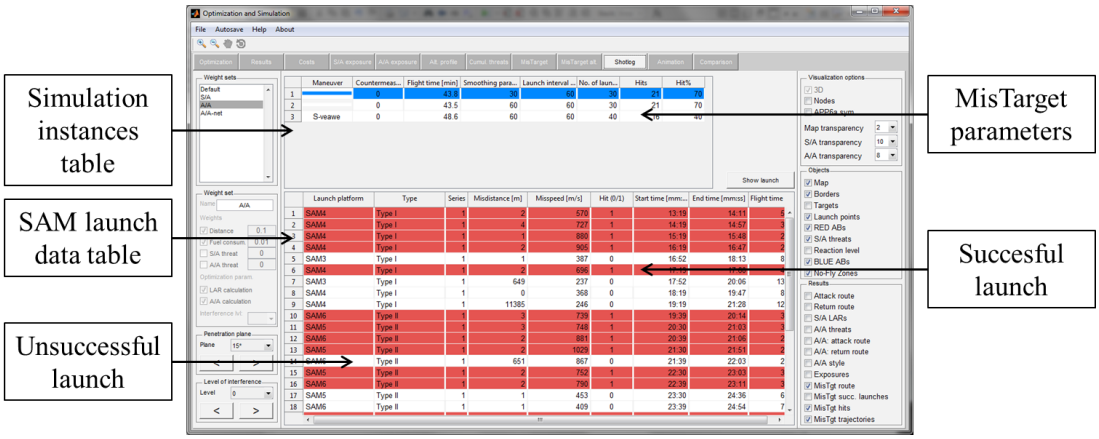


Figure 5.21: MisTarget shotlog panel.

SAM, launch time, the duration of flight, and the terminal state of the missile. Animation visualizing the flight of a SAM can be started by selecting a row, i.e., a single launch, from the table.

The animation panel (Figure 5.22) has an interface to control the animation of the selected optimal route. The speed of the animation as well as the camera position and angle can be controlled. In the animation, the LARs of the S/A threats, missile trajectories, and the expansion of the A/A threat are visualized as the Blue aircraft moves along its route. The launched SAMs are annotated with a distance to the Blue aircraft to aid the interpretation of their position.

Optimization results related to alternative weight sets can be compared in the weight set comparison panel (Figure 5.23). A line plot and bar plots of each

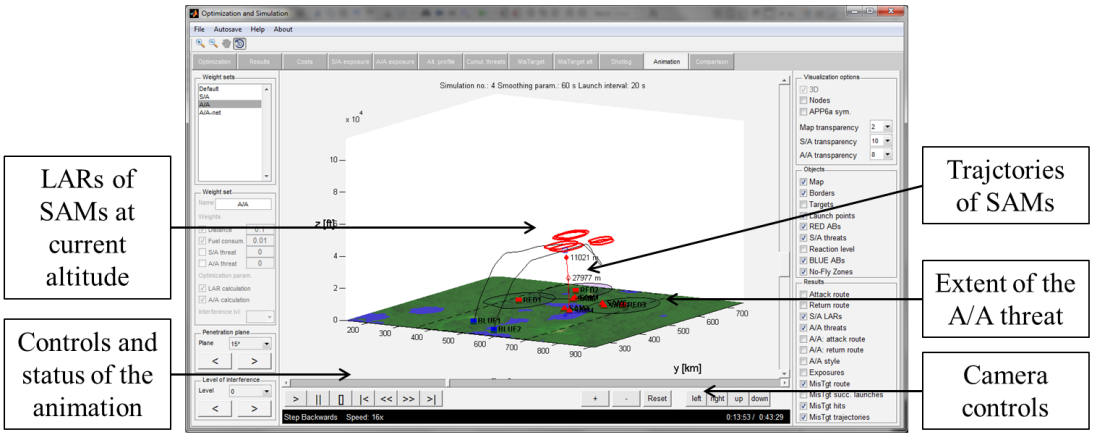


Figure 5.22: Animation panel.

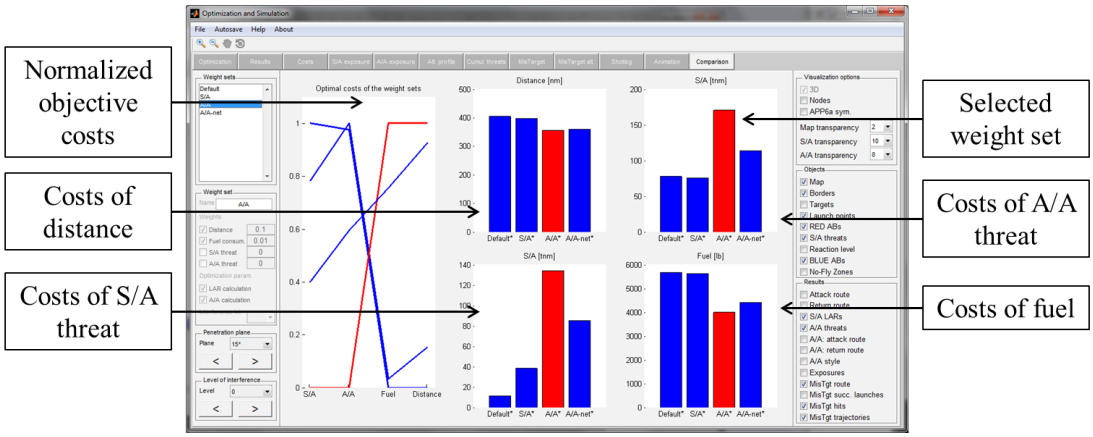


Figure 5.23: Comparison of objective costs panel.

objective costs related to the objectives are presented so that the effect of each weight set on the costs can be examined.

### 5.1.3 Area of influence calculation window

The area having targets that the Blue aircraft can influence with A/G weapons without exposing itself to the S/A threat can be analyzed in the area of influence calculation window (Figure 5.24). The window consists of optimization and simulation, results, and animation panels as well as visualization controls similar to the optimization and simulation window. In the optimization and simulation panel (Figure 5.24), the target area is defined as a four edged polygon within the AO. The target coordinates are defined by setting a distance between neigh-

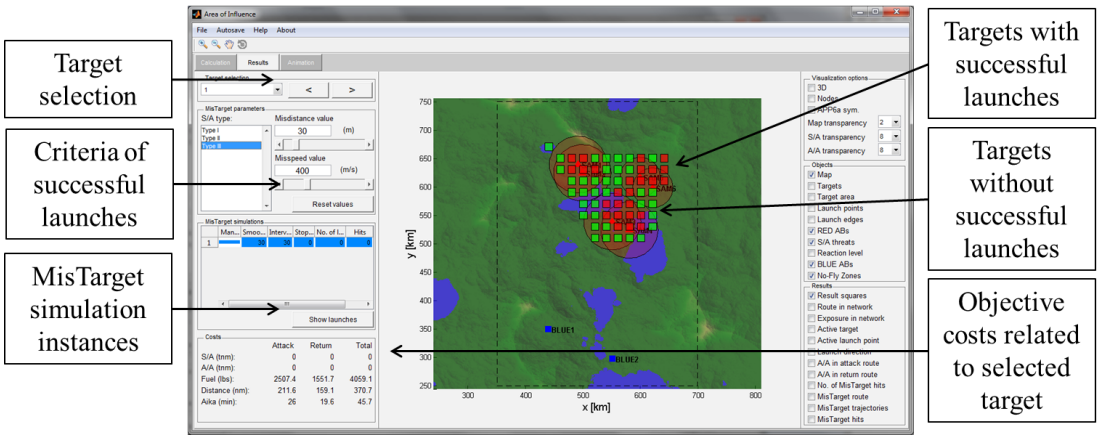


Figure 5.24: Results panel of the area of influence calculation window.

boring targets that is used to cover the target area with an evenly spaced grid of coordinates. The optimization and simulation parameters similar to the ones used in the optimization and simulation window are also given. As a additional parameter of the simulation model, an optional stop condition in the case that a successful SAM launch occurs during the simulation. If a successful launch is detected when evaluating a route, the simulations of successive launches do not give additional information and they can be passed in order to decrease the time needed to conduct the simulations.

After the optimization and the simulation are conducted, the results panel is shown (Figure 5.24). In the panel, the area of operations is displayed with the visualization of the target area. In addition, the optimal route for a given target is shown. The costs of the optimal route, the smoothened route used in the simulation as well as the SAM trajectories are also presented. The targets involving a route with no successful SAM launches are highlighted with green squares and the routes with successful launches with read squares. The simulation instances with their parameters and SAM launch tables are listed in order to enable comparison between alternative parameters of the simulation. In addition, the criteria of successful launch for each SAM can be varied to study how strongly they are fulfilled as well as how they effect in the size of the area that can be influenced.

## 5.2 Computational performance

Example computations of SARSS presented in Chapter 6 are carried out with a laptop computer with 2.6 GHz Intel Core i5 processor, 16 gigabytes of RAM, 64-bit Microsoft Windows 7 operating system, and MATLAB version 2012b.

Solving the shortest path problem with Dijkstra's algorithm is relatively fast. Even in the case of large networks involving hundreds of thousands of nodes and dozens of millions of edges that can be stored wholly in the physical memory of the computer, the solution time is in the neighborhood of one second. Forming the adjacency matrices of the objective costs for distance, fuel consumption, and the A/A threat also takes only a short amount of time. In the case of the S/A threat, each edge in the vicinity of the threat has to be examined in order to determine the part of the edge that is inside the threat. For a complicated network and large maximum ranges of SAMs, this can take several minutes. However, because of the symmetry of the threat model, each threat type is needed to calculate only once. After that, the S/A threats are saved as mat-files and are copied to any location of the network in negligible time.

As the weights of objective costs are changed, the adjacency matrices of the costs have to be aggregated again in order to form the adjacency matrix of the weighted sum of the costs. Here, the adjacency matrix related to A/A threat is recalculated for different penetration planes of the reaction level. Depending on the available physical memory, this can take a considerable time. If the physical memory runs out during the aggregation, data is temporarily stored on the hard drive, i.e., memory swapping occurs, which is time consuming. To avoid this problem, the network panel of the mission planning window (Figure 5.4) has a meter showing the expected need of physical memory.

The simulation of SAM launches is another time consuming task and it can take a relatively long time to conduct. This is not such an issue when evaluating a single route. However, when multiple routes are evaluated in the area of influence calculation, the computation time can be extensive. A single simulation run takes approximately two to five seconds depending on the position of the aircraft relative to the launch platform and the maximum range of the SAM. Means to overcome this issue are suggested in Chapter 7 dealing with future research.

## 5.3 Utilization

In the basic setting, SARSS can be used to solve an optimal route employed in A/G mission involving a single target and a single base that is both the initial and the terminal base of the mission. Using the solution procedure presented in Chapter 4, the optimal route is found by first repeating the optimization phase and adjusting the weights of the objective costs until an optimal route with satisfactory costs is found. For example, the consumption of fuel can be greater than the capacity of the fuel tanks of the aircraft with the given weight set. Then, the weight of the consumption of fuel is increased until a route with sufficiently low consumption is found.

In addition to finding the optimal route through air defenses, SARSS can be used to determine the optimal target out of a group of alternative targets. Adding a dummy node in the network that acts as the terminal node, the optimal route travels through the launch point that determines the target that involves the smallest total cost. Furthermore, the same idea is used for the optimal selection of the initial and terminal bases of the mission. This enables a what-if analysis where the effect of disabling and enabling bases on the optimal target and the optimal route can be studied.

The additional information, e.g., the table of SAM launches in the shotlog panel, provided by the GUI can be used to assess which enemy bases and launch platforms pose the most risk on the optimal route. Based on this knowledge, potential targets for SEAD mission can be identified. In the same manner, SARSS can be used inversely to identify the weak areas of friendly air defenses as well as the critical bases and launch platforms.

The area of influence calculation feature of SARSS can be used to determine the areas that can be influenced safely. With the help of the feature, one can quickly asses which targets in the area of operations are possible to neutralize with available A/G weapons. The area of influence calculation window also enables the varying of the criteria of successful launches to quickly assess the possible effects of evasive maneuvering and countermeasures on the results of the simulation of SAM launches.

The area of influence calculation can also be applied in the planning of SEAD missions. By defining the target area so that it covers the positions of the S/A launch platforms and the enemy bases, one can easily determine which platforms or bases can be neutralized without exposing the aircraft to the risk of getting shot down. This information is then used in the calculation of a single optimal route. By removing individual platforms or bases and comparing the effects on the optimal route, the launch platform which elimination leads to a route with the least cost is found out.

The area of influence calculation can also be used inversely when considering the allocation of the resources of friendly air defenses. By defining the target area to cover the coordinates of friendly launch platforms or bases, the weak spots of the defenses are determined. These results are then used to re-position the launch platforms and the bases such that the coverage of the defenses takes into consideration the vulnerable areas.

# Chapter 6

# Analysis of example mission

In this chapter, the MRPP of an example A/G mission is analyzed. The optimal route is determined using the solution procedure and SARSS described in Chapters 4 and 5, respectively. The details of the A/G mission are presented in Section 6.1. In Section 6.2, the parameterization phase of the solution procedure is discussed. In the optimization phase considered in Section 6.3, the optimal route is determined and the updating of the weights of the objective costs is demonstrated. The evaluation of the optimal route is conducted according to the simulation phase described in Section 6.4. The updating of the parameters of the threat models based on the simulation results is also demonstrated. In Section 6.5, the area of influence calculation enabled by SARSS is utilized in the planning of suppression of enemy air defenses mission. Based on the results, a new optimal route is determined in the case that one of the SAMs involved in the mission is neutralized. Results of the example analysis are summarized in Section 6.6.

## 6.1 Mission description

The A/G mission considered in the example analysis is depicted in Figure 6.1. The bottom left corner of the area of operations is located at coordinates (250,300) and the upper right corner at (700,750). The 3D view of the area of operations is presented in Figure 6.2. In the mission, the goal of the Blue force is to find a fast and fuel efficient route for a strike aircraft from a Blue base to the launch

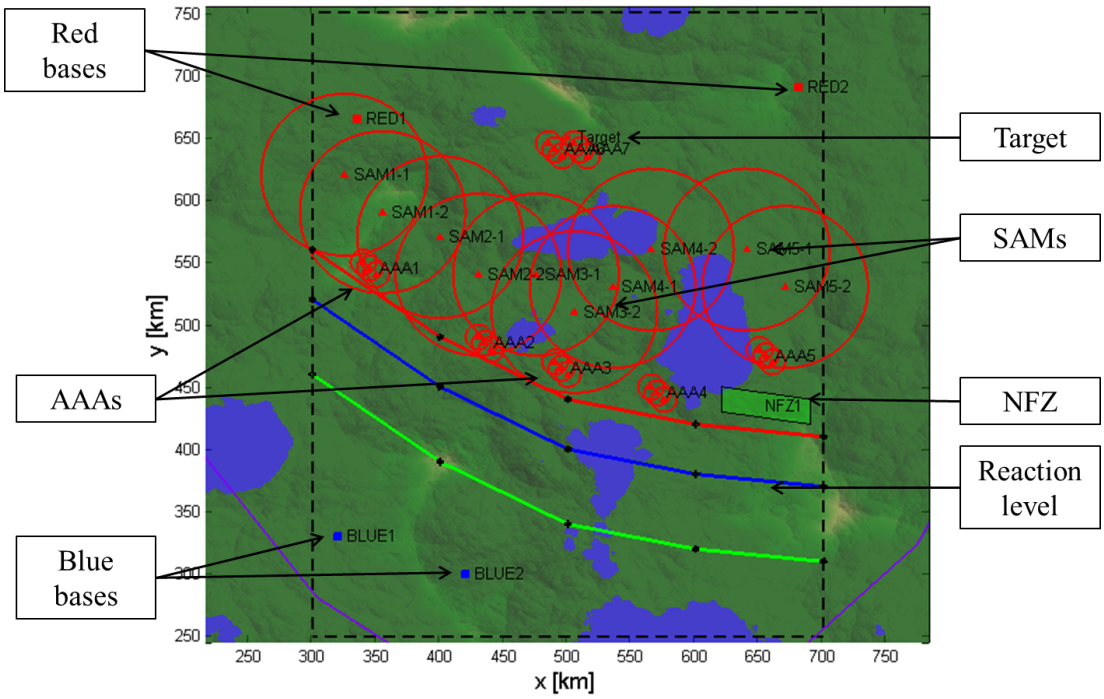


Figure 6.1: Example mission.

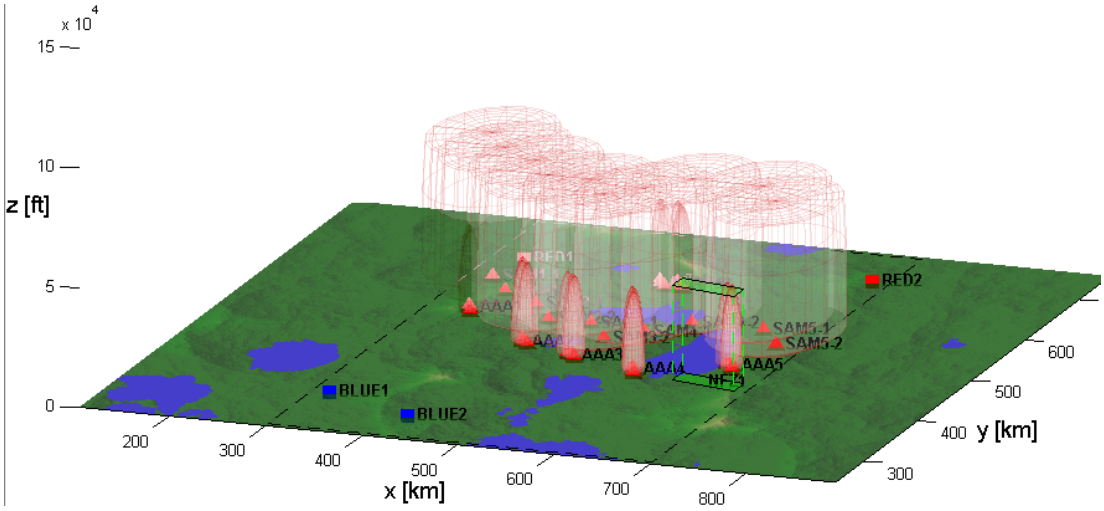


Figure 6.2: 3D view of the example mission.

point of an A/G weapon while avoiding the S/A and A/A threats posed by the air defenses and the Red aircraft. The mission can start from either of two Blue bases that are denoted with BLUE1-2 in Figure 6.1. The bases are located at coordinates (320,330) and (420,300). Similarly, the mission can end in either of the bases.

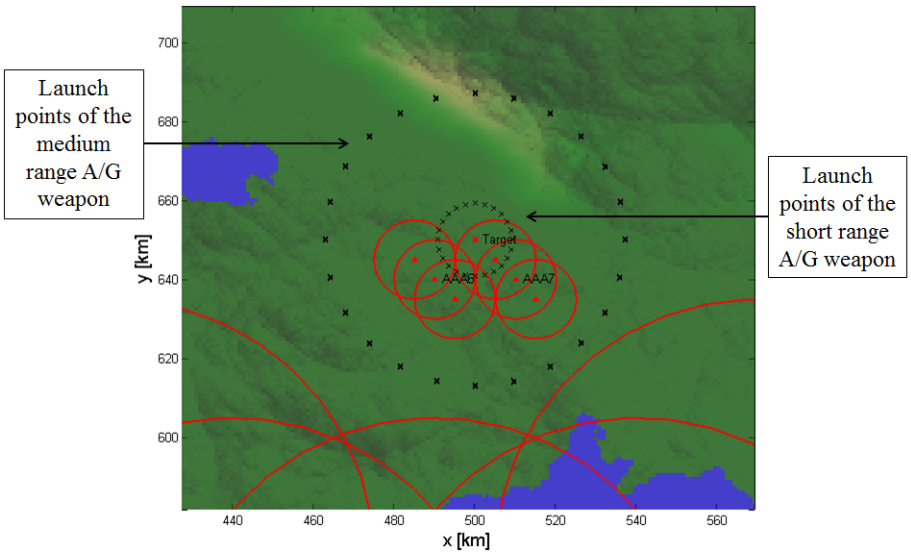


Figure 6.3: Launch points of A/G weapons in the example mission.

The target of the mission is located at the coordinates (500,650). Two optional A/G weapons are considered. Practically unlimited number of launch distances and altitudes for each A/G weapon could be applied but for simplicity, one group of launch points for each weapon is considered. The first weapon can be deployed from a distance of 5 nm and at the altitude of 10,000 ft. The second weapon can be deployed from 20 nm at 25,000 ft. These launch distances and altitudes are typical to short and medium range A/G weapons (see, e.g., [125] [126]). The direction of the launch, i.e., the launch sector, is set to 360° with the launch points divided into 15° intervals. This results in 24 evenly spaced launch points around the target at the launch distance. The launch points are depicted in Figure 6.3.

The reaction level that triggers the A/A threat is set to go through coordinates (300,560), (400,490), (500,440), (600,420), and (700,410) at the altitude of 1,500 ft. At 15,000 ft, the reaction level reaches 26 nm further and at 25,000 ft, it is 54 nm south of the first coordinates. An NFZ is located in the East near the reaction level and the coordinates of its corners are (620,430), (620,450), (690,440), and (690,420). The NFZ is active for the whole altitude range of the optimization network and during both attack and return routes.

## 6.2 Parameterization phase

### 6.2.1 Optimization network

The optimization network is constructed by dividing the area of operations into a 55x68x20 grid of nodes with horizontal and vertical spacing of 2 nm and 1063 ft, respectively. The minimum and maximum flight altitudes are set to 300 ft and 35,000 ft. The vertical spacing is determined by the smallest ascent or descent angle of 5° of the Blue aircraft. The maximum grid levels that the Blue aircraft can ascend and descend in one move are set to 12 and 15 that represent angles of 46.39° and 52.69°. The optimization network therefore consists of 563.312 nodes and approximately 71.2 x $10^6$ edges.

### 6.2.2 S/A threats

Two types of S/A threats are considered in the example analysis. The first type is a medium range SAM with the maximum range of 35.1 nm. In the vertical direction, the range is limited to 60,000 ft. The second S/A threat type is an AAA with the effective range of 6.48 nm in both horizontal and vertical directions. The parameters of the S/A threats are shown in Table 6.1.

Table 6.1: Parameters of the S/A threats.

| | SAM | AAA |
|---|---|---|
| Maximum range | 35.1 nm | 6.48 nm |
| Vertical ceiling | 60,000 ft | - |
| Minimum operating angle | 1.5° | 2.0° |
| Dead zone adjustment | 16.7 nm | 2.16 nm |
| Height of the radar antenna | 20 ft | 10 ft |
| LAR coefficients a, b and c | 0.85, 2.0, 0.8 | - |

The SAMs consist of 5 batteries each of which has two launch platforms situated within approximately 22 nm from each other. The batteries are located at coordinates (340,605), (415,555), (490,525), (550,555), and (655,545) (see, Figure 6.1). The AAAs consist of 7 batteries with 3 firing units in each battery within

a range of 8 nm. The batteries are located at coordinates (345,545), (435.485), (495.465), (570,455), (655,475), (490,640), and (510,640) which are presented in Figure 6.1.

### 6.2.3 A/A threats

The Red bases, labeled RED1 and RED2, are located at coordinates (335,665) and (680,690) (see, Figure 6.1). The aircraft type DCA1 is stationed at the base RED1 and type DCA2 at the base RED2. The aircraft type DCA1 represents a modern fighter aircraft with higher top speed than the Blue aircraft. The aircraft type DCA2 depicts an older fighter aircraft with shorter combat radius, longer reaction delay, and lower top speed. The parameters of the aircraft types are shown in Table 6.2. The extent of the A/A threat is limited by the reaction level at its lowest altitude, i.e., the red line segment in Figure 6.1. This level is thought to be the frontline of the underlying conflict and heavily defended by the Blue side so that the Red aircraft cannot pursue the Blue aircraft beyond it.

Table 6.2: Parameters of the A/A threats.

| | DCA1 | DCA2 |
|---|---|---|
| Combat radius | 400 nm | 300 nm |
| Reaction delay | 2 min | 3 min |
| Speed | Mach 0.95 | Mach 0.7 |

## 6.3 Optimization phase

### 6.3.1 Weights of objectives

In the example analysis, the S/A and A/A threats are initially considered equally costly by the DM, i.e., $w^{S/A} = w^{A/A}$. If one nautical mile under either threat can be avoided, an increase of 10 nm in the total length of the route is accepted. Therefore, $w^D = w^{A/A}/10$. Furthermore, a decrease of 1 nm in the total length of the route is acceptable, if it leads to a 10 lb increase in the fuel consumption, i.e., $w^F = w^D/10$. If one define $w^{S/A} = w^{A/A} = 1$, then $w^D = 0.1$ and $w^F = 0.01$.

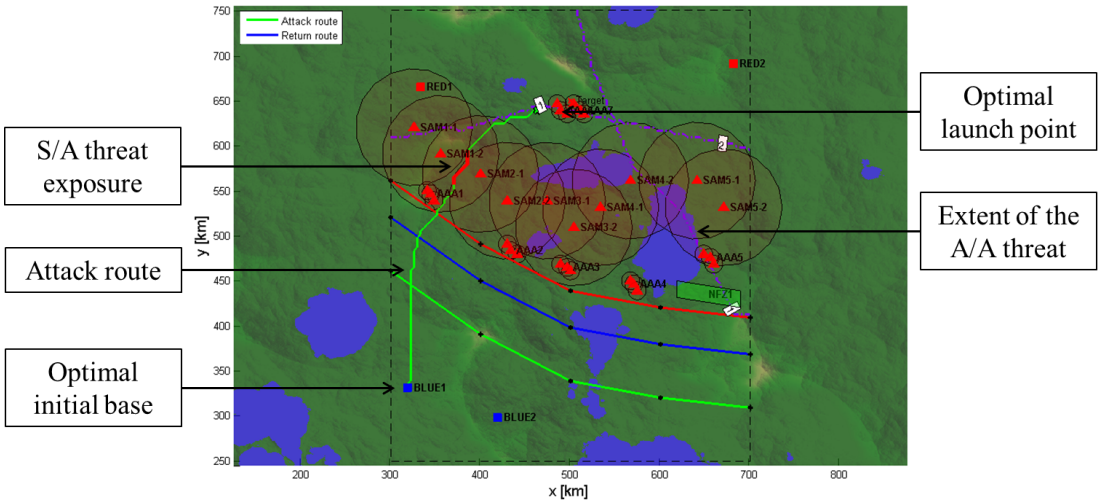


Figure 6.4: Attack route with the initial weights.

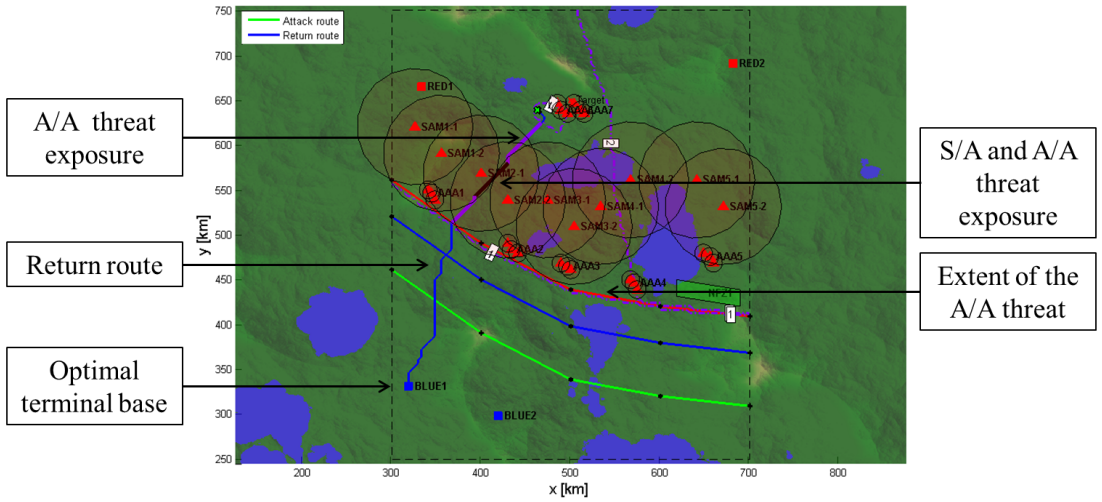


Figure 6.5: Return route with the initial weights.

The optimal attack and return routes corresponding to the above weights of the objective costs are solved with SARSS and presented in Figure 6.4 and Figure 6.5. The 3D view of the optimal route is displayed in Figure 6.6.

### 6.3.2 Evaluation of optimal routes

The objective costs of the optimal route are given in Table 6.3. The duration of the attack and return routes are 23.8 min and 23.3 min, respectively, and the duration of the whole route is 47.1 min. The route starts from the base BLUE1 and

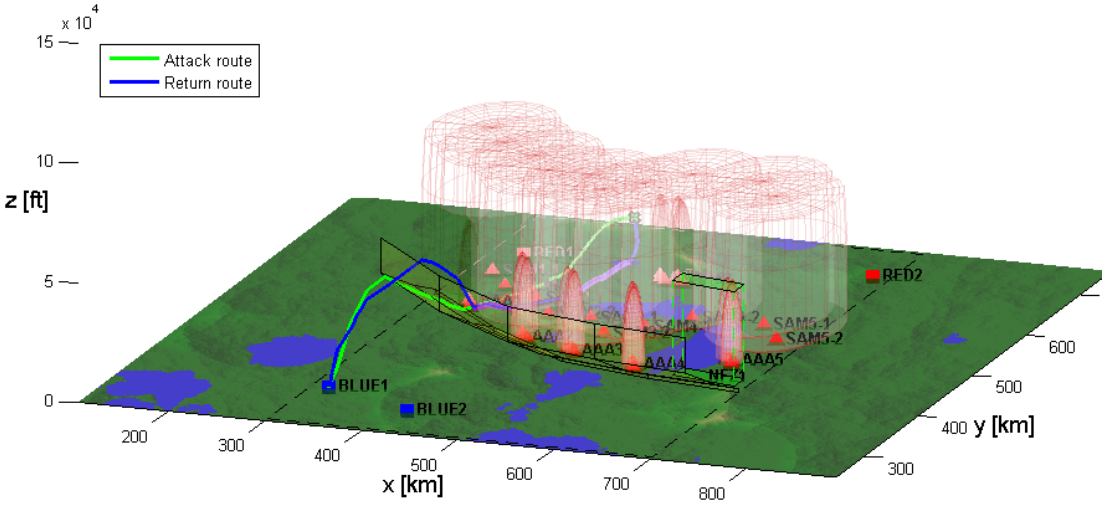


Figure 6.6: 3D view of the optimal route with the initial weights.

ascends to 30,000 ft while heading north. After flying for 70 nm, the route turns northeast and descends along the reaction level until it penetrates the level at 300 ft at coordinates (352,525). The route then progresses northeast for another 30 nm while maintaining the minimum flight altitude of 300 ft. At coordinates (415,624), the route turns east towards the launch point of the medium range A/G weapon at coordinates (463,639) and begins to ascend to the launch altitude of 25,000 ft. After the launch point, the route makes a 45° turn and heads southwest for 10 nm while descending to 10,000 ft. At coordinates (470,362), the route starts to decent to the minimum flight altitude and turns southwest and heads for the frontline. After reaching the frontline at (367,514) and clearing the A/A threat, the route ascends to 35,000 ft. Then, the aircraft continues south towards the base BLUE2 where it lands after travelling 413 nm. The altitude profile of the route resembles the typical high-low-low-high altitude profile of an A/G mission (see, Figure 4.5) discussed in Section 4.2.1. The Low penetration altitude of the reaction level gives the A/A threats less time to expand and therefore decrease the extent of the A/A threat.

The optimal route obtained with the initial weights involves flying within the LAR of the SAM2-1 for the total of 49.8 nm. It should be noted that the route crosses the LAR at low altitude where the LAR is smaller due to the dead zone of the radar of the weapon system. Additionally, the Blue aircraft traverses the maximum ranges of SAM1-2 and SAM2-2 for several nautical miles which is

Table 6.3: Costs of the optimal route with the initial weights.

| | Attack | Return | Total |
|---|---|---|---|
| Flight distance | 209.7 nm | 202.9 nm | 412.6 nm |
| Fuel consumption | 4116.8lb | 3364.2 lb | 7481.0 lb |
| S/A threat | 21.6 nm | 28.3 nm | 49.8 nm |
| A/A threat | 0 nm | 81.9 nm | 81.9 nm |

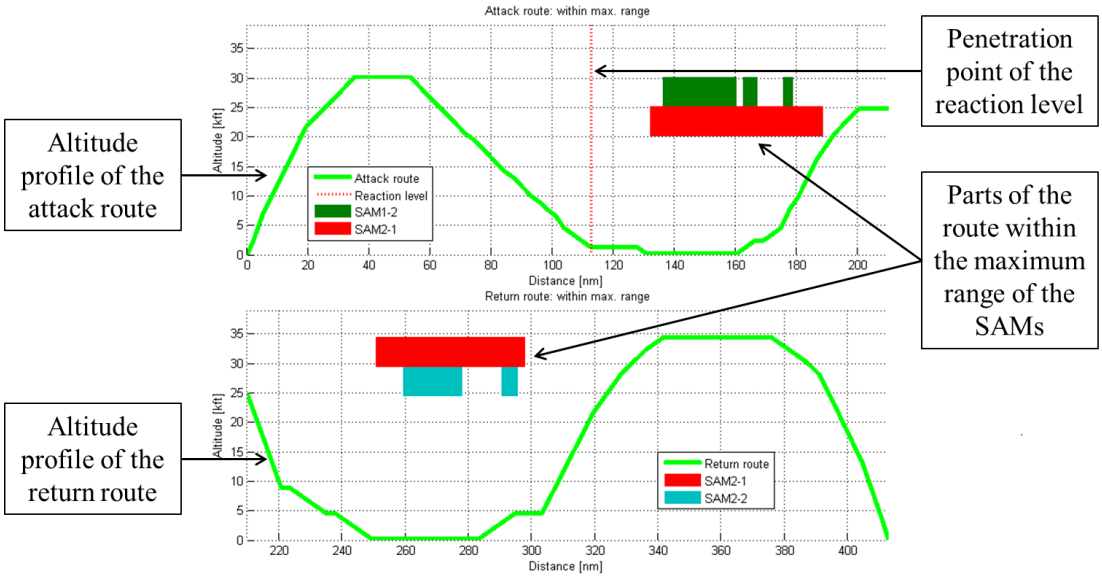


Figure 6.7: Parts of the optimal route within the maximum range of the SAMs.

pointed out in Figure 6.7. While the attack route does not involve exposure to the A/A threat, the extent of the A/A threat posed by the faster Red aircraft from the base RED1 surrounds the Blue aircraft during the return route. This leads to inevitable exposure to the threat for the major part of the return route.

While the optimal route represents the preferences reflected by the given weights of the objective costs, the DM might be discontent with the exposure to the S/A threat during the attack route. Flying within the LAR of a SAM before reaching the launch point sets the whole mission under risk. Additionally, conducting the necessary evasive maneuvers in the case of the SAM launch means diversion from the optimal route and makes it harder for the Blue aircraft to reach the launch point. Therefore, the weight of the S/A threat is increased to 3 in order to study if a route with less exposure to the S/A threat can be found. Then, the DM is willing to accept three times as much exposure to the A/A threat for the

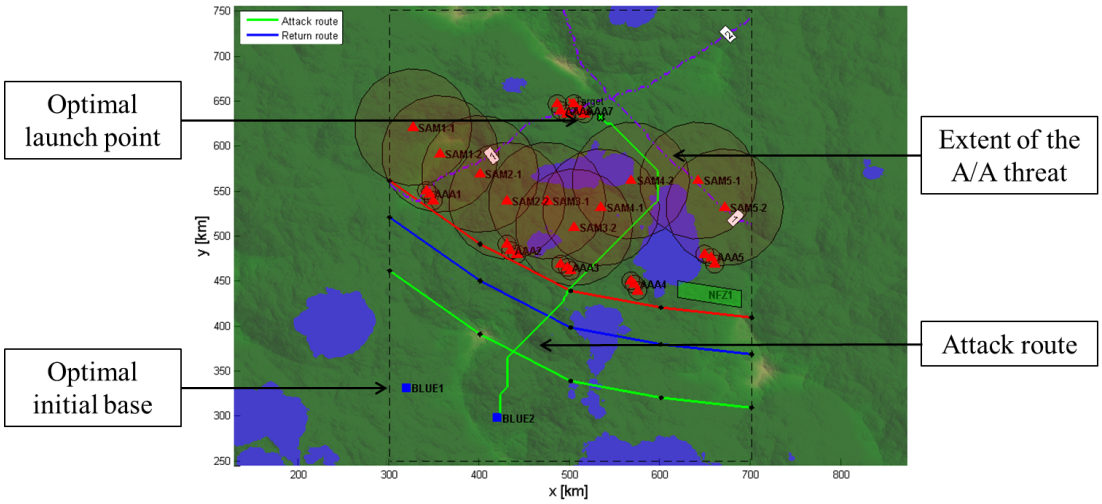


Figure 6.8: Attack route with the updated weights.

amount of decrease of the S/A threat than in the initial setting. Additionally, three times as long flight distance and three times as great fuel consumption are considered acceptable in order to avoid the S/A threat than with the initial weights. Therefore, $w^{S/A}/w^{A/A} = 3$ while the weights of the objective costs of the flight distance and the consumption of fuel stay the same.

The optimal route obtained with the updated weights ($w^{S/A} = 3, w^{A/A} = 1$, $w^D = 0.1$, and $w^F = 0.01$) is presented in Figures 6.8 and 6.9. The 3D view of the route is displayed in Figure 6.10 and the costs are given in Table 6.4. Now, the time needed to fly the optimal route is 49.6 min where the attack route takes 26.7 min and the return route 22.9 min. The new optimal route takes 2 minutes and 30 seconds longer to fly than the initial route. It is also 37.2 nm longer, requires 1347.8 lb more fuel, and involves additional 27.2 nm of travelling within the extent of the A/A threat. However, the route involves only 24.5 nm of travelling within the LARs of the SAMs which is almost half of the original exposure to the S/A threat.

The initial base of the optimal route is now BLUE2 from where the Blue aircraft ascends to 26,000 ft while heading northeast. The route descends along the reaction level and penetrates it at coordinates (498,440) as well as at the altitude of 1500 ft. Then, the route continues northeast for 30 nm while ascending to 3,5000 ft. The route then gradually descends to the minimum flight altitude and at coordinates (596,539) turns north between SAM4-2 and SAM5-1. After clearing

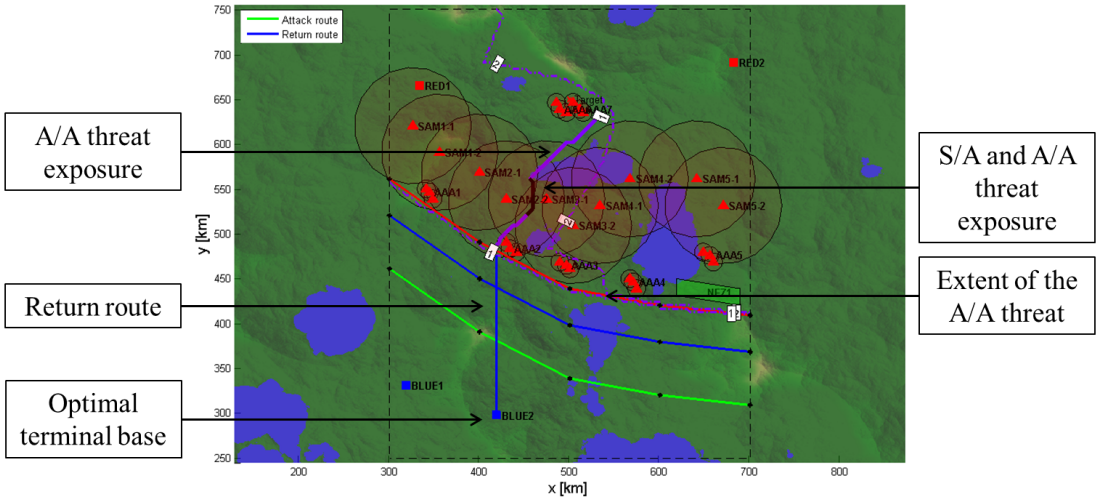


Figure 6.9: Return route with the updated weights.

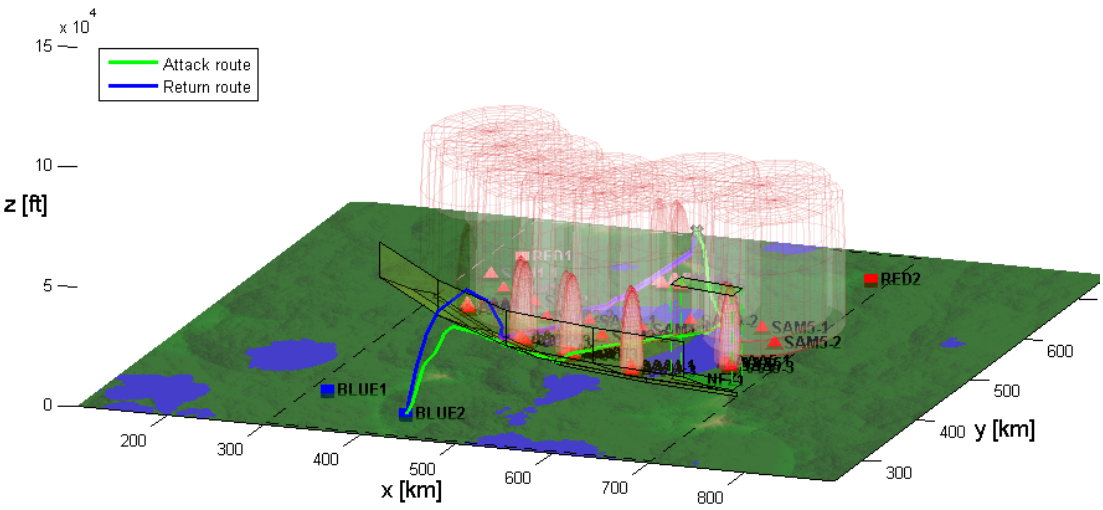


Figure 6.10: 3D view of the optimal route with the updated weights.

Table 6.4: Costs of the optimal route with the updated weights.

| | Attack | Return | Total |
|---|---|---|---|
| Flight distance | 235.9 nm | 213.9 nm | 449.8 nm |
| Fuel consumption | 5044.8 lb | 3784.0 lb | 8828.8 lb |
| S/A threat | 0 nm | 24.5 nm | 24.5 nm |
| A/A threat | 0 nm | 109.1 nm | 109.1 nm |

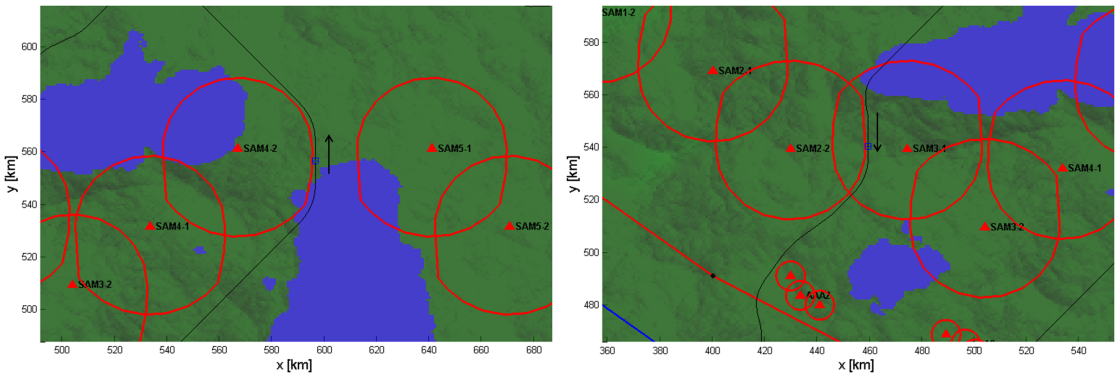


(a) LARs and the position of the Blue aircraft at time instant t = 19 min 45 s.

(b) LARs and the position of the Blue aircraft at time instant t = 33 min 21 s.

Figure 6.11: LARs of the SAMs during the optimal route. The position of the Blue aircraft is denoted with a blue rectangle.

the SAMs, the route turns northwest towards the launch point of a medium range A/G weapon at coordinates (533,632) while ascending to the launch altitude of 25,000 ft. After the launch point, the route travels 105 nm southwest towards the frontline. It then descends to the minimum flight altitude and flies south from coordinates (456,561) to (459,528) in order to navigate between SAM2-2 and SAM3-1. Before reaching the frontline at coordinates (415,483), the route deviates a few nm to the west in order to avoid the AAA battery AAA2. From the frontline, the aircraft following the route ascends to 33,000 ft and travels 100 nm south before landing in the base BLUE2.

Recall that the updated weights result in the optimal route that is longer, involves greater consumption of fuel, and is exposed to the A/A threat longer. However, the attack route has no S/A threat. By taking a detour to the west, the attack route is able to avoid the LARs of the SAMs completely. The route takes advantage of the dead zones of SAM4-2 and SAM5-1 which provides a corridor between the LARs of the SAMs. This is illustrated with the snapshot of the animation of the LARs in Figure 6.11a in which the Blue aircraft is marked with a blue rectangle. In the return route, the Blue aircraft flies within the LAR of SAM3-1 (see, Figure 6.11b). While the optimal route avoids most of the LARs, it still traverses the maximum ranges of multiple SAMs which is implied in Figure 6.12. Before accepting the route as the final solution of the MRPP, these parts of the route must be analyzed in the simulation phase of the solution procedure.

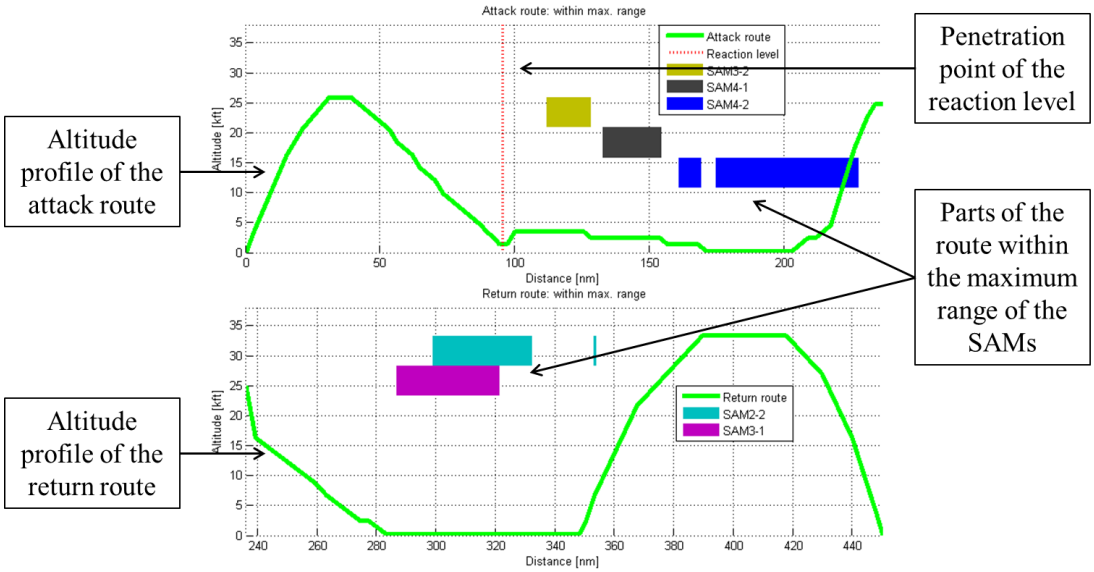


Figure 6.12: Parts of the optimal route obtained with the updated weights within the maximum range of the SAMs.

Similar to the attack route obtained with the initial weights, the attack route obtained with the updated weights does not involve exposure to the A/A threat. However, due to the longer attack route, the A/A threats have more time to expand. The threat posed by RED2 is still avoided but the threat by RED1 reaches the launch point approximately at the same time with the Blue aircraft even though the launch point is further from the base RED1. Because the distance from the launch point to the frontline is also greater, the return route has more exposure to the A/A threat as illustrated in Figure 6.9.

## 6.4 Simulation phase

### 6.4.1 Evaluation of S/A threat models

The optimal route obtained with the updated weights is evaluated with the simulation of SAM launches in order to study the threat caused by the SAMs on the optimal route. The simulation of SAM launches is conducted using the MisTarget simulation model with the launch interval of 10 seconds. The optimal route is smoothened using a moving average over 60 seconds. Figure 6.13 illustrates

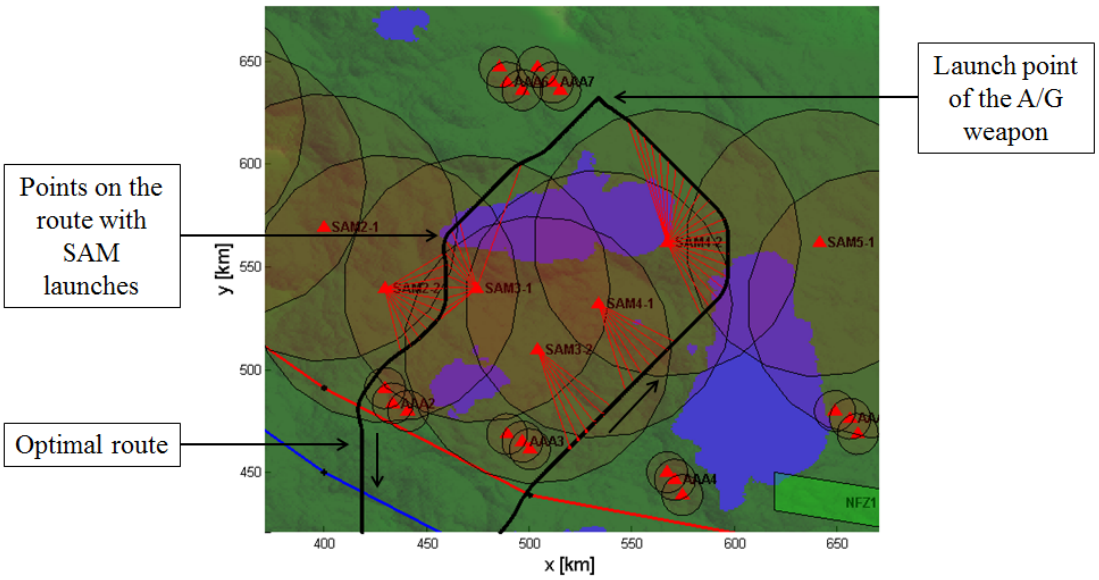


Figure 6.13: Simulation of SAM launches when the optimal route is obtained with the updated weights.

the route as well as the lines connecting the SAMs to the points on the route that correspond to the instances of the launches. The launch interval is set to 20 seconds in the figure which yields more comprehensible illustration.

The missile model of the SAM in the example analysis represents a typical medium range SAM. The minimum launch angle of the launch platform is 30°. The maximum flight time of the missile 180 seconds. In order to be able to achieve a successful launch, the missile must get within 30 meters of the aircraft at the minimum speed of 400 m/s. Otherwise, the launch is determined as unsuccessful.

The simulation consists of 114 launches by SAM2-2, SAM3-1, SAM3-2, SAM4-1, and SAM4-2. 43 of the launches are considered as successful. Illustrations of the trajectories of the SAMs are displayed in Figures 6.14a and 6.14b. The launch interval of 20 seconds is again used in the illustrations.

The platforms responsible for the successful launches in the simulation are SAM2-2, SAM3-1, and SAM4-2. This contradicts to the optimization results as the Blue aircraft travels only within the LAR of SAM3-1 (see, Figure 6.11). Therefore, SAM3-1 should be the only SAM to achieve successful launches. By examining the data of the launches (see, Figure 6.15), one can obtain that in the case of SAM4-2, the criteria of a successful launch are only barely fulfilled. Furthermore, these

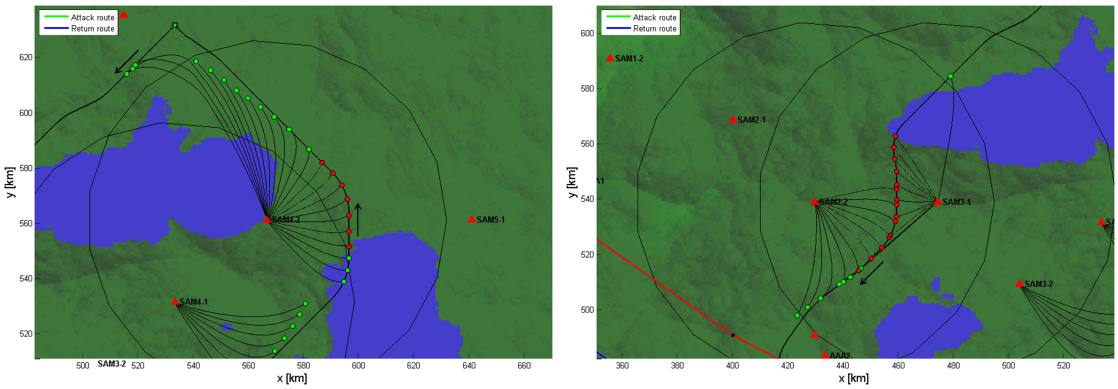


(a) Trajectories of SAM4-2.

(b) Trajectories of SAM2-2 and SAM3-1.

Figure 6.14: Trajectories of the SAMs when the optimal route is obtained with the updated weights.

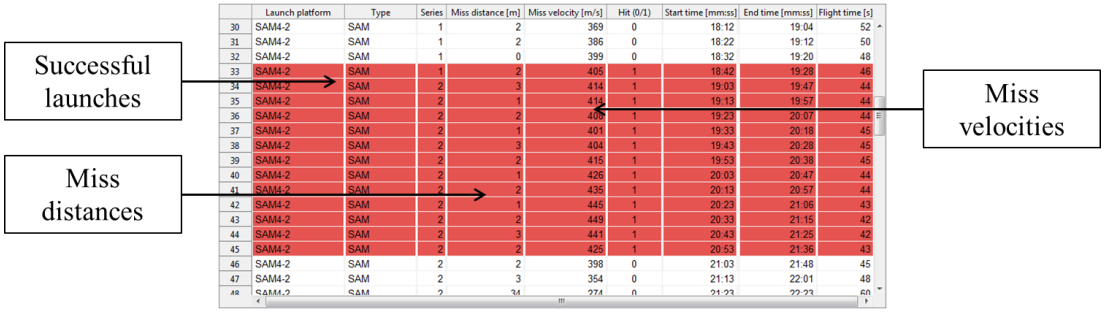


Figure 6.15: Launch data of the simulation of SAM launches.

launches occur when the Blue aircraft is flying at the minimum flight altitude. These facts indicate that the dead zone adjustment parameter of 32 km in the model of the SAM used in the optimization is slightly too small. A new value of 34 km is set and the optimization is repeated.

The optimal route obtained with the updated weights and the updated parameters of the S/A threat is depicted in Figures 6.16 and 6.17. The 3D view of the route is displayed in Figure 6.18 and the costs of the route are given in Table 6.5. The time needed to fly the optimal route is 50.5 min where the flight times of the attack and return routes are 27.0 min and 23.5 min, respectively. Compared to the earlier route, the flight time is approximately 30 seconds longer.

The initial base of the optimal route is again BLUE2. The rest of the attack route is similar to the earlier attack route with the exception of the route extending

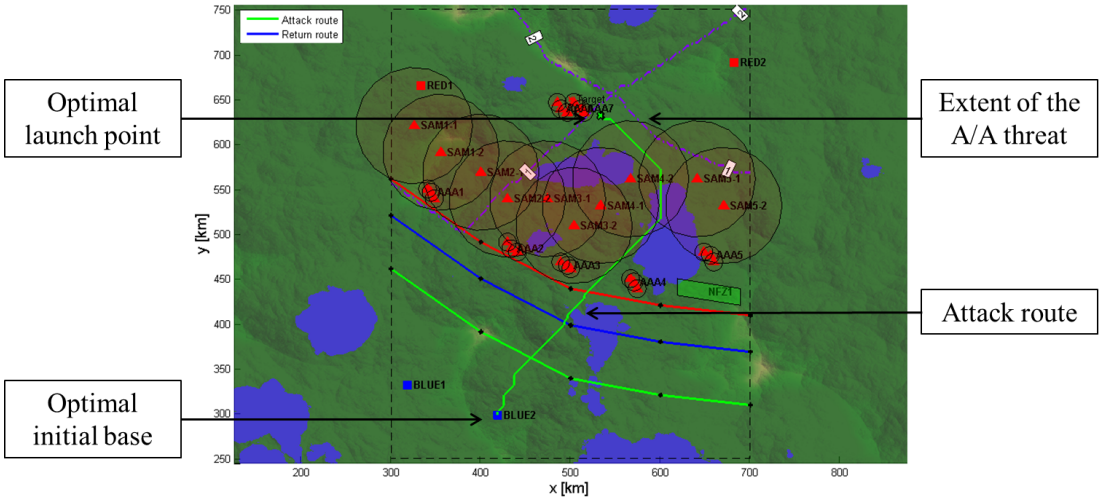


Figure 6.16: Attack route with the updated parameters of the S/A threat.

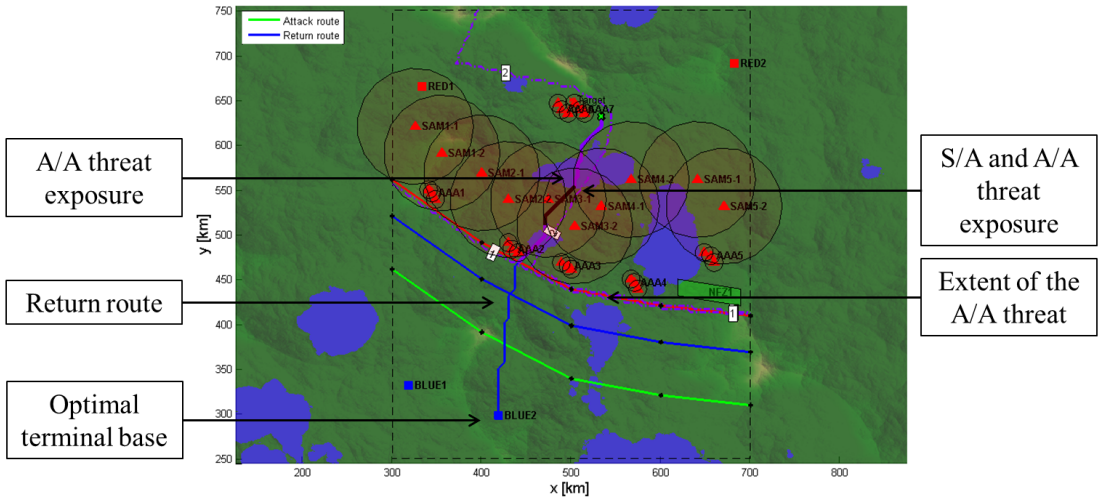


Figure 6.17: Return route with the updated parameters of the S/A threat.

Table 6.5: Costs of the optimal route with the updated parameters of the S/A threat.

| | Attack | Return | Total |
|---|---|---|---|
| Flight distance | 239.2 nm | 206.9 nm | 446.0 nm |
| Fuel consumption | 4829.6 lb | 3607.1 lb | 8436.7 lb |
| S/A threat | 0 nm | 31.5 nm | 31.5 nm |
| A/A threat | 0 nm | 108.4 nm | 108.4 nm |

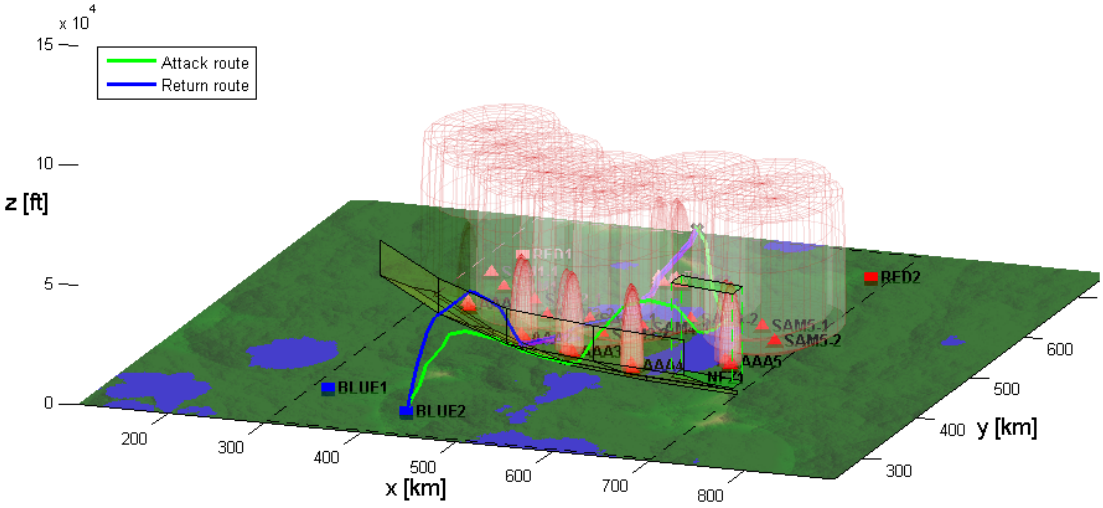


Figure 6.18: 3D view of the optimal route with the updated parameters of the S/A threat.

a few nautical miles more to the east leading to the avoidance of the increased LAR of SAM4-2. The corridor between the LARs of SAM4-2 and SAM5-1 remains despite the updated dead zone parameter, see Figure 6.19. The launch point is also the same at coordinates (530,628). The return route, instead of turning southwest, makes a 90° turn from the launch point to the south while descending gradually. Then, compared to the earlier route, the new return route travels approximately 30 nm more to the east. It ascends to the minimum flight altitude and continues between SAM3-1 and SAM3-2. After clearing the SAMs and avoiding the AAA battery AAA2, the route crosses the frontline at (441,469) and heads south while ascending to 33,000 ft. Then, the route ends in the base BLUE2 after travelling 446.0 nm. The objective costs of the route after updating the dead zone parameter are similar to the earlier route and include only small differences. The new route involves flying additional 7 nm within the LARs of the SAMs which is anticipated as the LARs are increased.

The simulation of SAM launches is conducted using the MisTarget simulation model with the launch interval of 10 seconds as well as using a moving average over 60 seconds in the smoothing of the optimal route. Figure 6.20 illustrates the route and the lines connecting the SAMs to the points of the route that correspond to the launches.

The simulation consists of 131 launches by SAM3-2, SAM3-2, SAM1, and SAM4-

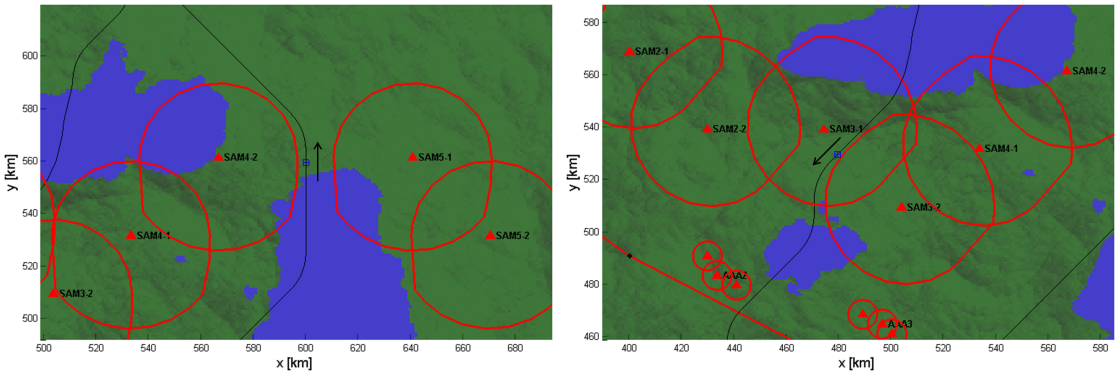


(a) LARs and the position of the Blue aircraft at time instant t = 20 min 17 s.

(b) LARs and the position of the Blue aircraft at time instant t = 33 min 37 s.

Figure 6.19: LARs of the SAMs when the optimal route is obtained with the updated threat parameters. The position of the Blue aircraft is denoted with a blue rectangle.

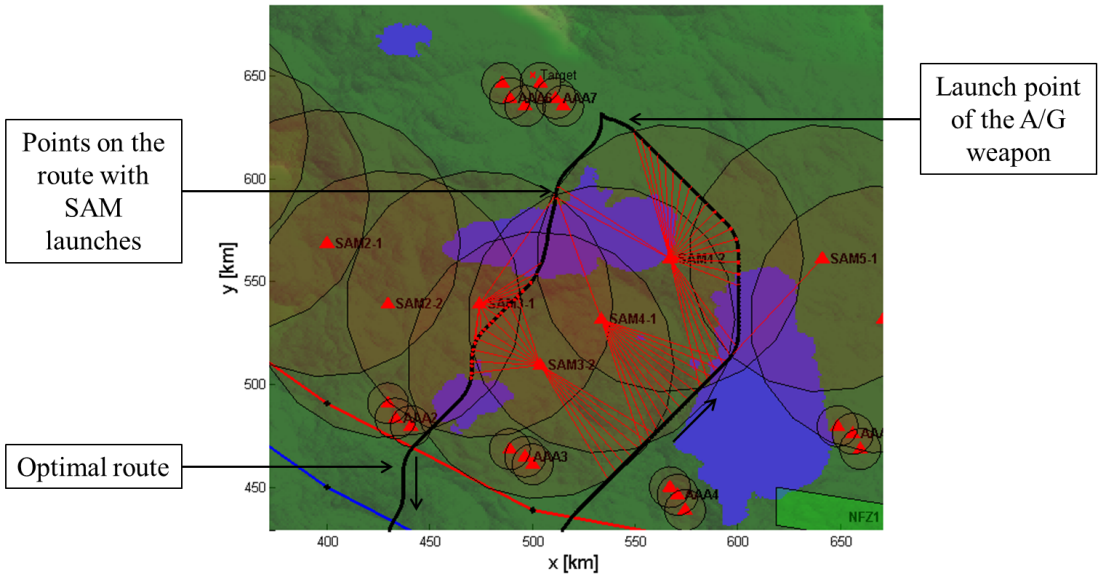


Figure 6.20: Simulation of the SAM launches when the optimal route is obtained with the updated parameters of the S/A threat.

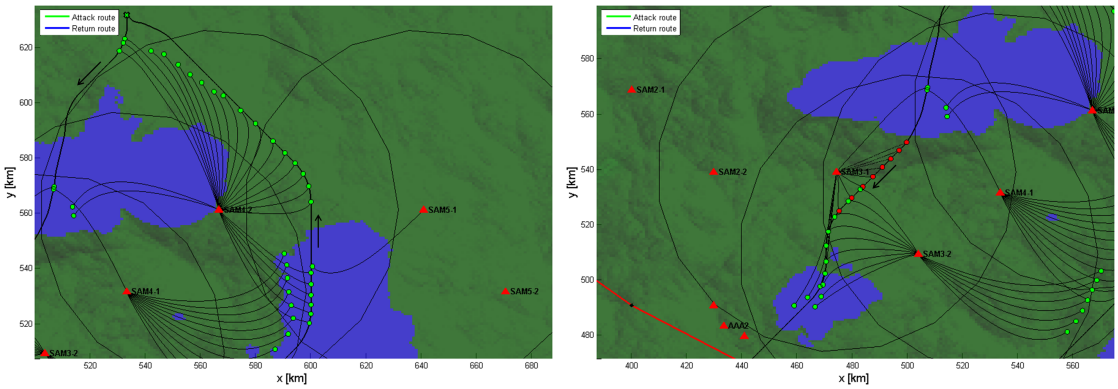


(a) Trajectories of SAM4-2.

(b) Trajectories of SAM2-2 and SAM3-1.

Figure 6.21: Trajectories of the SAMs when the optimal route is obtained with the updated parameters of the S/A threat.

2. 18 of the launches are considered as successful. The illustrations of the trajectories of the SAMs are displayed in Figures 6.21a and 6.21b.

Compared to the earlier route, the launches of SAM4-2 do not fulfill the criteria of the successful launch. Additionally, the new route involves 25 fewer successful launches compared to the earlier route. The only launch platform achieving successful launches is SAM3-1. This concurs with the results obtained in the optimization phase as the LAR of SAM3-1 is the only LAR the optimal route intersects. As optimization and simulation results concur, the optimal route is determined as feasible in terms of the S/A threat. However, using the updated weights of the objective costs, the successful launches of the SAMs cannot be avoided. It should be noted that the mission can be executed without any exposure to the S/A threat if the return route follows the attack route back to the frontline. By employing this return route, in addition to the A/A threat from RED1 also the A/A threat from RED2 reaches the Blue aircraft. This results in the amount of the A/A threat that exceeds the costs that are saved by avoiding the S/A threat and the route is not therefore optimal with the updated weights of the objective costs.

### 6.4.2 Evaluation of A/A threat models

Next, the A/A threat on the optimal route obtained with the updated weights and the updated parameters of the S/A threat (see, Figures 6.16 and 6.17) is examined with the help of the simulation model. The A/A threats are simulated with the parameters given in Table 6.2. The extent of the A/A threat at various time instances of the simulation is presented in Figures 6.22a - 6.22c. The position of the Blue aircraft is marked with a blue rectangle. The reaction level at the altitude of 1500 ft, i.e., the frontline, is denoted with a red line. In the simulation, the A/A threats start to expand after the Blue aircraft penetrates the reaction level and the delay times of the A/A threats have been passed (see, Figure 6.22a). The Blue aircraft launches the A/G weapon at the launch point and the A/A threat from the base RED1 reaches the position of the aircraft (see, Figure 6.22b) approximately at the same time. Similar to the optimization results, the Blue aircraft stays within the extent of the threat until it reaches the frontline. Because of the slower speed of the A/A threat type DCA2, the threat from the base RED2 does not reach the Blue aircraft before it reaches the frontline (see, Figure 6.22c). These results of the simulation of the A/A threats concur with the results provided by the optimization model. Thus, the parameters of the A/A threat do not need revision. Therefore, the optimal route obtained with the updated weights and parameters of the S/A threat as well as with the original parameters of the A/A threat is feasible, and therefore is the optimal solution of the MRPP at hand.

## 6.5 Area of influence calculation

Flying the optimal and feasible route of the example A/G mission discovered in Sections 6.3 and 6.4 involves exposure to the S/A threat which poses risk to the success of the mission. Therefore, it is useful to study if any of the S/A platforms could be neutralized in order to find new routes with less exposure to the threats. As noted in the introduction of this thesis, the mission type where the goal is to weaken the capability of the enemy to defend its airspace is called SEAD. Using the feature of area of influence calculation of SARSS, this kind of study can be conducted. In the following, the S/A platforms that can be neutralized with A/G

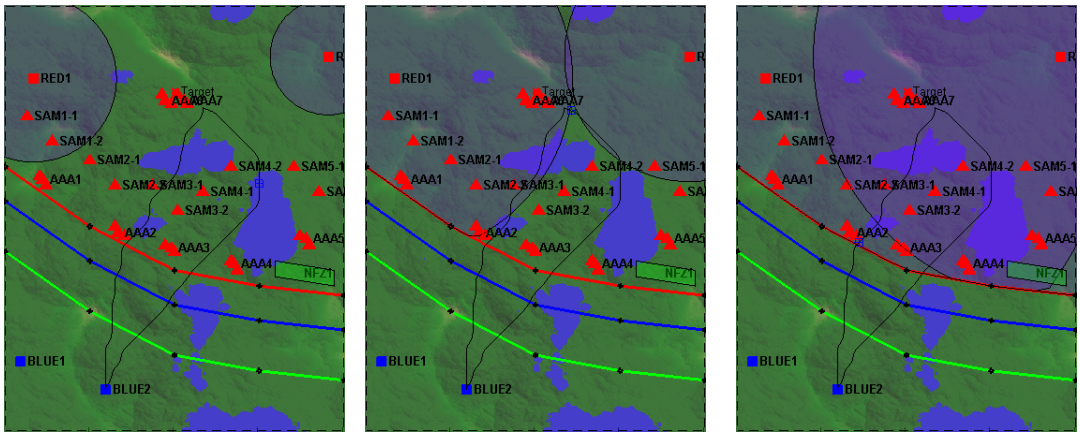


(a) t = 19 min 13 s. (b) t = 25 min 45 s. (c) t = 37 min 45 s.

Figure 6.22: Extent of the A/A threats at different time instants of the simulation. The red line denotes the frontline and the blue rectangle the position of the Blue aircraft, respectively.

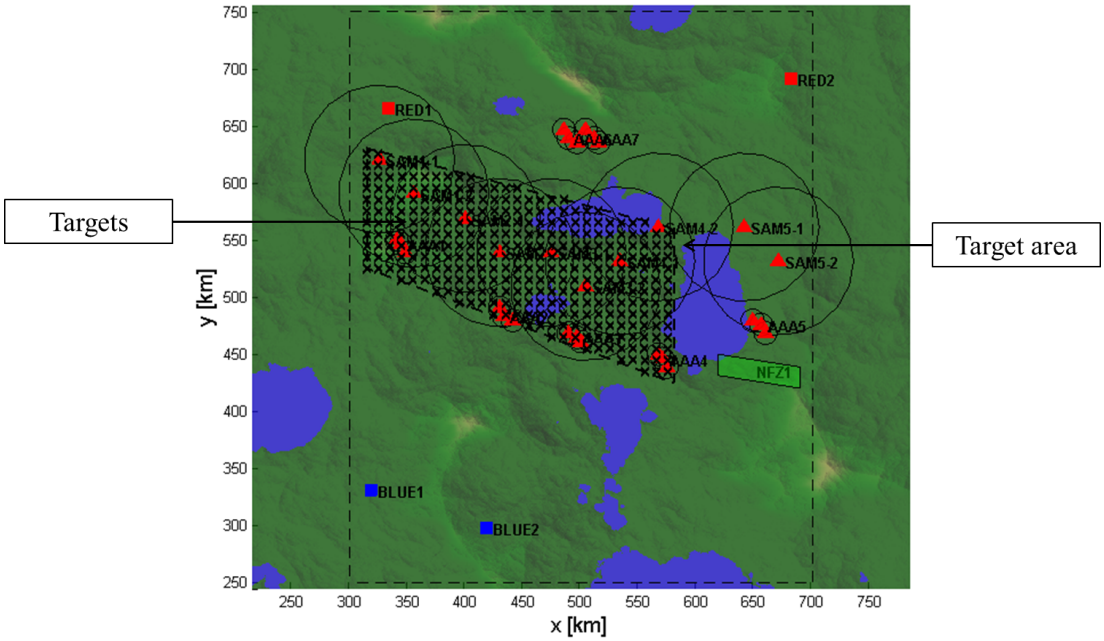


Figure 6.23: Targets in the area of influence calculation. x refers to a position of the target.

weapons without the exposure to the S/A threats are identified. Then, one of the S/A platform is removed and a new optimal route is determined through the weakened defenses.

The target area is depicted in Figure 6.23. The corners of the area are set to

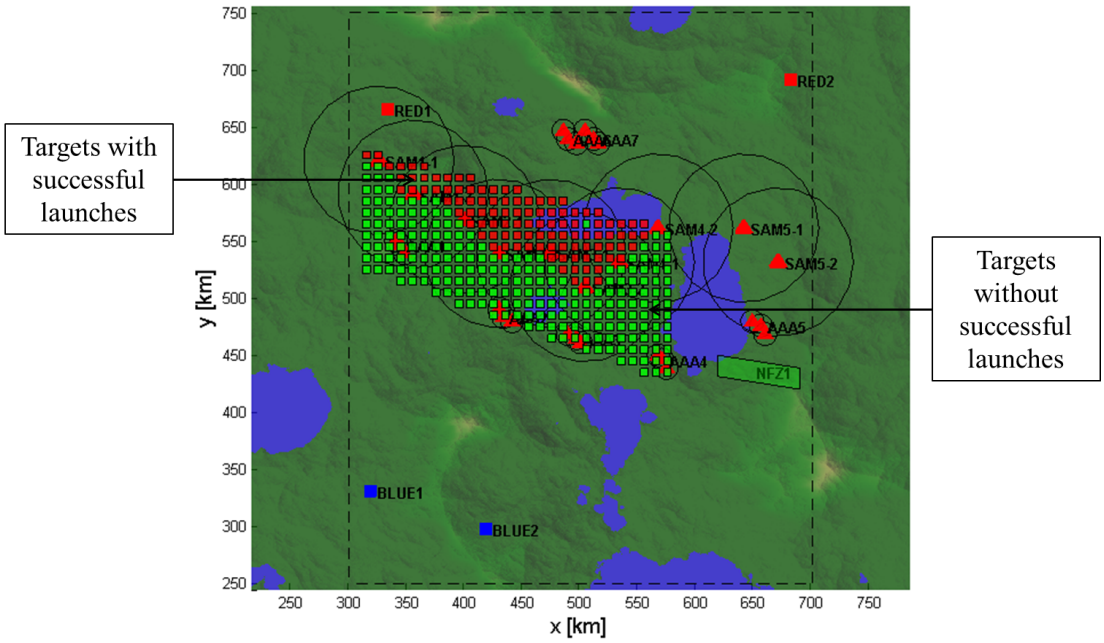


Figure 6.24: Results obtained in the area of influence calculation. The red squares implicate the targets that involve successful launches and the green squares the targets that can be influenced safely.

coordinates (315,525), (315,630), (580,560), and (580,425) so that the area envelopes the SAMs SAM1-1 to SAM4-2 and the AAA batteries AAA1 - AAA4. The target coordinates are laid over the target area with 10 km intervals. In total, the area consists of 324 targets. The same launch points 10 nm and 25 nm from the targets at altitudes 10,000 ft and 25,000 ft are considered as before. The weights of the objective costs are kept same as in Section 6.4. Additionally, the same simulation parameters are used.

The results of the area of influence calculation are illustrated in Figure 6.24. The red rectangles denote the targets which cannot be influenced with the A/G weapons without the successful launches of the SAMs when flying the optimal route. The targets that can be influenced without the successful launches when employing the optimal route are denoted with green rectangles. Now, one can notice that only SAM2-1 and SAM3-1 have red rectangles at their coordinates. All the other SAMs are located in the area with green rectangles and can therefore be neutralized with the A/G weapons without flying a route that involves successful launches. Additionally, all the AAAs in the target area are located at coordinates that can be safely influenced with the A/G weapons.

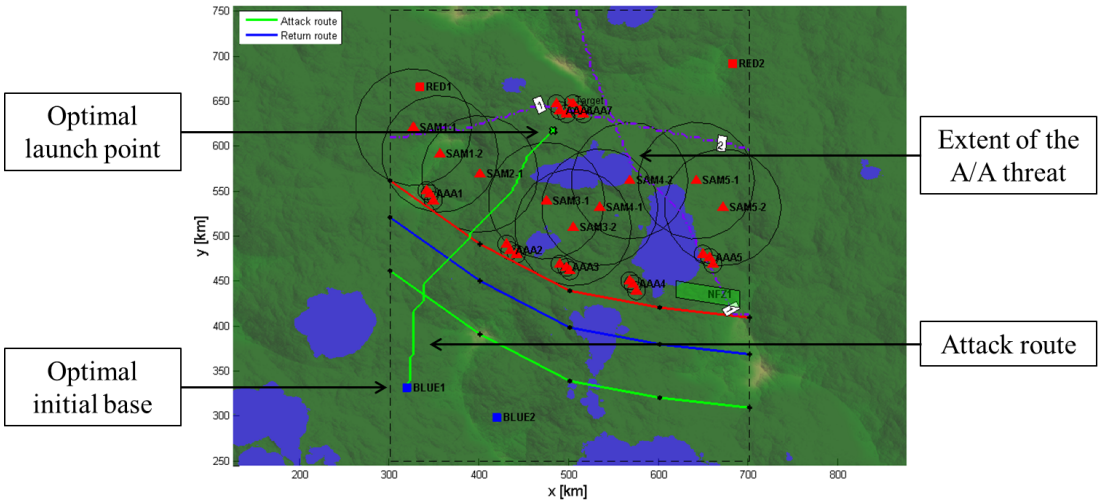


Figure 6.25: Optimal attack route after the SEAD mission.

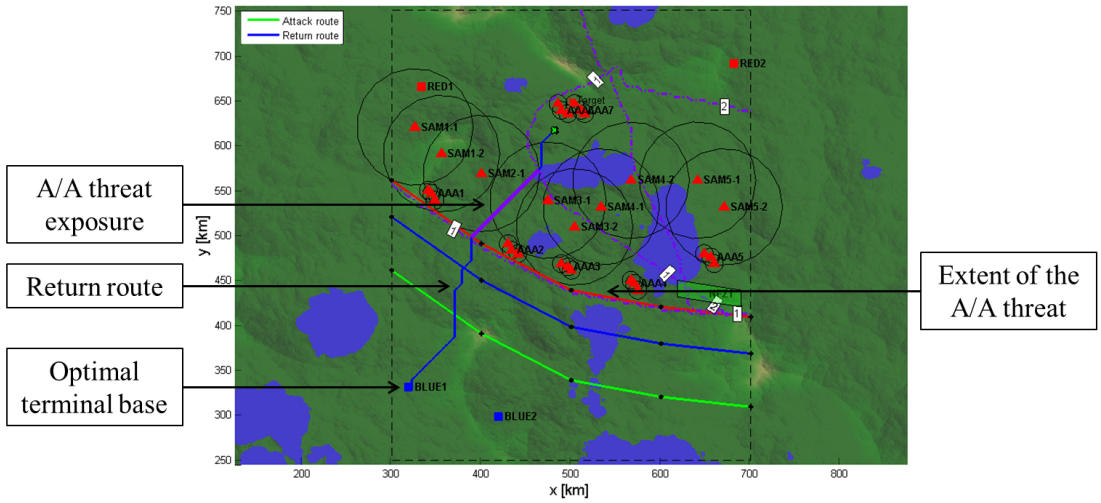


Figure 6.26: Optimal return route after the SEAD mission.

Next, an optimal route is determined in the case that SAM2-2 is first neutralized with the help of a SEAD mission. SAM2-2 is the logical choice as it is located on the straightest path from the base BLUE1 to the launch point. The weights of the objective costs as well as the simulation parameters are kept the same as before. The resulting optimal route is presented in Figures 6.25 and 6.26, and the objective costs of the route are given in Table 6.6. The time needed to fly the optimal route is 43.8 min where the attack route takes 21.7 min and the return route 22.1 min, respectively.

The optimal initial base after neutralizing SAM2-2 is still BLUE1. The attack

Table 6.6: Costs of the optimal route after the SEAD mission.

| | Attack | Return | Total |
|---|---|---|---|
| Flight distance | 191.4 nm | 191.9 nm | 383.2 nm |
| Fuel consumption | 3788.6 lb | 3156.3 lb | 6944.9 lb |
| S/A threat | 0 nm | 0 nm | 0 nm |
| A/A threat | 0 nm | 56.4 nm | 56.4 nm |

route first ascends to 30,000 ft and then descends along the reaction level. It penetrates the level at coordinates (389,499) and at the altitude of 1,500 ft. The route then heads northeast towards the launch point and stays under 5,000 ft leading to the avoidance the LARs of SAM2-1 and SAM3-1. After clearing the SAMs, the route ascends to the launch point, i.e., the altitude of 25,000 ft at coordinates (482,617). After the launch point, the route turns southwest back towards the frontline while descending to the minimum flight altitude in order to avoid the LARs of the SAMs. After the frontline, the route ascends to 35,000 ft and heads back to the base BLUE1.

The optimal route after neutralizing SAM2-2 does not involve any exposure to the S/A threat. The gap between SAM2-1 and SAM3-2 is wide enough which enables a safe passage to the Blue aircraft. This is also validated by the simulation of SAM launches as no successful launches of SAMs occur. Because the attack route is straighter than before, the extent of the A/A threat does not reach as far. This results in almost half of the cost caused by the threat. Additionally, the route has significantly lower fuel consumption and it takes several minutes less time to fly. The simulation of the A/A threat also yields similar results as the optimization model and therefore the obtained optimal route can be determined the feasible and the final solution of the MRPP.

## 6.6 Summary

Based on the results of the example analysis carried out in sections 6.3, 6.4, and 6.5 the A/G mission under consideration is possible to conduct with moderate exposure to the S/A and A/A threats posed by the Red force. In addition, the

length of the optimal route as well as the consumption of fuel are within an acceptable range. The optimal route provided by the optimization model takes advantage of the dead zones of the S/A threats in order to be able to reach the launch point of the medium range A/G weapon. Additionally, the optimization identifies the low altitude penetration point of the reaction level which results in the avoidance of the A/A threats on the attack route. Because the triggering of the A/A threats occurs later than the penetration of the reaction level on higher altitudes, the Red aircraft do not have the necessary time to intercept the Blue aircraft before the launch point. The optimal route is evaluated with the simulation of the S/A and A/A threats. The simulation results concur with those of the optimization model. Therefore, the route obtained with SARSS can be regarded as the feasible and optimal solution of the example MRPP although it involves the successful launches of the SAMs.

The area of influence calculation implies that most of the SAM launch platforms and AAA units can be neutralized without the risk of successful SAM launches. According to the results, removing one of the SAMs that can be neutralized safely from the mission description enables the mission to be conducted without exposure to the S/A threats. Additionally, as the new optimal route to the launch point is shorter, the A/A threats from the bases have less time to reach the Blue aircraft. Coupled with the shorter route, this results in the reduction of the aggregated cost and therefore the reduction of the risks related to conducting the mission.

# Chapter 7

# Future research

In this chapter, the future research avenues regarding the approach towards the automated solution of the MRPP as well as SARSS are discussed. While SARSS is at this stage a comprehensive tool for solving MRPPs, additional research questions remain. The future research categories include exploring different shortest path algorithms, adding new optimization objectives to the optimization model as well as improving the GUI of SARSS. Additionally, the current representations of flight mechanics, threats and fuel consumption can be developed in the optimization model.

## 7.1 Computational improvements

SARSS uses an explicitly defined network in solving the shortest path problem. The whole optimization network is formed before applying the optimization algorithm and it is stored wholly in the memory of the computer. While Dijkstra's algorithm solves the problem fast, the memory requirements for storing the whole network can be extensive. Furthermore, aggregating the objective costs and applying the weights can slow down the optimization significantly, if the physical memory runs out. An implicitly defined network can be more efficient in these cases. In the case of the implicitly defined optimization network, the costs of the edges are calculated as the algorithm reaches the node from where the edges originate. If the implicit network is used with an algorithm, e.g., A* search [87],

that does not require the whole network to be constructed, memory requirements are lower. A* search algorithm has been used successfully in the previous studies of the MRRP (see, e.g., [3, 2]) and could be used in SARSS as well. Using the A* search also allows the use of constraints for the fuel consumption and the turn radius of an aircraft as well as for flight time and threat exposures. Additionally, using the A* search, time dependent costs such as the expanding of the A/A threat can be taken into account. However, calculating the costs individually for each edge of the network might be slower than constructing the whole network at once.

The updating of the threat models as well as the repetition of the optimization and the simulation are now left to the user of SARSS. These tasks could be automated so that the threat models are updated automatically based on the simulation results and the calculations are repeated. The iteration is then continued until the results of the optimization and the simulation concur.

## 7.2 Modeling improvements

Terrain is not considered in SARSS as aircraft conducting an A/G mission fly at relatively high altitude and can rarely benefit from terrain masking. However, the option of terrain masking should be taken into consideration in the further development of SARSS. Then, in addition to aircraft, one could study the optimal use of low flying helicopters and unmanned aerial vehicles that can safely maneuver behind elevated terrain. For these types of air vehicles, the structure of the optimization network should also be reconstructed to reflect their performance.

Using parallel edges in the network, different flying speeds could be implemented. Aircraft speed has an effect on, e.g., fuel consumption, the LARs of the SAMs, and the extent of the A/A threat. Such an implementation has been used in the planning of the route of submarine through the network of sonars trying to detect it [127].

Reaching the launch point of an A/G weapon is only a part of a successful mission. Therefore, it would be useful to more closely study the route of the weapon itself. As modern precision guided ammunitions are able to maneuver independently, the

route optimization could be extended to consider the routes of the ammunitions as well. On the other hand, by calculating risks posed by the close range air defenses of the enemy, a terminal cost can be assigned to each launch point. These costs can be taken into account when determining the optimal route of the aircraft.

The optimal route obtained with SARSS can seem counter-intuitive. In this vein, it can be convenient to present routes from non-optimal bases to non-optimal launch points as well. Because Dijkstra's algorithm solves the single source shortest path problem, the routes to the non-optimal launch points are calculated as well. Visualizing these routes and presenting their costs increases the understanding of the DM about the optimal route. Additionally, the what-if analysis of which bases to use can be conducted at the same time.

The Red bases could include multiple types of A/A threats. This would reflect the situation where different types of aircraft are scrambled at alternative times from the base. Currently, only one A/A threat with a single reaction time can be situated in a base. Additionally, reaction times could be base specific to represent the effect of the infrastructure and other factors on the reaction time. They could also represent the time interval in which consecutive squadrons of aircraft can be scrambled.

Because of the nature of the optimization network, the optimal routes are not smooth and might therefore have steep turns. If the spacing of the network is tight relative to the performance of the aircraft, this might make the routes challenging to follow in practice. While the routes are smoothened in the simulation phase, the question should the route actually be able to be flown, is not addressed. One possibility to verify that the route is flyable would be to smoothen the route as long as the horizontal and vertical accelerations on the route would not exceed the operational limits of the aircraft.

Currently, the MisTarget simulation model is used to evaluate optimal routes. It could also be used to determine the LARs of SAMs by simulating cases where the aircraft flies using alternative speeds, altitudes, and distances from the launch platform. In the current implementation of SARSS, initial LAR coefficients are determined by the DM using expert assessment. The determination of the co-

efficients with Mistaget would save time as they are correct from the start and would not need revision.

More advanced simulations could also be conducted and linked to SARSS. At this moment, simulating the SAM launches related to a single route can take several minutes. Adding the launch logic of a SAM weapon system to the simulation would greatly lower the number of launches as the simulation is started only when the launch occurs in practice. Such a launch logic has been studied, e.g., using the FLAMES simulation environment [24] and could be used to determine the times for launches in SARSS as well.

## 7.3 Improvements to GUI of SARSS

While the GUI of SARSS is comprehensive and easy to use, it still needs refining. Even though an extensive error checking exists for user inputs in the GUI, there are few occasions where invalid inputs can cause the optimization routine to crash. Additionally, more detailed error messages in the case of invalid inputs can help better understand the origin of the error.

The overall usability of the GUI can be improved as well. For example, the position of the objects, e.g., SAMs or bases, on the map could be changed by dragging the objects with the cursor of a mouse. Fine tuning the positions by typing the coordinates is time consuming. Fortunately, MATLAB has built-in functions for this kind of functionality.

The map of the GUI is fixed at a certain resolution. When zooming the map, pixelation can make the map unreadable. A higher resolution map uses more memory and takes longer time to load on the screen. A dynamic map that changes its resolution according to the level of zoom and draws only the needed part of the map would be ideal. Using higher resolution maps also require an intelligent map image loading routine because displaying images in MATLAB is memory intensive.

An imbedded help documentation in SARSS would improve the user experience. Because of the number of parameters in the optimization and simulation mod-

els, a reference guide on the impact of the parameters would make the use of SARSS more comprehensible. The utilization of XML in the implementation of the documentation pages would enable them to be browsed with the help of the MATLAB's help browser.

# Chapter 8

# Conclusions

This thesis introduced a novel approach towards the automated solution of the mission route planning problem (MRPP) based on network optimization and simulation. In the approach, the MRPP is formulated as a multi-objective shortest path problem where the optimization network represents the possible waypoints and movements of the aircraft. The objectives are flight distance, fuel consumption, and exposures to threats posed by surface-to-air and air-to-air weapon systems. The multi-objective shortest path problem is reduced to a single-objective optimization problem by forming an aggregate objective function using a weighted sum of the objective costs. A trade-off method is applied to elicit the weights from the decision maker. The optimal route is calculated using a modified version of Dijkstra's algorithm. The threats involved in flying the optimal route are evaluated with a sophisticated simulation model in order to assess the results acquired by optimization. If the simulation results contradict the optimization results, the models of the threats used in the optimization are modified, and the optimization as well as the simulation are repeated.

In the approach, more elaborate models for fuel consumption and the ascent and descend capabilities of the aircraft are applied compared to the existing network optimization formulations of the MRPP. The modeling of the surface-to-air threats takes into consideration the state of the aircraft as well as the kinematic capability of the missile to reach the aircraft which have not been addressed before. Additionally, a new cost that represents the air-to-air threat posed by

enemy aircraft is introduced. On the other hand, the selection of the optimal initial and terminal bases of the mission as well as the optimal launch point of an air-to-ground weapon is also conducted when determining the optimal route. The selection of the launch point enables the determination of the corresponding air-to-ground weapon. The novel feature of the approach is also the use of the continuous time simulation model in order to more accurately analyze the surface-to-air and air-to-air threats involved in flying the optimal route.

The solution procedure of the approach is implemented in a software named Strike Aircraft Routing Software Suite (SARSS). SARSS includes modules for defining air-to-ground missions and calculating optimal routes as well as evaluating the optimal routes with simulation. In addition, MisTarget simulation model for simulating surface-to-air missiles is integrated in the simulation module. The modules are controlled with the graphical user interface of SARSS. The results of the optimization and the simulation are presented as 2D and 3D visualizations of the optimal route. Additional metrics such as the altitude profile of the optimal route and the cumulation of the threats are presented. The trajectories of the surface-to-air missiles and the expanding of the extent of the air-to-air threat over time can be studied using the animation of the simulation results.

SARSS produces optimal routes for air-to-ground missions with multiple objectives. SARSS can also be applied to study the effects of alternative initial and terminal bases as well as targets on the costs of flying the mission. The comparison of different weight sets of the objective costs is also conducted by examining the objective costs of the optimal routes related to the weight sets. SARSS can also be used in the planning of suppression of enemy air defenses missions by determining the threats that pose the highest risk on the optimal route. This information reveals which threats must be neutralized in order to carry out the mission safely. In addition, SARSS can be employed inversely by studying optimal routes through friendly air defenses. Then, the costs of the optimal routes imply how well targets on friendly territory are defended.

One of the features of SARSS is the identification of areas that can be safely influenced with air-to-ground weapons. This feature allows the determination of optimal routes to multiple targets at the same time. The results are visualized as a color coded grid of the targets that can be influenced without exposure to the

threats. This feature can also be utilized in the planning of suppression of enemy air defenses missions as illustrated in the example analysis of the thesis. Additionally, one can identify the vulnerable areas of friendly air defenses. Therefore, SARSS allows the allocation of the defensive resources as well.

SARSS provides an efficient and easy way to plan routes for air-to-ground missions involving multiple objectives. The fast construction of the optimization network as well as the efficient optimization and simulation routines allow the use of larger, as well as more complex and more realistic, representation of the MRPP that has previously been possible. An issue related to many existing software implementations dealing with MRPPs is that they require special knowledge of the underlying optimization models. In SARSS, however, knowledge of network optimization, simulation or programming is not needed. The parameters of the optimization and simulation models are well explained and controlled by the graphical user interface of SARSS. The comprehensiveness of the graphical user interface was found essential in the preliminary testing of SARSS. The preliminary tests with SARSS imply that the decision maker is able to define air-to-ground missions as well as to produce and analyze optimal routes with little training.

SARSS calculates an optimal route for a realistic air-to-ground mission involving multiple bases, threats, and targets in a few seconds when using a standard PC. However, if the memory requirements are exceeded, calculation times can add up to several minutes. A typical mission requires about 1GB of free RAM which should be available in almost every modern computer. Contrary to many existing implementations, the number of surface-to-air threats has negligible effect on the computational effort required by the optimization model. The evaluation of routes with simulation takes time that is related to the number of launches of surface-to-air missiles. It can be anything between seconds and hours depending on the launch interval and the total amount of time the aircraft travels within the maximum range of the missiles.

Based on the experience acquired in the example analysis as well as in the preliminary tests conducted with SARSS, the approach presented in this thesis for solving automatically the MRPP offers a transparent and tractable procedure to support the calculation of optimal routes employed in air-to-ground missions. Using the optimization model that generates optimal routes promptly and then

evaluating them with the sophisticated simulation model proved to be an efficient way to solve the MRPP. The updating of the weights of the objective costs and the parameters of the threat models provides optimal routes that are realistic and obey to the preferences of the decision maker.

Although SARSS is a comprehensive tool for solving MRPPs, many ideas for improvements and additions are under consideration. These additions include studying alternative optimization algorithms and the improvements to the current representations of the threats in the optimization model. The automatization of modifying the parameters of the optimization model based on the simulation results is also considered in the future research.

The automated solution approach presented in the thesis can also be applied to other multi-objective nonlinear dynamic optimization problems. Solving the approximate formulation of a dynamic optimization problem by using network optimization requires less computational effort than solving the original problem. Using the simulation model representing the dynamic system at hand, the quality, realism, and feasibility of the resulting optimal solution can be assessed. If the assessment implies shortcomings, the approximate formulation is updated according to the simulation results, and the calculations are repeated until the optimal and feasible solution for the original problem is obtained.

# Bibliography


[1] W.A. Menner. The Navy's Tactical Aircraft Strike Planning Process. *Johns Hopkins APL Technical Digest*, 18(1):90–104, 1997.

[2] E. Sezer. Mission Route Planning with Multiple Aircraft & Targets Using Parallel A* Algorithm. Master's thesis, Air Force Institute of Technology, School of Engineering and Management, OH, 2000.

[3] M. S. Gudaitis. Multicriteria Mission Route Planning Using a Parallel A* Search. Master's thesis, Air Force Institute of Technology, School of Engineering and Management, OH, 1994.

[4] K. Yavuz. Multi-Objective Mission Route Planning Using Particle Swarm Optimization. Master's thesis, Air Force Institute of Technology, School of Engineering and Management, OH, 2002.

[5] D. Bertsekas. *Network Optimization: Continuous and Discrete Models*. Athena Scientific, 1998.

[6] A.M. Law, W.D. Kelton, and W.D. Kelton. *Simulation modeling and analysis*, volume 2. McGraw-Hill, 1991.

[7] K. Virtanen, H. Ehtamo, T. Raivio, and R.P. Hamalainen. VIATO-visual interactive aircraft trajectory optimization. *IEEE Transactions on Systems, Man, and Cybernetics, Part C: Applications and Reviews*, 29(3):409–421, 1999.

[8] J. Karelahti, K. Virtanen, and T. Raivio. Near-optimal missile avoidance trajectories via receding horizon control. *Journal of Guidance Control and Dynamics*, 30(5):1287–1298, 2007.

[9] J.M. Hebert. *Air Vehicle Path Planning*. PhD thesis, Air Force Institute of Technology, School of Engineering and Management, OH, 2001.

[10] M. Zabarankin, S. Uryasev, and R. Murphey. Aircraft routing under the risk of detection. *Naval Research Logistics*, 53(8):728–747, 2006.

[11] T. Inanc, K. Misovec, and R.M. Murray. Nonlinear trajectory generation for unmanned air vehicles with multiple radars. In *43rd IEEE Conference on Decision and Control*, 2005.

[12] T. Schouwenaars, B. De Moor, E. Feron, and J. How. Mixed integer programming for multi-vehicle path planning. In *European Control Conference*, 2001.

[13] C. S. Ma and R. H. Miller. MILP optimal path planning for real-time applications. In *Proceedings of the 2006 American Control Conference*, 2006.

[14] A. Richards and J. P How. Aircraft trajectory planning with collision avoidance using mixed integer linear programming. In *Proceedings of the 2002 American Control Conference*, 2002.

[15] A. Chaudhry, K. Misovec, and R. D'Andrea. Low observability path planning for an unmanned air vehicle using mixed integer linear programming. In *43rd IEEE Conference on Decision and Control*, 2005.

[16] M. John, D. Panton, and K. White. Mission planning for regional surveillance. *Annals of Operations Research*, 108(1):157–173, 2001.

[17] S.H. Lee. Route Optimization Model for Strike Aircraft. Master's thesis, Naval Postgraduate School, CA, 1995.

[18] W.M. Carlyle, J.O. Royset, and R.K. Wood. Routing Military Aircraft with a Constrained Shortest-Path Algorithm. Technical report, Naval Postgraduate School, CA, 2007.

[19] K. Virtanen, J. Karelahti, and T. Raivio. Modeling air combat by a moving horizon influence diagram game. *Journal of Guidance Control and Dynamics*, 29(5):1080–1091, 2006.

[20] J. Poropudas and K. Virtanen. Game-theoretic validation and analysis of air combat simulation models. *IEEE Transactions on Systems, Man and Cybernetics, Part A: Systems and Humans*, 40(5):1057–1070, 2010.

[21] J.B. Cruz Jr, M.A. Simaan, A. Gacic, H. Jiang, B. Letelliier, M. Li, and Y. Liu. Game-theoretic modeling and control of a military air operation. *IEEE Transactions on Aerospace and Electronic Systems*, 37(4):1393–1405, 2001.

[22] J.B. Cruz Jr, M.A. Simaan, A. Gacic, and Y. Liu. Moving horizon Nash strategies for a military air operation. *IEEE Transactions on Aerospace and Electronic Systems*, 38(3):989–999, 2002.

[23] Y. Liu, M.A. Simaan, and J.B. Cruz Jr. An application of dynamic Nash task assignment strategies to multi-team military air operations. *Automatica*, 39(8):1469–1478, 2003.

[24] Ternion Corporation. The FLexible Analysis, Modeling, and Exercise System (FLAMES). `http://www.ternion.com`, September 2013.

[25] R.M. Jones, J.E. Laird, P.E. Nielsen, K.J. Coulter, P. Kenny, and F.V. Koss. Automated intelligent pilots for combat flight simulation. *AI magazine*, 20(1):27–41, 1999.

[26] S. Glærum. TALUS-an object oriented air combat simulation. In *Proceedings of the 1999 Winter Simulation Conference*, 1999.

[27] J. S. Hammond, R. L. Keeney, and H. Raiffa. Even swaps: a rational method for making trade-offs. *Harvard Business Review*, 76(2):137–149, 1998.

[28] E.W. Dijkstra. A note on two problems in connexion with graphs. *Numerische mathematik*, 1(1):269–271, 1959.

[29] M.L. Fredman and R.E. Tarjan. Fibonacci heaps and their uses in improved network optimization algorithms. *Journal of the Association for Computing Machinery*, 34(3):596–615, 1987.

[30] J. Hoffren and T. Sailaranta. Realististen lentokone- ja ohjussimulaatioiden yhistäminen. Technical Report N:o T-177, Series T, Helsinki University of Technology, Laboratory of Aerodynamics, 2002.

[31] C. Bolkcom. Military Suppression of Enemy Air Defenses (SEAD): Assessing Future Needs. Technical report, 2005.

[32] J.B. Olsan. Genetic Algorithms Applied to a Mission Routing Problem. Technical report, The Defense Technical Information Center, 1993.

[33] Air Force Doctrine Center. Targeting. *Air Force Doctrine Document*, 2006.

[34] E.L. Fleeman. Technologies for future precision strike missile systems. Technical report, 2001.

[35] Air Force Doctrine Center. Air Warfare. *Air Force Doctrine Document*, 2000.

[36] N.H. Quttineh. *Models and Methods for Costly Global Optimization and Military Decision Support Systems*. PhD thesis, Linköping University, Department of Mathematics, 2012.

[37] P. Toth and D. Vigo. *The vehicle routing problem*, volume 9. Society for Industrial and Applied Mathematics, 2002.

[38] D. Delling, P. Sanders, D. Schultes, and D. Wagner. *Algorithmics of Large and Complex Networks*. Springer, 2009.

[39] J. Poropudas and K. Virtanen. Analyzing air combat simulation results with dynamic Bayesian networks. In *Proceedings of the 2007 Winter Simulation Conference*, 2007.

[40] A.E. Bryson. *Dynamic optimization*. Addison-Wesley, 1999.

[41] K. Virtanen et al. *Optimal pilot decisions and flight trajectories in air combat*. PhD thesis, Helsinki University of Technology, Systems Analysis Laboratory, 2005.

[42] D.E. Kirk. *Optimal control theory*. Dover Publications, 2004.

[43] A.E. Bryson Jr. Optimal control-1950 to 1985. *Control Systems, IEEE*, 16(3):26–33, 1996.

[44] IBM. ILOG CPLEX Optimization Studio. `http://www-01.ibm.com/software/integration/optimization/cplex-optimization-studio/`, September 2013.

[45] J. Bellingham, A. Richards, and J. How. Receding horizon control of autonomous aerial vehicles. In *Proceedings of the 2002 American Control Conference*, 2002.

[46] T. Schouwenaars, J. How, and E. Feron. Receding horizon path planning with implicit safety guarantees. In *Proceedings of the 2004 American Control Conference.*, volume 6, pages 5576–5581. IEEE, 2004.

[47] B.V. Cherkassky, A.V. Goldberg, and T. Radzik. Shortest paths algorithms: theory and experimental evaluation. *Mathematical programming*, 73(2):129–174, 1996.

[48] G. Gutin and A.P. Punnen. *The traveling salesman problem and its variations*, volume 12. Springer, 2002.

[49] D. Bertsimas and J.N. Tsitsiklis. *Introduction to linear optimization.* Athena Scientific, 1997.

[50] C. Papadimitriou and K. Steiglitz. *Combinatorial optimization: algorithms and complexity.* Courier Dover Publications, 1998.

[51] R. Gibbons. *A primer in game theory.* Prentice Hall, 1992.

[52] Y Ho, A Bryson, and S Baron. Differential games and optimal pursuit-evasion strategies. *Automatic Control, IEEE Transactions on*, 10(4):385–389, 1965.

[53] R. Isaacs. *Differential games: a mathematical theory with applications to warfare and pursuit, control and optimization.* Dover Publications, 1999.

[54] V. Turetsky and J. Shinar. Missile guidance laws based on pursuit-evasion game formulations* 1. *Automatica*, 39(4):607–618, 2003.

[55] T. Basar and G.J. Olsder. *Dynamic noncooperative game theory*, volume 200. Society for Industrial and Applied Mathematics, 1995.

[56] G. Tidhar, C. Heinze, and M. Selvestrel. Flying together: Modelling air mission teams. *Applied Intelligence*, 8(3):195–218, 1998.

[57] M.C. Fu. Optimization for simulation: Theory vs. practice. *INFORMS Journal on Computing*, 14(3):192–215, 2002.

[58] D. McIlroy and C. Heinze. Air combat tactics implementation in the smart whole air mission model (SWARMM). In *Proceedings of the First International SimTecT Conference*, 1996.

[59] Science Applications International Corp. SAIC Mission Planning System. `http://www.saic.com/`, September 2013.

[60] Northrop Grumman Information Technology. Joint Mission Planning System (JMPS). `http://www.is.northropgrumman.com/`, September 2013.

[61] BAES Systems. Common Low Observable Autorouter (CLOAR). `http://www.baesystems.com`, September 2013.

[62] OR Concepts Applied. ORCA Planning and Utility System (OPUS). `http://www.orconceptsapplied.com/opus`, September 2013.

[63] Northrop Grumman Information Technology. Joint Routing and Analysis Planning System (JRAPS). `http://www.is.northropgrumman.com/`, September 2013.

[64] Tybrin Corporation. Portable Flight Mission Planning Software (PFPS). `http://www.tybrin.com/`, September 2013.

[65] Janne Karelahti, Kai Virtanen, and John Öström. Automated generation of realistic near-optimal aircraft trajectories. *Journal of guidance, control, and dynamics*, 31(3):674–688, 2008.

[66] NASA. Program to Optimize Simulated Trajectories II (POST II). `http://post2.larc.nasa.gov/index.html`, September 2013.

[67] NASA. Optimal Trajectories by Implicit Simulation program (OTIS). `http://otis.grc.nasa.gov/`, September 2013.

[68] Astos Solutions. Aero Space Trajectory Optimization Software (ASTOS). `http://www.astos.de/`, September 2013.

[69] Tactical Technologies Inc. The Tactical Engagement Simulation Software (TESS). `http://tti-ecm.com/`, September 2013.

[70] S.R. Proulx, D.E.L. Promislow, and P.C. Phillips. Network thinking in ecology and evolution. *Trends in Ecology & Evolution*, 20(6):345–353, 2005.

[71] J.E. Flood. *Telecommunication networks*. The Institution of Engineering and Technology, 1997.

[72] S. Goyal. *Connections: an introduction to the economics of networks*. Princeton University Press, 2009.

[73] J. M. Mulvey and H. Vladimirou. Stochastic network optimization models for investment planning. *Annals of Operations Research*, 20(1):187–217, 1989.

[74] B. Latour. *Reassembling the social-an introduction to actor-network-theory*, volume 1. Oxford University Press, 2005.

[75] J.A. Bondy and U.S.R. Murty. *Graph theory with applications*, volume 290. Macmillan, 1976.

[76] L. Euler. Solutio problematis ad geometriam situs pertinentis. *Commentarii Academiae Scientiarum Imperialis Petropolitanae*, 8:128–140, 1741.

[77] B. Golany, M. Kress, M. Penn, and U.G. Rothblum. Network optimization models for resource allocation in developing military countermeasures. *Operations Research*, 60(1):48–63, 2012.

[78] D. Shrimpton and A.M. Newman. The US Army uses a network optimization model to designate career fields for officers. *Interfaces*, 35(3):230–237, 2005.

[79] R. Bellman. On a routing problem. Technical report, The Defense Technical Information Center, 1956.

[80] K. Menger. Das botenproblem. *Ergebnisse eines mathematischen kolloquiums*, 2:11–12, 1932.

[81] M. Grötschel and O. Holland. Solution of large-scale symmetric travelling salesman problems. *Mathematical Programming*, 51(1):141–202, 1991.

[82] J. Current and M. Marsh. Multiobjective transportation network design and routing problems: Taxonomy and annotation. *European Journal of Operational Research*, 65(1):4–19, 1993.

[83] B.M. Waxman. Routing of multipoint connections. *IEEE Journal on Selected Areas in Communications*, 6(9):1617–1622, 2002.

[84] J.J. Xu and H. Chen. Fighting organized crimes: using shortest-path algorithms to identify associations in criminal networks. *Decision Support Systems*, 38(3):473–487, 2004.

[85] R. Bellman. Bottleneck problems and dynamic programming. *Proceedings of the National Academy of Sciences of the United States of America*, 39(9):947–951, 1953.

[86] Charles E Leiserson, Ronald L Rivest, Clifford Stein, and Thomas H Cormen. *Introduction to algorithms*. The MIT press, 2001.

[87] P.E. Hart, N.J. Nilsson, and B. Raphael. A formal basis for the heuristic determination of minimum cost paths. *IEEE transactions on Systems Science and Cybernetics*, 4(2):100–107, 1968.

[88] J.C.N. Clımaco and M.M.B. Pascoal. Multicriteria Path and Tree Problems–Discussion on Exact Algorithms. Technical Report No. 3, INESC-Coimbra, 2010.

[89] M. Ehrgott and X. Gandibleux. A survey and annotated bibliography of multiobjective combinatorial optimization. *OR Spectrum*, 22(4):425–460, 2000.

[90] M. Gen, R. Cheng, and D. Wang. Genetic algorithms for solving shortest path problems. In *IEEE International Conference on Evolutionary Computation, 1997.*, 1997.

[91] C.W. Ahn and RS Ramakrishna. A genetic algorithm for shortest path routing problem and the sizing of populations. *IEEE Transactions on Evolutionary Computation*, 6(6):566–579, 2002.

[92] E.Q.V. Martins. On a multicriteria shortest path problem. *European Journal of Operational Research*, 16(2):236–245, 1984.

[93] M. Mollaghasemi and J. Pet-Edwards. *Technical briefing: making multiple-objective decisions*. IEEE computer society press, 1997.

[94] L Zadeh. Optimality and non-scalar-valued performance criteria. *IEEE Transactions on Automatic Control*, 8(1):59–60, 1963.

[95] Z. Tarapata. Selected multicriteria shortest path problems: An analysis of complexity, models and adaptation of standard algorithms. *International Journal of Applied Mathematics and Computer Science*, 17(2):269–287, 2007.

[96] R. Clemen. *Making hard decisions: an introduction to decision analysis*. Cengage Learning, 1996.

[97] K. Miettinen. *Nonlinear multiobjective optimization*, volume 12. Springer, 1999.

[98] K. Miettinen, F. Ruiz, and A. Wierzbicki. Introduction to multiobjective optimization: interactive approaches. *Multiobjective Optimization*, pages 27–57, 2008.

[99] S. Zionts and J. Wallenius. An interactive programming method for solving the multiple criteria problem. *Management Science*, 22(6):652–663, 1976.

[100] A.M. Geoffrion, J.S. Dyer, and A. Feinberg. An interactive approach for multi-criterion optimization, with an application to the operation of an academic department. *Management Science*, 39(4):357–368, 1972.

[101] A.P. Wierzbicki. The Use of Reference Objectives in Multiobjective Optimization-Theoretical Implications and Practical Experience. *International Institution of Applied System Analysis, Laxenburg, Austria, Working Paper WP-79-66*, 1979.

[102] K. Miettinen and M.M. Mäkelä. Interactive multiobjective optimization system WWW-NIMBUS on the internet. *Computers & Operations Research*, 27(7):709–723, 2000.

[103] R. T. Marler and J. S. Arora. The weighted sum method for multi-objective optimization: new insights. *Structural and multidisciplinary optimization*, 41(6):853–862, 2010.

[104] A. Messac and C.A. Mattson. Generating well-distributed sets of Pareto points for engineering design using physical programming. *Optimization and Engineering*, 3(4):431–450, 2002.

[105] J. Koski. Defectiveness of weighting method in multicriterion optimization of structures. *Communications in applied numerical methods*, 1(6):333–337, 1985.

[106] I. Das and JE Dennis. A closer look at drawbacks of minimizing weighted sums of objectives for Pareto set generation in multicriteria optimization problems. *Structural and Multidisciplinary Optimization*, 14(1):63–69, 1997.

[107] R.L. Keeney and H. Raiffa. *Decision making with multiple objectives: preferences and value tradeoffs*. John Wiley and Sons, 1976.

[108] A. Messac. Physical programming: effective optimization for computational design. *AIAA journal*, 34(1):149–158, 1996.

[109] I. Das and J. Dennis. Normal-boundary intersection: A new method for generating the Pareto surface in nonlinear multicriteria optimization problems. *SIAM Journal on Optimization*, 8(3):631–657, 1998.

[110] A. Messac, A. Ismail-Yahaya, and C.A. Mattson. The normalized normal constraint method for generating the Pareto frontier. *Structural and multidisciplinary optimization*, 25(2):86–98, 2003.

[111] M. Zeleny. *Multiple criteria decision making*, volume 25. McGraw-Hill, 1982.

[112] S. Kirkpatrick. Optimization by simulated annealing: Quantitative studies. *Journal of Statistical Physics*, 34(5):975–986, 1984.

[113] C.A.C. Coello, D.A. Van Veldhuizen, and G.B. Lamont. *Evolutionary algorithms for solving multi-objective problems*. Plenum Publishing Corporation, 2002.

[114] C. Prins. A simple and effective evolutionary algorithm for the vehicle routing problem. *Computers & Operations Research*, 31(12):1985–2002, 2004.

[115] M. Dorigo, M. Birattari, and T. Stutzle. Ant colony optimization. *IEEE Computational Intelligence Magazine*, 1(4):28–39, 2006.

[116] J. Kennedy, R. Eberhart, et al. Particle swarm optimization. In *Proceedings of IEEE international conference on neural networks*, 1995.

[117] Department of Defense Standard Practice. MIL-STD-3013A: GLOSSARY OF DEFINITIONS, GROUND RULES, AND MISSION PROFILES TO DEFINE AIR VEHICLE PERFORMANCE CAPABILITY United States Military Standard, 2003.

[118] M. Waddell. Surface-To-Air Guided Missile Systems Methods Of Tactical Analysis. Technical report, The Defense Technical Information Center, 1961.

[119] G. Siouris. *Missile guidance and control systems*. Springer, 2004.

[120] G.R. Curry. *Radar system performance modeling*, volume 1. Artech House, 2005.

[121] M. Guelman. A qualitative study of proportional navigation. *IEEE Transactions on Aerospace and Electronic Systems*, 7(4):637–643, 1971.

[122] G. E. Straight. An Open Loop Missile Evasion Algorithm for Fighters. Technical report, The Defense Technical Information Center, 1983.

[123] MathWorks. MATLAB R2012b. `http://www.mathworks.com/`, September 2013.

[124] ProFantasy Software Ltd. Fractal Terrains 3. `http://www.profantasy.com/products/ft.asp`, September 2013.

[125] U.S. Air Force. JOINT DIRECT ATTACK MUNITION GBU- 31/32/38 Factsheet. `http://www.navy.mil/navydata/fact_display.asp?cid=2100&tid=400&ct=2`, September 2013.

[126] U.S. Navy. AGM-154 Joint Standoff Weapon (JSOW) Fact File. `http://www.navy.mil/navydata/fact_display.asp?cid=2100&tid=300&ct=2`, September 2013.

[127] C. Hallam, K. J. Harrison, and J. A. Ward. A multiobjective optimal path algorithm. *Digital Signal Processing*, 11(2):133–143, 2001.